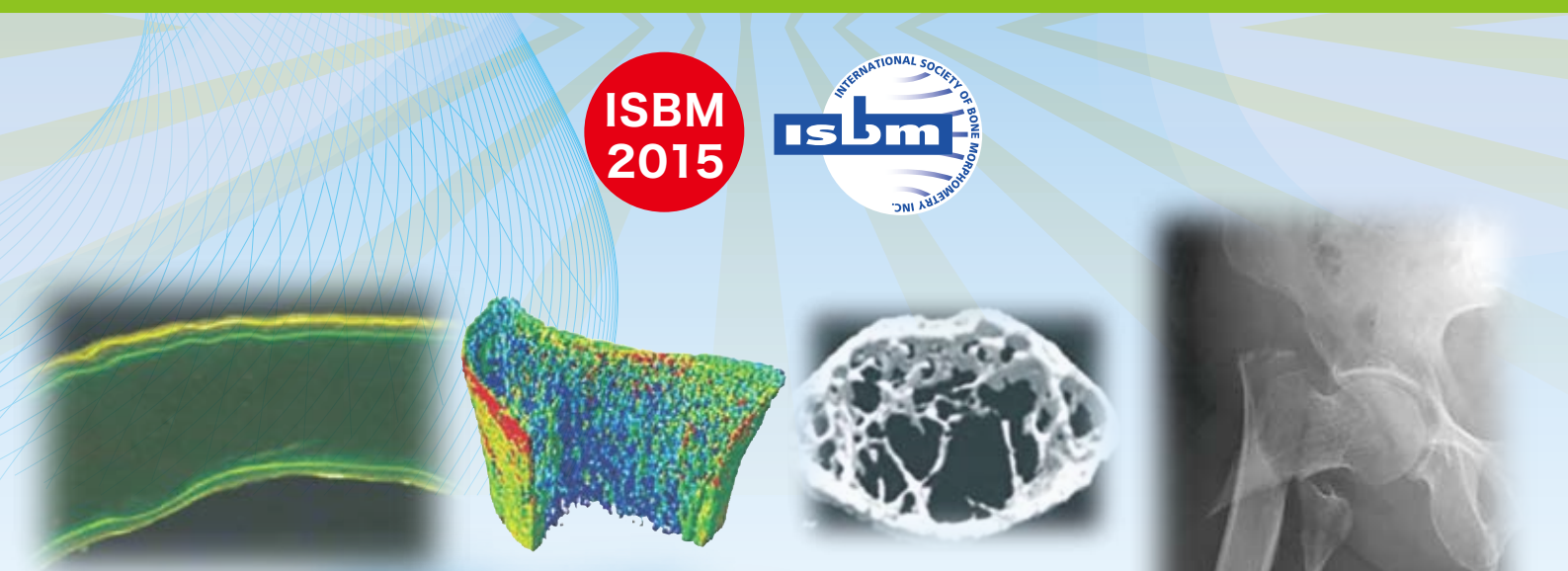


# 13<sup>th</sup> Congress of the International Society of Bone Morphometry

ISBM  
2015



**Program Book**

**Date** April 27-29, 2015

**Venue** Tokyo Garden Palace Hotel, Tokyo

**President** Masaki Noda  
Tokyo Medical and Dental University

<http://www.procomu.jp/isbm2015/>

# NEW FORCE

6ヵ月に1回の皮下注\*で、  
骨粗鬆症による骨折リスクを抑制

薬価基準収載

ヒト型抗RANKLモノクローナル抗体製剤

**プラリア® 皮下注60mg  
シリンジ**

一般名 / デノスマブ (遺伝子組換え)

生物由来製品、劇薬、処方せん医薬品\*

※注意—医師等の処方せんにより使用すること

\*プラリアの用法・用量：通常、成人にはデノスマブ (遺伝子組換え) として  
60mgを6ヵ月に1回、皮下投与する。

## 【禁 忌】(次の患者には投与しないこと)

1. 本剤の成分に対し過敏症の既往歴のある患者
2. 低カルシウム血症の患者 (「重要な基本的注意」の項参照)
3. 妊婦又は妊娠している可能性のある婦人 (「妊婦、産婦、授乳婦等への投与」の項参照)

## 【効能・効果】

骨粗鬆症

### <効能・効果に関連する使用上の注意>

本剤の適用にあたっては、日本骨代謝学会の診断基準等を参考に、骨粗鬆症との診断が確定している患者を対象とすること。

## 【用法・用量】

通常、成人にはデノスマブ (遺伝子組換え) として60mgを6ヵ月に1回、皮下投与する。

## 【使用上の注意】

### 1. 慎重投与 (次の患者には慎重に投与すること)

- (1) 低カルシウム血症を起こすおそれのある患者 [低カルシウム血症が発現するおそれがある (「重要な基本的注意」の項参照)。]
- (2) 重度の腎機能障害のある患者 [使用経験が少ない。低カルシウム血症を起こすおそれがある。]

### 2. 重要な基本的注意

(1) 本剤はランマークと同一成分 (デノスマブ) を含むため、本剤投与中の患者にはランマークの投与を避けること。(2) 本剤投与開始前に血清補正カルシウム値を確認すること。低カルシウム血症のある患者は、本剤投与前に低カルシウム血症を治療すること。(3) 本剤投与により低カルシウム血症があらわれることがあるため、血清補正カルシウム値が高値でない限り、毎日カルシウム及びビタミンDの経口補充のもとに本剤を投与すること。ただし、腎機能障害患者や、既に活性型ビタミンDを使用している患者においては、適宜、活性型ビタミンDを使用するとともに、カルシウムについては投与の必要性を判断し、投与量を調整すること。また、投与開始後早期及びその後も定期的に血清カルシウム値を測定し、血清補正カルシウム値の変動や、痙攣、しびれ、失見当識等の症状に注意すること。なお、本剤の国内第Ⅲ相臨床試験では、全ての患者に対して、治験期間中に毎日少なくとも600mgのカルシウム及び400IUの天然型ビタミンDが補充された (「重大な副作用」、「臨床成績」の項参照)。また、本剤の海外市販後の自発報告において、重篤な低カルシウム血症が認められている。このうち、発現日が確認できた症例の約半数は、初回投与から7日以内の発現であった。(4) 骨粗鬆症の発症にエストロゲン欠乏、加齢以外の要因が関与していることもあるので、治療に際してはこのような要因を考慮する必要がある。(5) 顎骨壊死・顎骨骨髓炎があらわれることがある。報告された症例の多くが抜歯等の顎骨に対する侵襲的な歯科処置や局所感染に関連して発現している。リスク因子としては、悪性腫瘍、化学療法、コルチコステロイド治療、放射線療法、口腔の不衛生、歯科処置の既往等が知られている。本剤の投与開始前は口腔内の管理状態を確認し、必要に応じて、患者に

対し適切な歯科検査を受け、侵襲的な歯科処置をできる限り済ませておくよう指導すること。本剤投与中に侵襲的な歯科処置が必要になった場合には、本剤の休薬等を考慮すること。また、口腔内を清潔に保つこと、定期的な歯科検査を受けること、歯科受診時に本剤の使用を歯科医師に告知して侵襲的な歯科処置はできる限り避けることなどを患者に十分説明し、異常が認められた場合には、直ちに歯科・口腔外科を受診するように指導すること (「重大な副作用」の項参照)。(6) 本剤又はビスホスホネート系薬剤を長期使用している患者において、非外傷性的大腿骨転子下及び近位大腿骨骨幹部の非定型骨折が発現したとの報告がある。これらの報告では、完全骨折が起こる数週間から数カ月前に大腿部や鼠径部等において前駆痛が認められている報告もあることから、本剤の投与開始後にこのような症状が認められた場合には、X線検査等を行い、適切な処置を行うこと。また、両側性の骨折が生じる可能性があることから、片側で非定型骨折が起きた場合には、反対側の大腿部の症状等を確認し、X線検査を行うなど、慎重に観察すること。X線検査時には骨皮質の肥厚等、特徴的な画像所見がみられており、そのような場合には適切な処置を行うこと。(7) 本剤のシリンジ注射針カバーは、天然ゴム (ラテックス) を含み、アレルギー反応を起こすことがあるので、投与に際し、問診を行うこと。また、観察を十分に行い、異常が認められた場合には投与を中止し、適切な処置を行うこと。

### 3. 副作用

骨粗鬆症患者を対象とした国内第Ⅲ相臨床試験において、総症例881例中159例 (18.0%) に副作用 (臨床検査値異常を含む) が認められた。主なものは、低カルシウム血症7例 (0.8%)、背部痛7例 (0.8%)、γ-GTP上昇7例 (0.8%)、高血圧7例 (0.8%)、湿疹6例 (0.7%)、関節痛5例 (0.6%) 等であった。〔承認時〕

(1) 重大な副作用 ① 低カルシウム血症 (0.8%) : 痙攣、しびれ、失見当識等の臨床症状を伴う低カルシウム血症があらわれることがあるので、観察を十分に行うこと。低カルシウム血症が認められた場合には、カルシウム及びビタミンDの補充に加えて、緊急時には、カルシウムの点滴投与を併用するなど、適切な処置を速やかに行うこと。

② 顎骨壊死・顎骨骨髓炎 (0.1%) : 顎骨壊死・顎骨骨髓炎があらわれることがあるので、観察を十分に行い、異常が認められた場合には投与を中止するなど、適切な処置を行うこと。

③ アナフィラキシー (頻度不明<sup>※1</sup>) : アナフィラキシーがあらわれることがあるので、観察を十分に行い、異常が認められた場合には投与を中止し、適切な処置を行うこと。

④ 大腿骨転子下及び近位大腿骨骨幹部の非定型骨折 (頻度不明<sup>※1</sup>) : 大腿骨転子下及び近位大腿骨骨幹部の非定型骨折を生じることがあるので、観察を十分に行い、異常が認められた場合には投与を中止するなど、適切な処置を行うこと (「重要な基本的注意」の項参照)。

⑤ 重篤な皮膚感染症 (頻度不明<sup>※1</sup>) : 重篤な蜂巣炎等の皮膚感染症があらわれることがあるので、観察を十分に行い、発赤、腫脹、疼痛、発熱等の症状が認められた場合には、適切な処置を行うこと。

注) 海外において認められている副作用のため頻度不明。

その他の使用上の注意につきましては製品添付文書をご参照ください。

製造販売元 (資料請求先)



Daiichi-Sankyo

第一三共株式会社

東京都中央区日本橋本町3-5-1

提携



**13<sup>th</sup> Congress of the  
International Society of  
Bone Morphometry**





## Welcome to the XIII<sup>th</sup> Congress of the International Society of Bone Morphometry



**Masaki Noda, M.D., Ph.D.**

President  
Department of Molecular Pharmacology  
Medical Research Institute  
Tokyo Medical and Dental University,  
Tokyo, Japan

As a president, I would like to welcome all of you to the 13th congress of The International Society of Bone Morphometry (ISBM) in Tokyo. ISBM was founded in 1973, and incorporated as a non-profit organization in 1996. The mission of ISBM is to emphasize the importance of traditional morphometric techniques in the field of bone research, to embrace new technologies that result in refinements and advances in bone morphometric analyses, and to facilitate the education and training of basic scientists and clinicians in all aspects of bone morphometry. Many preclinical and clinical studies utilize bone morphometry as an essential technique to assess changes in bone structure and function in response to a variety of influences such as hormones, cytokines, growth factors, mechanical loading, and bone-active drugs. Bone morphometry is also essential for skeletal phenotyping of knockout and transgenic mice. Recent rapid advances in human bone imaging are emphasizing the importance of bone morphometry as a tool for patient evaluation and monitoring drug efficacy in clinical practice.

This meeting, the 13th Congress of the Society, will be held on April 27-29, 2015 in Tokyo. We will begin the congress by a wonderful keynote speaker, Jack Martin. Following his presentation, there will be main six sessions where distinguished invited scientists in the field of skeletal diseases and basic research will present spectacular series of talks. We are also welcoming delegations from 12 countries. Their papers will be presented in oral or poster presentation sessions.

I express my sincere gratitude to Professor Masako Ito, the President of Japanese Society for Bone Morphometry for her very kind and full support for this meeting. I am also very much thankful to Dr. Hideaki Takahashi, Professor Emeritus of Niigata University, the past president of the 5th Congress of ISBM held in Japan, who has been wonderfully leading this field of bone morphometry for many years.

The congress would not be possible without the generous supports of our sponsors, exhibitors, and donors. Special thanks are in order for these companies whose names are listed in a knowledge page.

ISBM congress serves as a unique opportunity for graduate students, postdocs, and young and senior scientists for innovation in clinical and basic research based on a merging of molecular biology, preclinical and clinical pathophysiology, and future development of bone-active drugs. Please join and enjoy ISBM Tokyo 2015 to become more innovative, connected and interactive in the field of skeletal clinical and basic sciences.

April 3, 2015

*Masaki Noda*





# Table of Contents

Welcome to the XIIIth Congress of the International Society of Bone Morphometry .....	i
Officers and Board Members of the International Society of Bone Morphometry .....	v
To Participants .....	vi
To Poster Session Chairpersons and Speakers .....	viii
Floor Plan .....	ix
Poster & Exhibition Layout .....	ix
Venue for Receptions .....	x
Special Thanks to our Congress Sponsors and Exhibitors.....	xi
Program at a Glance .....	xii
Congress Agenda .....	xv
Keynote Lecture .....	1
Main Sessions .....	5
Work Shop .....	23
Luncheon & Evening Seminars .....	27
Oral Presentations .....	39
Poster Sessions .....	63







## **To Participants**

### **1. Main Reception Desk**

The registration/information desk is located in the lobby of the Banquet Hall “Takachiho” in the TOKYO GARDEN PALACE

Dates and Times: April 27 (Monday) –April 29 (Wednesday) 8:00 a.m. - 5:00 p.m.

### **2. On-Site Registration**

On-site registrants must fill out a registration form and pay their fees. At registration, participants will be given a badge on which to write their name and affiliation. These badges should be worn at all times during the conference. Students must present their student ID cards at registration.

### **3. Registration Fees**

Member: JPY 30,000 Non-Member JPY 32,000

Post Graduate Student/Resident: JPY 27,000

### **4. During question-and-answer and discussion sessions, please follow the chairman's directions and state your name and affiliation when you first approach the microphone.**

### **5. Smoking is not permitted in any of the conference venues.**

### **6. Mobile phones should be turned off or in silent mode.**

### **7. Lunch will be provided at luncheon seminars. Participants also may dine at the hotel's restaurants and coffee shops.**

### **8. The recording of all or part of any scientific presentation or poster presentation is prohibited.**

## **To Invited Speakers of Main Sessions**

Presentation data and PC

<Presentation time>

50minutes for presentation and 10 minutes for Q&A

<Presentation equipment>

### **1. All presentation materials should be prepared in Microsoft PowerPoint 2010 or 2013 for Windows PC.**

### **2. You can bring your presentation data on a USB memory stick or CD-R in the above format.**

### **3. You are advised to bring your own laptop PC if your presentation materials including video/movies cannot be prepared in the above mentioned format.**

### **4. Please make sure that your laptop is equipped with mini D-sub (15pins). If you are using Macintosh, please make sure to bring AC adaptor and connector to mini D-sub (15pins).**

### **5. Please deactivate your screensaver and power saving settings.**

### **6. Please bring your own power cable. Presentations using batteries may result in problems.**

### **7. To avoid losing important data saved on the PC used for your presentation, be sure to backup such data beforehand.**

## **To Speakers of Oral Presentations**

### Presentation registration

After registering for the conference at the reception desk of the site, all speakers for the oral sessions are asked to come to the “PC Center” to check in their presentation data. You are advised to come to the PC Center before 30 minutes prior to their presentations.

New investigator award winners need to attend the closing ceremony on April 29th 2015 to receive the awards.

### <Presentation time>

9 minutes for presentation and 3 minutes for Q&A

### <Presentation equipment>

1. All presentation materials should be prepared in Microsoft PowerPoint 2010 or 2013 for Windows PC.
2. You can bring your presentation data on a USB memory stick or CD-R in the above format.
3. You are advised to bring your own laptop PC if your presentation materials including video/movies cannot be prepared in the above mentioned format.
4. Please make sure that your laptop is equipped with mini D-sub (15pins). If you are using Macintosh, please make sure to bring AC adaptor and connector to mini D-sub (15pins).
5. Please deactivate your screensaver and power saving settings.
6. Please bring your own power cable. Presentations using batteries may result in problems.
7. To avoid losing important data saved on the PC used for your presentation, be sure to backup such data beforehand.



## **To Poster Session Chairpersons and Speakers**

### **[Presentation time]**

1 minutes for presentation and 2 minutes for Q&A

(There will be a chairperson in front of your poster. Please follow his instruction and present your poster for 4 min at the indicated date and time shown above. There will be 2 min discussion (Q & A) period just after your presentation.)

### **[Venue]**

Tenku A (2nd floor)

### **[Poster dimension]**

Poster maximum size:

Height: 210 cm

Width: 90 cm

### **[Poster setup time]**

April 27th (Mon.) 8:30-12:00

### **[Poster presentation time]**

April 28th (Tues.) 13:00-14:00

### **[Poster presentation session frame]**

April 28th (Tues.) Poster Presentation 1 13:10-13:46

April 29th (Wed.) Poster Presentation 2 13:10-13:46

\*Please stand by your poster 5 minutes before the session starts.

\*Please follow the instruction given by your chairperson

### **[Poster removal time]**

April 29th (Wed.) 14:00-18:00

Note : All posters should be taken down from the boards by the above time. Conference secretariat will not assume responsibility for possible loss of posters left on the board , in particular posters left after the last day of the congress.

For Poster Session Speakers

#### **1. Poster Board Size**

90cm wide by 210cm high, including 20cm for title, name and affiliation.

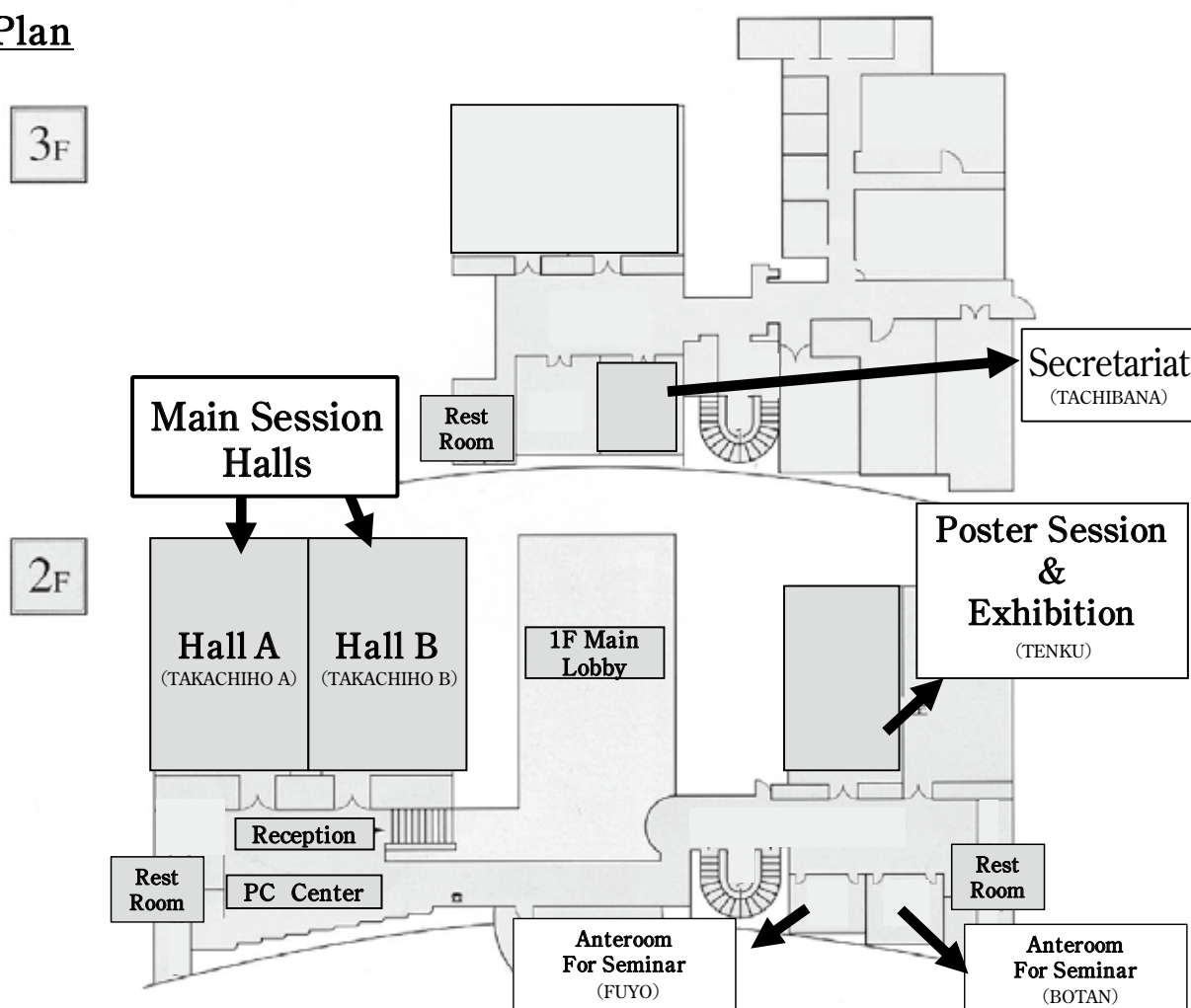
In preparing your presentation, we ask that you keep your name, title, and affiliation at 70cm wide by 20cm high. The poster number (20cm by 20cm) will be added by the secretariat.

The poster display space is 190cm high by 90cm wide. If more space is needed, use the space allotted for the name, title, and affiliation, as information in the lower portion of the poster board will be difficult to see.

#### **2. Ribbons and push-pins for the speakers will be at the poster session reception desk. Speakers also should wear their ribbons during the poster presentation.**

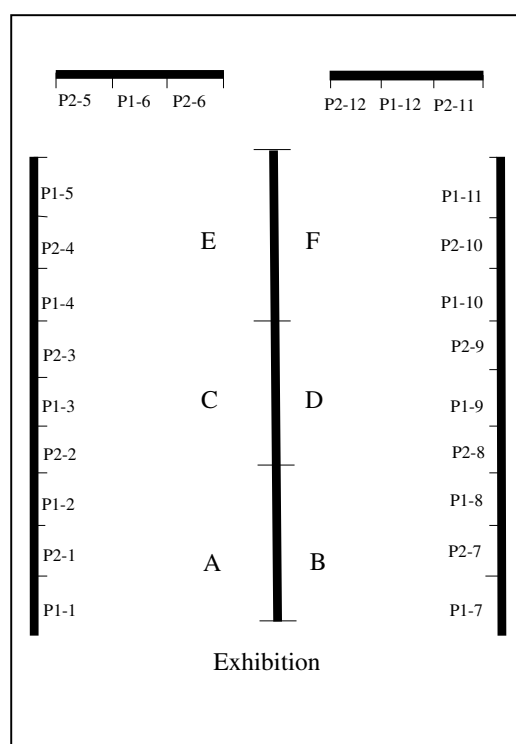
New investigator award winners need to attend the closing ceremony on April 29th 2015 to receive the awards.

## Floor Plan



### Poster Session / Exhibition

(Tenku A)



## Venue for Receptions

### April 27, 2015 (Monday)

Social Evening 7:00 p.m. ~ 8:30 p.m.

Venue : Garden Palece Hotel (Takachiho B)

Tokyo Night View from Sky Lounge (26F) 8:30 p.m. ~ 9:00 p.m.

Venue : Tokyo Medical and Dental University MD-Tower, 26F Floor

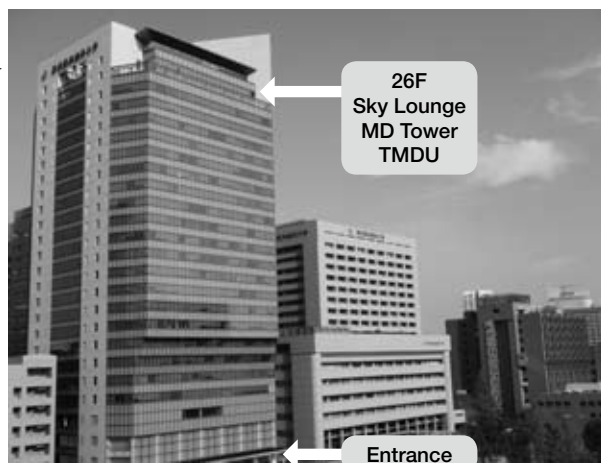
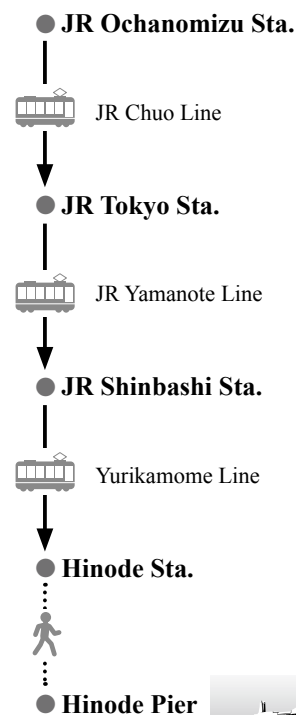
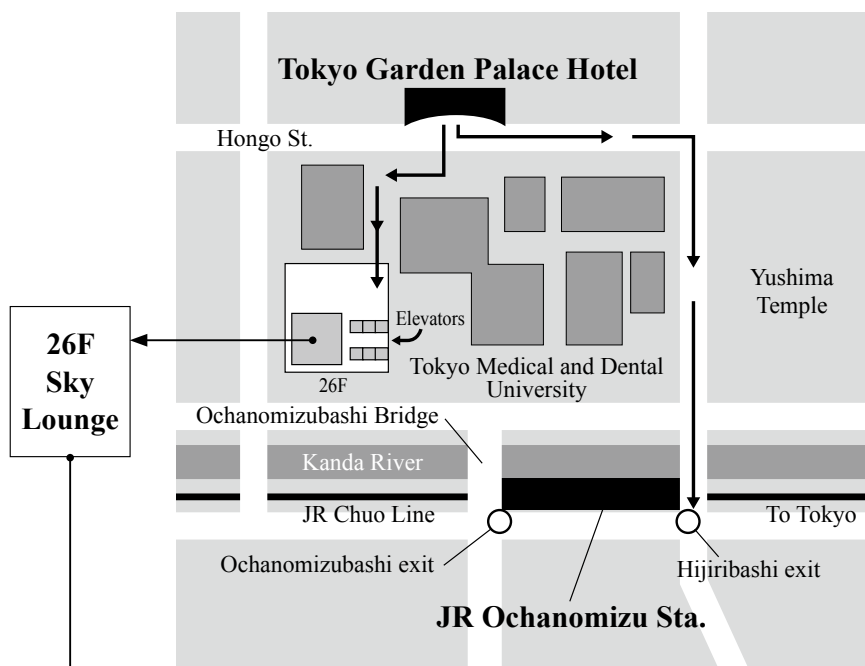
### April 28, 2015 (Tuesday)

International Evening (Bus will depart from the Hotel at 6:10 p.m.)

Venue : Symphony Cruise (Departing at 7:00 p.m.)

Hinode Pier in Tokyo Bay

### Access & Map





## Special Thanks to our Congress Sponsors and Exhibitors

### **Gold Sponsors :**

#### Luncheon Seminar

- CHUGAI PHARMACEUTICAL Co., Ltd.
- Taisho Toyama Pharmaceutical Co., Ltd.
- Asahi Kasei Corporation.
- Pfizer Inc.
- DAIICHI SANKYO COMPANY, LIMITED.
- MSD K.K. a subsidiary of Merck & Co., Inc.

#### Evening Seminar

- Hisamitsu Pharmaceutical Co., Inc.
- Eli Lilly Japan K.K.

### **Silver Sponsors :**

#### Contribution

- Sumitomo Dainippon Pharm Co., Ltd
- Taisho Toyama Pharmaceutical Co., Ltd.
- Novartis Pharma K.K.
- Osteometrics, Inc.
- Astellas Pharma Inc.

#### Exhibition

- SHIMADZU CORPORATION.
- RATOC Systems, Inc.
- Summit Pharmaceuticals International Corporation.
- Bean Stalk Snow Co., Ltd. (MEGMILK SNOW BRAND Group)
- SHOSHIN EM Corporation.
- TOYO Corporation.

### **Bronze Sponsors :**

#### Advertisement

- SHIMADZU CORPORATION.
- Astellas Pharma Inc.
- Eisai Co., Ltd.
- RATOC Systems, Inc.
- Hologic Japan, Inc
- ZEISS
- DAIICHI SANKYO COMPANY, LIMITED
- RIKAKEN CO., LTD.
- John Wiley & Sons (Asia) Pte. Ltd.
- Summit Pharmaceuticals International Corporation.

## Program at a Glance

April 27(Mon)				
	Hall A(2F) Room "Takachiho A"	Hall B (2F) Room "Takachiho B"	Poster (3F) Room "Tenku A"	
8:00				
8:30	<b>8:40 Opening Remark</b> <b>8:45 Keynote Lecture</b>		<b>8:30-12:00</b>	
9:00	How concepts of bone remodeling influence therapeutic development in osteoporosis <b>Jack Martin</b>			
	<b>9:45</b> <b>Session 1 : New Treatment and Diagnosis for Osteoporosis</b>			Poster setup time
10:00	New imaging techniques in the diagnosis of bone diseases <b>Thomas Link</b>			
11:00	Targeting cathepsin k for the treatment of osteoporosis <b>Le Duong</b>			
	<b>11:45 Group Picture</b>			
12:00	<b>12:00 Luncheon Seminar</b>	<b>12:00 Luncheon Seminar</b>		
	Novel modes of action of anti-bone resorptive drugs revealed by intravital two-photon bone imaging technology <b>Masaru Ishii</b> Chugai Pharmaceutical Co., Ltd	Locomotive syndrome – Measures for increasing healthy life expectancy  <b>Kozo Nakamura</b> Taisho Toyama Pharmaceutical Co., Ltd.		
13:00	<b>13:00</b> <b>Oral Presentation 1</b>			
	<b>O1-1-O1-5</b>			
14:00	<b>14:00</b> <b>Session 2 : Bone Diseases and Cell Regulation</b>		<b>Poster Exhibition</b>	
	Cell communication in osteoimmunology <b>Hiroshi Takayanagi</b>			
15:00	Effects of sclerostin antibody on different bone surfaces with shorter- and longer- term treatment <b>David Ke</b>			
16:00	Cartilage and meniscus regenerationby synovial stem cells : from bench to clinic <b>Ichiro Sekiya</b>			
17:00	<b>17:00</b> <b>Oral Presentation 2</b>			
	<b>O2-1-O2-5</b>			
18:00	<b>18:00</b> <b>Evening Seminar</b> Geometry of lower extremities and atypical femoral fractures <b>Muneaki Ishijima</b> Hisamitsu Pharmaceutical Co., Inc.			
19:00		<b>19:00-20:30</b> <b>Social Evening</b> Garden Palace Hotel <b>20:30-21:00</b> TMDU MD Tower 26F Sky Lounge		
21:00				

April 28(Tues)			
	Hall A(2F) Room "Takachiho A"	Hall B (2F) Room "Takachiho B"	Poster (3F) Room "Tenku A"
8:00			
8:30	<b>8:30 Session 3 : Fracture and Bone Structure</b>		
9:00	Assessment of bone structure in relation to biomechanical properties <b>Masako Ito</b>		
10:00	Hierarchical imaging of bone failure <b>Ralph Muller</b>		
10:30	<b>Oral Presentation 3</b>		
11:00	<b>O3-1-O3-6</b>		Poster Exhibition
12:00	<b>12:00 Luncheon Seminar</b>	<b>12:00 Luncheon Seminar</b>	
13:00	Morphological examination on anabolic effects of intermittent administration of PTH in bone <b>Norio Amizuka</b> Asahi Kasei Corporation.	Bone histomorphometry in orthopedic clinical practice <b>Noriaki Yamamoto</b> Pfizer Inc.	
14:00			<b>13:10-13:46</b> <b>Poster Presentation 1-A, 1-B</b>
14:00	<b>14:00 Session 4 : Bone Impairment and Clinical Bases</b>		Talk & Discussion <b>P1-1-P1-12</b>
15:00	Clinical management of osteoporosis : new options <b>Robert Recker</b>		
16:00	Genetic and molecular bases of osteolytic/osteoporotic disorders <b>Yoichi Ezura</b>		
17:00	Rapid and reproducible ex vivo imaging of mouse articular cartilage using confocal microscopy <b>Matthew Warman</b>		
17:00	<b>17:00 Evening Seminar</b> Anabolic therapy for the skeleton with PTH – now and the future <b>Jack Martin</b> Eli Lilly Japan K.K.		
18:00	<b>18:10 Transportation to International Evening Venue</b> (Bus will depart from Garden Palace Hotel)		
19:00	<b>19:00-21:00</b> <b>International Evening on Symphony Cruise</b> <b>at Hinode Pier in Tokyo Bay</b>		
21:00			



April 29(Wed)			
	Hall A(2F) Room "Takachiho A"	Hall B (2F) Room "Takachiho B"	Poster (3F) Room "Tenku A"
8:00			
8:30	<b>8:30</b> <b>Session 5 : Instability and Skeletal Diseases</b>		
9:00	AFF: Clinical and histological features of atypical subtrochanteric and diaphyseal femoral fracture <b>Naoto Endo</b>		
10:00	Regulation of the catabolic cascade in osteoarthritis by the zinc /ZIP8 MTF1 axis <b>Jang-Soo Chun</b>		
10:30	<b>Oral Presentation 4</b>		
11:00	<b>O4-1-O4-6</b>		
12:00	<b>12:00 Luncheon Seminar</b> Imaging analysis of the effects of denosumab on bone structural properties <b>Masako Ito</b> Denosumab for the treatment of osteoporosis <b>Sakae Tanaka</b> Daiichi Sankyo Company, Ltd.	<b>12:00 Luncheon Seminar</b> Bone microarchitecture after alendronate treatment of osteoporotic women <b>Robert Recker</b> MSD K.K. A subsidiary of Merck & Co., Inc.	
13:00			<b>13:00-13:46</b> <b>Poster Presentation 2-A, 2-B</b>
14:00	<b>14:00 Workshop</b> Proper bone histomorphometry in rats <b>Thomas Wronski</b> Bone histomorphometry in mice: Getting it right! <b>Natalie Sims</b>		Talk & Discussion <b>P2-1-P2-12</b>
15:00	<b>15:00</b> <b>Session 6 : Molecular Bases for Skeletal Pathology</b> Dynamic live imaging of bones: opening a new era with 'Bone histodynametry' <b>Masaru Ishii</b> Histological aspects on the biological function of osteocytes <b>Norio Amizuka</b> Investigating the dynamic biology of osteocytes and bone extracellular matrix assembly using live cell imaging approaches <b>Sarah Dallas</b>		<b>14:00-18:00</b>  Poster removal time
16:00			
17:00			
18:00	<b>18:00 Award Ceremony</b> <b>Closing Remark</b> <b>18:10 Adjourn</b>		
19:00			
21:00			

# 13<sup>th</sup> Congress of the International Society of Bone Morphometry

## 2015.4.27 Monday

8:40am	Opening Remark	
8:45am-9:45am	Keynote Lecture	Chair : <b>Masaki Noda</b>
	• <b>Jack Martin</b> : How concepts of bone remodeling influence therapeutic development in osteoporosis	(p3)
<hr/>		
9:45am-11:45am	<b>Session 1</b> New Treatment and Diagnosis for Osteoporosis ( <i>Takachiho A</i> )	
	Chairs : <b>Tom Wronski, Natalie Sims</b>	
9:45am-10:45am	• <b>Thomas Link</b> : New imaging techniques in the diagnosis of bone diseases	(p7)
10:45am-11:45am	• <b>Le Duong</b> : Targeting cathepsin k for the treatment of osteoporosis	(p8)
<hr/>		
11:45am-11:50am	Group Picture ( <i>Takachiho A</i> )	
12:00pm-13:00pm	Luncheon Seminar Speaker : <b>Masaru Ishii</b> ( <i>Takachiho A</i> )	(p29)
	Dynamic live imaging of bones : opening a new era with 'bone histodynametry'	
	Sponsored by CHUGAI PHARMACEUTICAL Co., Ltd	
	Luncheon Seminar Speaker : <b>Kozo Nakamura</b> ( <i>Takachiho B</i> )	(p30)
	Locomotive syndrome –measures for increasing healthy life expectancy	
	Sponsored by Taisho Toyama Pharmaceutical Co., Ltd.	
1:00pm-2:00pm	Oral Presentation 1 Chairs : <b>Jean-Paul Roux, Akira Nifuji</b> ( <i>Takachiho A</i> )	
1:00pm-1:12pm	O1-1 <b>Yanfei Linda Ma</b> : Histomorphometric analyses of cortical effects of teriparatide in postmenopausal women with or without long-term alendronate therapy	(p41)
1:12pm-1:24pm	O1-2 <b>Ko Chiba</b> : In vivo bone microstructural analysis of osteoporosis using HR-pQCT	(p42)
1:24pm-1:36pm	O1-3 <b>Nobuhito Nango</b> : Measurement of bone strength and medication evaluation can be achieved using medical CT images	(p43)
1:36pm-1:48pm	O1-4 <b>J. Ignacio Aguirre</b> : Comparative analysis of the development of periodontal disease in rice rats and lewis rats	(p44)
1:48pm-2:00pm	O1-5 <b>Akira Nifuji</b> : G9a deficiency leads to impaired osteoblastic differentiation in mice	(p45)
<hr/>		
2:00pm-5:00pm	<b>Session 2</b> Bone Diseases and Cell Regulation ( <i>Takachiho A</i> )	
	Chairs : <b>Matthew Warman, Yoichi Ezura</b>	
2:00pm-3:00pm	• <b>Hiroshi Takayanagi</b> : Cell communication in osteoimmunology	(p9)

3:00pm-4:00pm	• <b>David Ke</b> : Effects of sclerostin antibody on different bone surfaces with shorter- and longer- term treatment (p10)
4:00pm-5:00pm	• <b>Ichiro Sekiya</b> : Cartilage and meniscus regeneration by synovial stem cells : from bench to clinic (p11)
<hr/>	
5:00pm-6:00pm	Oral Presentation 2 Chairs : <b>Linda Ma, Aguirre Ignacio</b> ( <i>Takachiho A</i> )
5:00pm-5:12pm	O2-1 <b>Christina Vrahnas</b> : Osteocytic ephrinB2 restrains mineralisation of murine bone (p46)
5:12pm-5:24pm	O2-2 <b>Andreas Johnathan Truessel</b> : Quantitative local in vivo environment (live) Imaging of osteocytes during dynamic bone remodeling (p47)
5:24pm-5:36pm	O2-3 <b>Guangyi Li</b> : Influence of subchondral bone plate integrity on subchondral bone homeostasis in osteoarthritis (p48)
5:36pm-5:48pm	O2-4 <b>Hiroshige Sano</b> : Intravital bone imaging by two-photon excitation microscopy to identify osteocytic osteolysis in vivo (p49)
5:48pm-6:00pm	O2-5 <b>Smriti Aryal</b> : Nck adaptor proteins control osteoblastic migration, bone formation and bone mass (p50)
6:00pm-7:00pm	Evening Seminar Speaker : <b>Muneaki Ishijima</b> ( <i>Takachiho A</i> ) (p36) Geometry of lower extremities and atypical femoral fractures Sponsored by Hisamitsu Pharmaceutical Co., Inc.
7:00pm-9:00pm	【Social Evening】 Garden Palace Hotel ( <i>Takachiho B</i> )
8:30pm-9:00pm	Night viewing of Tokyo (MD Tower 26th Floor)

**2015.4.28 Tuesday**

8:30am-10:30am	<b>Session 3</b> Fracture and Bone Structure ( <i>Takachiho A</i> )		
	Chairs : <b>Robert Recker, Thomas Link</b>		
8:30am-9:30am	• <b>Masako Ito</b> : Assessment of bone structure in relation to biomechanical properties		(p12)
9:30am-10:30am	• <b>Ralph Muller</b> : Hierarchical imaging of bone failure		(p13)
10:30am-11:45am	Oral Presentation 3 Chairs : <b>Urszula Iwaniec, Norio Amizuka</b> ( <i>Takachiho A</i> )		
10:30am-10:42am	O3-1 <b>Anders Palmquist</b> : Bone-implant interface: morphology and ultrastructure		(p51)
10:42am-10:54am	O3-2 <b>Paksinee Kamolratanakul</b> : Comparative histological study in maxillary sinus augmentation using coarse or fine particle of xenograft materials (preliminary report)		(p52)
10:54am-11:06am	O3-3 <b>Phil Salmon</b> : Is it time to say goodbye to SMI?		(p53)
11:06am-11:18am	O3-4 <b>Omar Omar</b> : Labeling and seeding of MSCs on hydroxyapatite bone substitute : cell behavior and in vivo tracking		(p54)
11:18am-11:30am	O3-5 <b>Furqan A. Shah</b> : Apatite orientation corresponds to the shape of the osteocyte lacuna in sheep trabecular bone		(p55)
11:30am-11:42am	O3-6 <b>Urszula T. Iwaniec</b> : Housing mice at room temperature results in premature bone loss : implications for the mouse as a model of osteoporosis		(p56)
12:00pm-1:00pm	Luncheon Seminar Speaker : <b>Norio Amizuka</b> ( <i>Takachiho A</i> ) (p31) Morphological examination on anabolic effects of intermittent administration of PTH in bone Sponsored by Asahi Kasei Corporation.		
	Luncheon Seminar Speaker : <b>Noriaki Yamamoto</b> ( <i>Takachiho B</i> ) (p32) Bone histomorphometry in orthopedic clinical practice Sponsored by Pfizer Inc.		
1:00pm-2:00pm	Poster Presentation 1-A Chair : <b>Noriaki Yamamoto</b> ( <i>Tenku A</i> )		
1:10pm-1:16pm	P1-1 <b>Eunji Kim</b> : Alveolar bone healing after the removal of temporary anchorage devices		(p65)
1:16pm-1:22pm	P1-2 <b>Nam Cong Nhat Huynh</b> : Inhibition of histone deacetylases enhances the osteogenic differentiation of human periodontal ligament cells		(p66)
1:22pm-1:28pm	P1-3 <b>Igor Zakharov</b> : Principles of selection methods of radiation diagnosis of postmenopausal osteoporosis		(p67)

1:28pm-1:34pm	P1-4	<b>Makiri Kawasaki</b> : TGF-beta impairs cilia morphology via suppression of Ifit88 expression in chondrocytic ATDC5 cells (p68)
1:34pm-1:40pm	P1-5	<b>Takuya Notomi</b> : Membrane depolarization regulates intracellular RANKL transport in non-excitable osteoblasts (p69)
1:40pm-1:46pm	P1-6	<b>Sakie Katsumura</b> : Poldip2 is expressed in osteoblasts and its expression is enhanced by osteogenic differentiation medium containing beta glycerophosphate and ascorbic acid or BMP (p70)

Poster Presentation 1-B Chair : **Sadakazu Ejiri**

1:10pm-1:16pm	P1-7	<b>Maureen Watson</b> : Bone regeneration is increased with local application of lactoferrin in critical-sized rat calvarial defects (p71)
1:16pm-1:22pm	P1-8	<b>Yayoi Izu</b> : Collagens vi and xii form complexes mediating osteoblast interaction during osteogenesis (p72)
1:22pm-1:28pm	P1-9	<b>Tomoki Uehara</b> : A rankl-binding peptide accelerates BMP-induced bone regeneration in murine maxilla by subperiosteal injections (p73)
1:28pm-1:34pm	P1-10	<b>Chantida Pawaputanonna Mahasarakham</b> : BMP-2 induction of LGR4 expression in osteoblastic MC3T3-E1 cells (p74)
1:34pm-1:40pm	P1-11	<b>Urszula T. Iwaniec</b> : Paradoxical effects of partial leptin deficiency on bone in growing female mice (p75)
1:40pm-1:46pm	P1-12	<b>Koji Mineta</b> : Osteocytes in primary cultures express higher levels of $\beta$ 2-adrenergic receptor mRNA while MLOY4 cells exhibit culture period dependent regulation of the expression levels (p76)

---

2:00pm-5:00pm	<b>Session 4</b> Bone Impairment and Clinical Bases ( <i>Takachiho A</i> ) Chairs : <b>Sarah Dallas, Naoto Endo</b>	
2:00pm-3:00pm	• <b>Robert Recker</b> : Clinical management of osteoporosis : new options	(p14)
3:00pm-4:00pm	• <b>Yoichi Ezura</b> : Genetic and molecular bases of osteolytic/osteoporotic disorders	(p15)
4:00pm-5:00pm	• <b>Matthew Warman</b> : Rapid and reproducible ex vivo imaging of mouse articular cartilage using confocal microscopy	(p16)

---

5:00pm-6:00pm	Evening Seminar Speaker : <b>Jack Martin</b> ( <i>Takachiho A</i> ) (p37) Anabolic therapy for the skeleton with PTH – now and the future Sponsored by Eli Lilly Japan K.K.
6:10pm-	Transportation to International Evening Venue. Hinode Pier in Tokyo Bay
7:00pm-9:30pm	<b>【International Evening】</b> Symphony Cruise Dinner
9:30pm-10:00pm	Transportation back to Garden Palace Hotel

**2015.4.29 Wednesday**

8:30am-10:30am	<b>Session 5</b> Instability and Skeletal Diseases ( <i>Takachiho A</i> ) Chairs : <b>Le Duong, Ralph Muller</b>	
8:30am-9:30am	• <b>Naoto Endo</b> : AFF: clinical and histological features of atypical subtrochanteric and diaphyseal femoral fracture	(p17)
9:30am-10:30am	• <b>Jang-Soo Chun</b> : Regulation of the catabolic cascade in osteoarthritis by the zinc·ZIP8·MTF1 axis	(p18)
10:30am-11:45am	Oral Presentation 4 Chairs : <b>Watson Maureen, Mika Ikegame</b> ( <i>Takachiho A</i> )	
10:30am-10:42am	O4-1 <b>Jean-Paul Roux</b> : Texture analysis improvement in cortical evaluation : influence of osteophyte in femoral neck in osteoarthritis	(p57)
10:42am-10:54am	O4-2 <b>Miyuki Takasu</b> : Accuracy of clinical computed tomography for measurement of bone quality : a study in cadavers	(p58)
10:54am-11:06am	O4-3 <b>Mika Ikegame</b> : Melatonin suppresses the microgravity-induced activation of osteoclasts in cultured goldfish scale	(p59)
11:06am-11:18am	O4-4 <b>Michael Dray</b> : Histomorphometric analysis of bone to assess safety and mechanical performance of low dose fluoride	(p60)
11:18am-11:30am	O4-5 <b>Hitoshi Amano</b> : Craniofacial anomalies in cartilage calcification insufficient (CCI) rat	(p61)
11:30am-11:42am	O4-6 <b>Yasuhiro Sawada</b> : Temporal association of tensin 1 and p130Cas at focal adhesions links actin inward flux to cell migration	(p62)
12:00pm-1:00pm	Luncheon Seminar Speakers ( <i>Takachiho A</i> ) <b>Masako Ito</b> Imaging analysis of the effects of denosumab on bone structural properties <b>Sakae Tanaka</b> Denosumab for the treatment of osteoporosis Sponsored by DAIICHI SANKYO COMPANY, LIMITED.	(p33-34)
	Luncheon Seminar Speaker : <b>Robert Recker</b> ( <i>Takachiho B</i> ) Bone microarchitecture after alendronate treatment of osteoporotic women Sponsored by MSD K.K. a subsidiary of Merck & Co., Inc.	(p35)
1:00pm-2:00pm	Poster Presentation 2-A Chair : <b>Takashi Teramoto</b> ( <i>Tenku A</i> )	
1:10pm-1:16pm	P2-1 <b>Mari Sato</b> : Potential role of osteocyte in the fracture healing: comparison of fishes with and without osteocytes	(p77)
1:16pm-1:22pm	P2-2 <b>Tadayoshi Hayata</b> : Dullard/Ctdnep1 regulates endochondral ossification via suppression of TGF- $\beta$ signaling	(p78)



1:22pm-1:28pm	P2-3	<b>Huayue Chen</b> : Masticatory activity affects bone remodeling in mice	(p79)
1:28pm-1:34pm	P2-4	<b>Shuichi Moriya</b> : $\beta$ 2-adrenergic receptor expression in osteoblastic MC3T3-E1 cells is regulated by PTH	(p80)
1:34pm-1:40pm	P2-5	<b>Wataru Yano</b> : Quantification analysis of cranial bones development among primates species using geometric morphometrics method	(p81)
1:40pm-1:46pm	P2-6	<b>Wanting Lin</b> : Deletion of Pfn1 has an effect on bone formation	(p82)

Poster Presentation 2-B Chair : **Omar Omar** (*Tenku A*)

1:10pm-1:16pm	P2-7	<b>Hiroyuki Nakano</b> : A novel measurement method for the morphology of the mandibular ramus using homologous modeling	(p83)
1:16pm-1:22pm	P2-8	<b>Takayuki Yamada</b> : BMP-induced alkaline phosphatase expression in osteoblast-like MC3T3E1 cells is suppressed by $\beta$ 2 adrenergic receptor activation	(p84)
1:22pm-1:28pm	P2-9	<b>Akira Minematsu</b> : Voluntary exercise prevents deterioration of trabecular bone architecture in diabetes mellitus model rats	(p85)
1:28pm-1:34pm	P2-10	<b>Jumpei Shirakawa</b> : Morphological and dynamic analysis of migration linked to FUCCI-indicated cell cycle under the influence of PTH and mechanical flow signals	(p86)
1:34pm-1:40pm	P2-11	<b>Yasue Nishii</b> : Influence of magnet implant on tibial trabecular bone microarchitecture in ovariectomized rats	(p87)
1:40pm-1:46pm	P2-12	<b>Jumpei Shirakawa</b> : PTH-induced proliferation in osteoblasts requires ubiquitin specific peptidase 2 (Usp2)	(p88)

2:00pm-2:30pm	<b>Workshop</b> ( <i>Takachiho A</i> )		
		<b>Thomas Wronski</b> : Proper bone histomorphometry in rats	(p25)
2:30pm-3:00pm		<b>Natalie Sims</b> : Bone histomorphometry in mice : Getting it right!	(p26)

---

3:00pm-6:00pm	<b>Session 6</b> Molecular Bases for Skeletal Pathology ( <i>Takachiho A</i> )		
	Chairs : <b>Jack Martin, Jang-Soo Chun</b>		
3:00pm-4:00pm	• <b>Masaru Ishii</b> : Dynamic live imaging of bone: opening a new era with bone histodynametry		(p19)
4:00pm-5:00pm	• <b>Norio Amizuka</b> : Histological aspects on the biological function of osteocytes		(p20)
5:00pm-6:00pm	• <b>Sarah Dallas</b> : Investigating the dynamic biology of osteocytes and bone extracellular matrix assembly using live cell imaging approaches		(p21)

---

6:00pm	Award Ceremony & Closing Remark
6:10pm	Adjourn

# Keynote Lecture

---



# How concepts of bone remodelling influence therapeutic development in osteoporosis



**T. John Martin**

St Vincent's Institute of Medical Research ;  
University of Melbourne Department of Medicine

Remodelling of bone takes place throughout life asynchronously in “basic multicellular units” (BMUs) throughout the skeleton, providing the mechanism for repair of micro-damage, removal of old bone, and adaptation to mechanical stress. Essential to remodelling is that at each BMU, equal volumes of bone are removed by osteoclasts and replaced by osteoblasts. Within any individual BMU the volume of bone replaced by formation is approximately equal to that removed by resorption, a mechanism referred to as “coupling”.

All approaches to prevention and treatment of osteoporosis are underpinned by the cellular and molecular control of the above events. Antiresorptives (bisphosphonates, anti-RANKL, estrogen, SERMs) reduce the rate of remodelling, either by inhibiting osteoclast formation or activity, hastening their death, or combinations of these.

With all of these drugs, inhibition of resorption is inevitably accompanied by inhibited bone formation within the BMUs, because of the coupling of the two processes. With increased understanding of coupling, attempts are being made to develop drugs that inhibit the volume of bone resorbed by each BMU and increasing the volume of bone formed by each BMU – in other words uncoupling bone formation from resorption. The first of these, using a cathepsin K inhibitor, arose from the finding that genetic blockade of cathepsin K resulted in decreased bone resorption without decline in formation. Preclinical studies indicated that cathepsin K null osteoclasts that had diminished resorptive capacity, were able to produce activity that promoted bone formation – in that case sphingosine-1-phosphate, one of a number of candidate coupling factors that are the subject of much current interest, and these will be discussed in depth.

Anabolic treatment with PTH increases the number of active BMUs upon intracortical, endocortical and trabecular surfaces and deposits new osteoid. PTH promotes differentiation of committed osteoblast precursors, activation of osteoclasts that produce coupling activities, promotes survival of osteoblasts and osteocytes, and inhibits sclerostin production by osteocytes. The possible involvement of local coupling activities in the anabolic action of PTH is of much interest. PTH treatment results in an increased amount of bone which is at first inadequately mineralized, so its enhancement of BMD is on an entirely different basis from the increase with anti-resorptive treatment.

Antibody against sclerostin has proven effective in preclinical and current clinical studies, showing clear evidence of increased bone formation. Anti-sclerostin treatment was associated with a transitory increase in formation marker PINP, that decreased to control levels, whereas the resorption marker, CTX, declined rapidly and remained so. The reason for the decrease in bone formation marker after an initial rise is unknown. The decreased resorption marker might be explained by a change in the osteoblast lineage population as a result of profoundly increased bone formation, with lesser availability of cells that stimulate RANKL production and therefore osteoclasts. These aspects of anti-sclerostin action draw attention to the fact that the mechanisms involved in sclerostin blockade are new to us. In rodents and non-human primates the tissue level mechanism by which anti-sclerostin increases bone is predominantly through quiescent surfaces – thus a modelling effect.

The intercellular communication mechanisms provide the challenges that bone presents to drug development. There are specific ways in which current and prospective anti – resorptive drugs differ from one another in their actions. There is a special need for effective, safe stimulators of bone formation, to provide for those who have undergone substantial bone loss. Exciting possibilities of new anabolic therapies are evident, the result of new insights emerging through mouse and human genetics



## **Main Sessions**

---



# New imaging techniques in the diagnosis of bone diseases



**Thomas M. Link, MD, PhD**

Department of Radiology and Biomedical Imaging,  
UCSF, San Francisco, CA, USA

Standard imaging techniques to quantitatively assess metabolic bone diseases include Dual X-ray Absorptiometry –DXA- and Quantitative Computed Tomography –QCT-, but it is well-known that these technologies to measure bone mineral density –BMD- have limitations in predicting fracture risk. To improve prediction of fracture risk the FRAX score was developed, allowing improved assessment of hip and major osteoporotic fracture risk by including BMD and clinical risk factors.

BMD, however, only provides information on bone mass but bone strength is also governed by the architecture of the trabecular and cortical bone. This prompted the Bone Quality Initiative by the National Institutes of Health approximately a decade ago and a number of new technologies have been investigated and used in clinical studies since then. Among the most promising candidates for measuring bone quality are high resolution peripheral QCT –HR-pQCT-, high resolution Magnetic Resonance Imaging –MRI-, MR Spectroscopy and QCT with finite element analysis:

1. HR-pQCT: HR-pQCT was developed for imaging of trabecular and cortical bone architecture of the distal radius and tibia. The HR-pQCT system is produced by a single manufacturer (XtremeCT, Scanco Medical AG, Brüttisellen, Switzerland) and has a substantially higher spatial resolution compared to standard cross-sectional imaging techniques. The reconstructed voxel size is 82  $\mu\text{m}$  for the standard patient HR-pQCT protocol and newer generation HR-pQCT systems have a voxel size down to 41  $\mu\text{m}$ . The effective radiation dose is low with <3 microSv. The system allows acquisition of BMD, trabecular and cortical bone architecture as well as finite element assessment. Previous clinical studies have shown promising results in differentiating postmenopausal females and older men with and without fragility fractures and in monitoring therapeutic interventions.
2. High Resolution MRI: High resolution MRI can be used for the distal radius, tibia, knee and proximal femur. With higher field strength (3 and 7 Tesla) excellent visualization of the proximal femur trabecular bone architecture has been achieved allowing finite element assessment. Previous studies have shown the technique's potential in differentiating patients with and without osteoporotic fractures also in those patients that do not differ by BMD.
3. MR Spectroscopy: Proton magnetic resonance spectroscopy allows to measure bone marrow fat non-invasively and previous studies have shown that bone marrow fat increases with decreasing BMD and is significantly elevated in postmenopausal females and older men. This technology may in particular allow to assess and monitor metabolic diseases such as Type 2 diabetes that have an increased risk of fragility fractures.
4. QCT with finite element analysis: Standard CT can be used to derive bone strength data through finite element modeling and this has been shown to provide improved monitoring of treatment effects compared to DXA and greater sensitivity in fracture risk assessment at the proximal femur and lumbar spine.

Also some additional technologies have been established and optimized which include Quantitative Ultrasound of Bone, Positron Emission Tomography and Texture analysis of DXA spine images (Trabecular Bone Score).

In summary in the last decade a number of new imaging technologies to measure trabecular bone structure and quality have been established that, though currently used mostly for research purposes, have shown to provide additional information beyond BMD in characterizing fracture risk and monitoring therapy.



## Targeting cathepsin k for the treatment of osteoporosis



**Le T. Duong**

Bone Biology, Merck Research Laboratories,  
West Point, Pennsylvania, PA, USA

Bone resorption requires cellular secretion of acid for dissolution of mineral as well as enzymes for degradation of collagen. The lysosomal cysteine protease cathepsin K (CatK), one of the most active collagenases, is responsible for degradation of bone matrix proteins. CatK is predominantly but not exclusively expressed by osteoclasts. Loss-of-function mutations in the CatK gene lead to pycnodysostosis, a rare autosomal recessive disorder in humans associated with osteosclerosis with increased risk of non-traumatic fractures, short stature, acro-osteolysis and skull deformities. CatK gene deletion in mice results in high bone mass phenotype due to defective osteoclastic resorption activity. However, the number of osteoclasts, osteoblasts and the bone formation rate (BFR) are all elevated in CatK knock-out mice. Several small molecular weight orally available inhibitors of CatK with varied selectivity profiles toward other human cathepsins have advanced into clinical development. Odanacatib (ODN) is a selective and reversible CatK inhibitor currently in Phase III for the treatment of postmenopausal osteoporosis. This inhibitor has been shown to reduce bone resorption efficiency without impairing osteoclast differentiation or survival in vitro. Daily administration of ODN clearly increases spine and hip bone mineral density (BMD) in ovariectomized (OVX) skeletally mature rabbits and monkeys. In rabbits, ODN reduces bone resorption while allowing bone remodeling as determined by BFR to continue in trabecular and endocortical bones. In monkeys, ODN reduces remodeling-based bone formation, while dose-dependently enhancing modeling-based bone formation in endocortical and periosteal femoral surfaces, leading to significantly increased cortical thickness and improved bone strength. In a phase II clinical trial extended over 5-years, postmenopausal women with osteoporosis receiving ODN 50mg once-weekly present a sustained reduction of bone resorption markers (NTx), whereas the bone formation markers (PINP) are modestly reduced and demonstrate an early return toward baseline. Consequently, areal BMD of spine and total hip increased continuously up to 5 years. Consistent with the mechanism of CatK inhibition observed from preclinical studies, trabecular mineralizing surface and BFR in transilial biopsies from patients on ODN are not different from those on placebo. After treatment for 2-years, hip QCT and radius/tibia HR-pQCT further show a gain of trabecular and cortical vBMD, and modest but significant improvement of cortical thickness at these sites. On the other hand, following discontinuation of ODN after 2-years of therapy, bone mass in these subjects reverses back to baseline within a year. The ODN fracture prevention clinical trial included ~16,000 PMOP for 3 years, with ~8000 of them continuing on in a 5-year extension with maintained randomization. ODN 50mg demonstrated significant reduction of vertebral, non-vertebral and hip fractures. In summary, the CatK inhibitor ODN has been demonstrated to be an effective therapy for the treatment of osteoporosis via a molecular mechanism distinct from the standard antiresorptives.

## Cell communication in osteoimmunology



**Hiroshi Takayanagi**

Department of Immunology, Graduate School of Medicine and Faculty of Medicine  
The University of Tokyo, Japan,

Bone cells and hematopoietic cells share the same microenvironments in the bone marrow, communicating through various factors. Osteoblasts, osteoclasts and osteocytes are not only degrading or forming bone but may have distinct roles in the immune regulation. However, the molecules involved in the cell communication in the bone marrow are poorly identified. IGF-1 and TGF- $\beta$  are among the classical coupling factors important in the transition phase. OPG, RANKL and sclerostin are important modulators of bone remodeling. Osteocytes are the critical source of these factors, suggesting that osteocytes regulate bone remodeling in response to mechanical stress utilizing these factors. Recent studies suggest that semaphorins play an essential role in the regulation of bone remodeling but they function in the distinct bone remodeling phases. I will discuss the recent progress in the field of osteoimmunology focusing on the molecules controlling the cell communication in the bone marrow as well as T cell interaction with osteoclasts in autoimmune arthritis.

## Effects of sclerostin antibody on different bone surfaces with shorter- and longer-term treatment



**Hua Zhu (David) Ke**

Bone Research, New Medicines Therapeutics,  
UCB Pharma, Slough, England.

Wnt/beta-catenin signaling plays an important role in bone formation and resorption. Sclerostin (Scl) binds to co-receptors Lrp5/6 and inhibits wnt/beta-catenin signaling in osteoblast lineage, results in decreased bone formation. Inactivation of sclerostin leads to substantially increased bone mass in humans and in genetically manipulated animals. A series of shorter-term preclinical studies demonstrated that monoclonal antibody targeting sclerostin (Scl-Ab) increases bone formation on all bone surfaces, decreases bone resorption on trabecular and endocortical surface, and increases BMD and bone strength in multiple skeletal sites in animal models of osteoporosis. In shorter-term (4-6 weeks) studies, it has been showed that increased bone formation induced by Scl-Ab was primary stemmed from activating bone formation on the quiescent bone surface (modeling-based bone formation) and prolong the formation of new bone on pre-existing bone remodeling surface in animal models. Scl-Ab treatment in OVX rats decreased osteoclastogenesis in bone marrow culture in vitro, and decreased osteoclast number and surface in vivo, suggesting that Scl-Ab treatment decreases bone resorption. In a longer-term (26 weeks) OVX rat study, despite continuously increased BMD and bone strength, trabecular and periosteal bone formation temporally increased and gradually returned to control level, while endocortical bone formation remained significantly elevated at end of the study. However, in this longer-term study, strong correlation between bone mass and bone strength was remained at the end of the study, indicating normal quality of bone was induced by longer-term Scl-Ab treatment, as observed from those shorter-term studies. Similarly, a humanized Scl-Ab, romosozumab, has been shown to simultaneously increase bone formation markers and decrease bone resorption markers, leading to a significant increase in BMD giving by monthly s.c. injection for 12 months. In this clinical study, serum bone formation markers were temporally increased and returned to baseline within 6 to 12 months while serum bone resorption markers remained decreased throughout the 12 months duration. The mechanism for time-dependent changes in bone formation and bone resorption on different bone surfaces with longer-term Scl-Ab treatment is not completely understood. Local bone mechanical signal and other feedback pathways may be involved. These data may indicate that the early bone gains with Scl-Ab treatment were accompanied by increased cortical and trabecular bone formation and reduced osteoclast activity, whereas later gains were attributed to residual endocortical and trabecular osteoblast stimulation and persistently low osteoclast activity.

## Cartilage and meniscus regeneration by synovial stem cells : from bench to clinic



**Ichiro Sekiya**

Center for Stem Cell and Regenerative Medicine  
Tokyo Medical and Dental University  
Tokyo, Japan

According to our previous studies, the number of mesenchymal stem cells (MSCs) in synovial fluid increase in knees with anterior cruciate ligament injury (Rheumatology 2008), meniscus injury (Clin Orthop Relat Res 2014), and osteoarthritis (J Orthop Res 2011). The morphology and gene profiles in synovial fluid MSCs were more similar to those in synovial MSCs than in bone marrow MSCs. Principal component analysis of gene profiles for various mesenchymal tissues-derived MSCs and chondrocytes demonstrated that MSCs from intraarticular tissues and chondrocytes were closer to each other than MSCs from extraarticular tissues (J Orthop Res 2008). Synovium may be a reservoir for MSCs to contribute to the intraarticular tissue repair. After intraarticular tissues, such as cartilage, meniscus, and ligament are injured, MSCs may be mobilized from synovium to synovial fluid, adhere to the injured site, and contribute to the repair. However, the number of MSCs is limited, therefore, the injured tissues cannot be healed in the natural course. Transplantation of enough number of synovial MSCs to the injured tissues will promote intraarticular tissue healing.

MSCs are attractive cell source for cartilage and meniscus regeneration. Our in vitro and in vivo chondrogenic assay demonstrated that synovial and bone marrow MSCs had a higher chondrogenic ability than adipose and muscle MSCs (Arthritis Rheum 2005, Cell Tissue Res 2007, Cell Tissue Res 2008). Human synovial MSCs expanded more in human serum than bone marrow MSCs (Arthritis Rheum 2008). In rat, rabbit, and pig studies, transplantation of synovial MSCs promoted cartilage and meniscus regeneration (Stem Cells 2007, Stem Cells 2009, Cytotherapy 2012, Osteoarthritis Cartilage 2012, J Bone Joint Surg Am 2012, Biochem Biophys Res Commun 2013). Also, transplantation of synovial MSCs promoted healing after meniscal repair with induction of synovium into the longitudinal tear in the avascular zone of meniscus in pigs (Osteoarthritis Cartilage 2015).

Current cell therapy for cartilage and meniscus regeneration requires invasive procedures. We have developed a novel implantation procedure with synovial MSCs. Cartilage or meniscus defect is filled with synovial MSC suspension for 10 minutes. According to our in vitro and in vivo studies, more than 60% cells adhered to the defect, and promoted cartilage and meniscus regeneration (Arthritis Res Ther 2008, J Orthop Res 2013).

Transplantation of MSCs is one possible strategy to achieve articular cartilage repair. We investigated whether transplantation of synovial MSCs regenerated cartilage defect. Patients with a symptomatic single cartilage lesion of the femoral condyle were indicated and 10 patients were enrolled in this study. Our method has such advantages that no periosteal coverage or scaffold were required and that transplantation is possible arthroscopically. For this small, initial case series, transplantation of synovial MSCs improved clinical outcomes (Clin Orthop Relat Res 2015). We are also trying to regenerate osteoarthritis of the knee with osteotomy or meniscus centralization (Arthrosc Tech 2012) by using synovial MSCs. We have started a clinical trial using transplantation of synovial MSCs to promote healing after meniscal suture repair.

## Assessment of bone structure in relation to biomechanical properties



**Masako Ito**

Center for Gender Equality,  
Nagasaki University  
Nagasaki, Japan

With the development of noninvasive imaging techniques such as computed tomography (CT), micro-CT, and high resolution peripheral quantitative CT (HR-pQCT), imaging of the bone architecture provides important information about age- and disease-related changes in bone microstructure and estimates of bone strength.

The pathogenesis of osteoporosis has been focused on dynamic trabecular bone loss due to menopause, which is strongly related to vertebral fractures, on the other hand relatively less attention given to non-vertebral fractures and cortical bone loss. However, since 80% of fractures are non-vertebral and occur at predominantly cortical sites. Recently, the researches have investigated the deterioration of microstructure of the cortical bone in relation to the risk of non-vertebral fracture, furthermore in relation to the diseases associated with adult lifestyle habits (type 2 diabetes mellitus, and chronic kidney disease), and to the effect of osteoporotic agents. In Japan, it is difficult to fulfill a clinical trial large enough to obtain high-level evidence to reduce the risk of hip fracture. So that, useful methods are required to evaluate the effect of agents on bone biomechanical properties, especially the effect of preventing femoral fracture.

In this lecture, I would like to review the articles of the treatment effects on the microarchitecture of the trabecular and cortical bone, and bone geometry.

# Hierarchical imaging of bone failure



**Ralph Müller**

Institute for Biomechanics,  
ETH Zurich, Zurich, Switzerland

Aging is on the verge of a new era. Humans are approaching old age in unprecedented numbers as a result of large baby boom cohorts born in the middle of the 20th century that are approaching traditional retirement ages. Increases in the prevalence of age-related disease, frailty, and disability are visible signs of the potential costs and social burdens arising from this historic demographic shift. One disease that will be affected dramatically by this shift will be osteoporosis and with it there will be marked increase in osteoporotic bone fractures. With recent advances in molecular medicine and disease treatment in osteoporosis, the development of diagnostic and monitoring tools must therefore be in the focus of aging and health-related research in order to allow early detection and control of the disease.

A number of new microstructural imaging modalities have been put forward over the last two decades allowing quantification with high precision and accuracy. Biomedical imaging technology such as MRI or CT is readily available, but few attempts have been made to expand the capabilities of these systems by integrating quantitative analysis tools as an integrative part of biomedical information technology and by exploring structure–function relationships in a hierarchical fashion over the different length scales. Nevertheless, such quantitative endpoints have become an important factor for success in basic research and the development of novel therapeutic strategies in biomedicine and clinical practice. Where the 20th century was the century of image formation, success in the 21st century will be judged by our ability to extract meaningful quantitative information from these images. Micro- and nano-computed tomography is key to these developments being an approach to image and quantify trabecular bone in three dimensions and providing multi-scale biological imaging capabilities with isotropic resolutions ranging from a few millimeter (clinical CT), to a few micrometers (microCT) down to one hundred nanometers (nanoCT).

As part of the presentation, new strategies for advanced hierarchical quantification of bone and their structure function relationship will be presented. The focus will be on hierarchical micro- and nano-imaging as well as image-guided biomechanics. At the microscopic level, bone microstructure is known to influence bone strength and failure mechanisms significantly. Biomechanical imaging allows direct time-lapsed visualization and computation of local displacements and strains for better quantification of bone fracture initiation and progression. Recent introduction of highly brilliant synchrotron radiation X-ray sources now permits to explore bone on the nanoscopic level to uncover the ultrastructure of bone including vascular and cellular structures and to investigate their role in the development of bone failure.

In conclusion, hierarchical microimaging is well suited to investigate quantitative structure function relationships and failure in both trabecular and cortical bone. The approach can help improve predictions of bone failure, clarify the pathophysiology of skeletal diseases, and define the response to therapy. We expect these findings to improve our understanding of bone failure and with that to also allow improved quality control and more successful outcomes in studies dealing with pharmacological treatment of bone.

## Clinical management of osteoporosis : new options



**Robert R. Recker, M.D., M.A.C.P., F.A.C.E.**

Head of Creighton University's Osteoporosis Research Center  
Omaha, NE, USA

Osteoporosis became recognized in the early 20<sup>th</sup> century as skeletal weakness due to loss of bone mass. In 1947 Fuller Albright recognized that bone removal and replacement (bone remodeling) occurred throughout life, and that loss of estrogen in women at menopause resulted in increased bone removal without a similar increase in bone formation. This resulted in a net loss of bone tissue at menopause which continued as time passed, and resulted in risk of major fractures. Thus, for most of the past 60 years osteoporosis was considered a disease of low bone mass and weakened skeleton. This idea was strengthened by the invention of dual photon-absorptiometry (DPA) in the late 70s followed by dual x-ray absorptiometry (DXA) in the 80s. With these inventions we were able to measure bone mass, and express the results as a two-dimensional density. Soon thereafter epidemiologic data became available which showed that fracture risk could be indexed to the T-score (DXA), which was the Standard Deviation of bone density in a healthy population in their 20s. We then began to focus on ways to increase bone mass, and/or to stop bone loss. The first successful intervention to stop bone loss was hormone (estrogen) replacement therapy which became widely used in the 1940s and 1950s in the United States and Europe, even in the absence of solid anti-fracture efficacy data.

In ~1995 the first bisphosphonate that slowed bone remodeling, slowed bone loss and reduced the risk of fracture became available. This was Alendronate the first effective anti-fracture treatment for osteoporosis. Subsequently, three other bisphosphonates were approved for use in the United States; Actonel, Ibandronate, and Zoledronic acid. At nearly the same time a selective estrogen receptor modulator, raloxifene, became available. All of these treatments reduce the risk of fracture by about 50%. They have been, and still are, used extensively throughout the world. However the ideal medical “cure” of osteoporosis would need to reduce the risk of fracture to perhaps 10 or 15%. It is unlikely that the risk of fracture can be completely eliminated; however, recent discoveries hold some promise that we might be able to reduce the risk of fracture in osteoporosis patients by 75 to 95%. This arises from the discovery of an autosomal dominant mutation in LRP5, (Lipoprotein-Related Receptor Protein 5). LRP5 activates the wnt signaling pathway that when linked with its co-receptor, Secreted Frizzled Protein (SFP), signals bone forming cells to form bone. The affected individuals in the family in which this mutation was discovered had T-scores of +5 or higher. The 19 affected individuals in that family had never had a fracture in lifespans ranging from childhood to age 86. The wnt pathway has at least two inhibitors that bind LRP5, sclerostin and DKK-1. Very recently an antibody to sclerostin has been formulated, and is being tested by two pharmaceutical companies. Preliminary results in humans show very remarkable gains in bone density of more than 15%, i.e., a more than one standard deviation increase in the T score. Soon we may be able to offer our osteoporosis patients something resembling a “cure”.

## Genetic and molecular bases of osteolytic/osteoporotic disorders



**Yoichi Ezura, Masaki Noda**

Department of Molecular Pharmacology  
Medical Research Institute  
Tokyo Medical and Dental University  
Tokyo, Japan

Osteolysis or regional bone loss is a serious complication in patients in orthopedics, dentistry, or rheumatology as the lesions around the implants, peri-articular erosion in chronic arthritis, and osteomyelitis or infectious bone diseases. Inflammatory responses for pathogens, materials, and autoantigens may be the triggers, whereas the metastatic or primary bone tumors could be the cause. Shared pathogenic mechanisms could be involved in osteoporosis (OP) in some extent, because OP also represents rapid bone loss in some instances. Indeed, genetic association studies for OP have partially implicated such possibilities. Here, I would like to discuss about such possibilities from three aspects of the molecular and genetic understandings of the inherited disorders associated with osteolysis.

First, a number of inherited human conditions are known to be caused by a defect in osteoclasts. In general, mutations leading to ineffective osteoclasts cause osteopetrosis, whereas mutations leading to osteoclast activation or production may cause osteolysis. For example, dominant negative mutations in osteoclast inhibiting factor, v-maf musculoaponeurotic fibrosarcoma oncogene ortholog B gene (MAFB) causes multicentric carpo-tarsal osteolysis (MCTO). Constitutive active mutations of the receptor activator of the nuclear kappa B gene (RANK) cause familial expansile osteolysis (FEO). Therefore, the repeatedly detected strong association of genetic variations in RANK locus, as well as RANKL and OPG loci by genome-wide association studies (GWAS) for low bone mineral density (BMD) in general population implies that acceleration of osteoclastogenesis may be involved in OP pathogenesis in part. The association of RANK polymorphisms in the 3'-untranslated region, for which we have shown a binding of the deadenylation complex forming Cnot3 by mouse study, may indicate the involvement of regulation in mRNA stability.

Secondly, the osteolysis could also be the result of accelerated inflammation. Cherubism is an autosomal dominant hereditary disorder characteristically presented by osteolytic lesions in facial bones of children accompanied by ballooning appearance. The disease is known to be caused by constitutive active mutations of the SH3-domain binding protein 2 gene (SH3BP2). The mutations results in enhanced TNF- $\alpha$  receptor and TLRs signaling by getting rid of the regulation through poly(ADP-ribose) polymerizing enzyme tankyrase, but the pathogenesis and the mechanisms explaining an interesting feature of this disease, the remission of the osteolysis after puberty is not fully understood yet. The accelerated inflammation is also the case in familial cold auto-inflammatory syndrome (FCAS1), caused by mutations in a gene encoding inflammasome protein Cryopyrin (also named as NLRP3). Osteolytic lesions in the leg are prevalent in the FCAS patients. We assume the accelerated inflammation could be involved in susceptibility for many other disorders including OP, as well as osteolysis causing rheumatoid arthritis and osteomyelitis.

Lastly, several osteolytic disorders are paradoxical or mysterious on its pathogenesis. Pycnodysostosis is caused by homozygous mutations in cathepsin K, and its major bone phenotype is systemic osteosclerosis. However, the patients sometimes represent paradoxical osteolysis in fingertips (acro-osteolysis). The acro-osteolysis is a symptom observed in several diseases. Sometimes it is explained by peripheral circulation and/or neurotic disorders, but basically its pathogenesis is not understood well. Paradoxical osteolysis is also the case in multicentric osteolysis nodulosis and arthropathy (MONA) that is caused by loss of function mutations in MMP2 gene, encoding a bone collagen degrading enzyme. The Nasu-Hakola disease (NHD, also known as polycystic lipomembranous osteodysplasia with sclerosing leukoencephalopathy; PLOSL) is also mysterious because the causative homozygous mutations are found in genes encoding transmembrane receptor molecules TREM2 and DAP12 that are known to be essential for osteoclastogenesis. Clarification of the mechanisms for such conditions is needed.



## **Rapid and reproducible ex vivo imaging of mouse articular cartilage using confocal microscopy.**



**Matthew L. Warman, M.D.**

Investigator, Howard Hughes Medical Institute

Professor of Genetics and Orthopaedic Surgery

Boston Children's Hospital and Harvard Medical School Boston, MA, USA

Mice are commonly used to study biologic pathways involved in articular cartilage development, homeostasis, and degeneration. However, the small size of articular cartilage surfaces in mice makes it challenging to evaluate the effects of genetic or environmental perturbations on cartilage structure and function. Current methods for evaluating mouse cartilage are time-consuming, labor intensive, and dependent upon the laboratory's expertise in obtaining appropriate images. I will describe a 3-D confocal microscope imaging technique Dr. Minjie Zhang has been developing in my laboratory that is easily applied to different mouse articular cartilage surfaces. This technique can rapidly and reliably measure chondrocyte number and distribution. It can also identify chondrocytes that incorporated EdU in vivo, an indicator of cell division, and chondrocytes that express cell-type-specific fluorescent proteins. I will show the utility of this imaging method in experiments we designed to determine if chondrocyte death causes cartilage surface damage and, conversely, if cartilage surface damage causes chondrocyte death. Confocal imaging offers advantages over other methods of evaluating mouse cartilage, in terms of the speed of data acquisition, the sample sizes needed to obtain statistically meaningful results, and the ability to provide new insights about articular cartilage biology.

## AFF: clinical and histological features of atypical subtrochanteric and diaphyseal femoral fracture



**Naoto Endo**

Division of Orthopedic Surgery, Niigata University Graduate School of Medical and Dental Sciences, Niigata, Japan

AFF, atypical subtrochanteric and diaphyseal femoral fracture have been reported in relation to SSBT (severely suppressed bone turnover) due to bisphosphonate treatment. Recently several cases with AFFs in denosmab treatment also were reported. This fracture site is atypical, such as subtrochanteric or diaphyseal area of femoral shaft, whereas osteoporosis-related hip fractures are located in the neck or trochanteric region of femur in aged population. Both fractures most often occur with minimal trauma. Since AFFs occur at very low rate, data on these patients with AFFs are limited. The mechanism and risk factors associated with AFFs are still unknown.

1. According to ASBMR Task Force 2014 (J Bone Miner Res 2014;29:1-23), these patients with AFF experienced thigh pain before fracture and had cortical thickening of femur. This is the unusual radiographic features, suggesting periosteal and/or endosteal stress reaction. This is the critical point to distinguish AFFs from osteoporotic fractures.
2. The data on the patients with AFFs in Japan reported from Japanese Orthopedic Association. More than 300 cases were reported in each year in 2010 – 2013.
3. Clinical and histological features in patients with AFFs reported by Niigata University showed that histomorphometric analysis indicated low ~ normal bone-turnover in patients with AFFs.
4. Treatment: Since AFFs are difficult to unite in most cases, surgical treatment for fracture with plate or nail and enhancement for fracture healing with bone grafting, bone-stimulating agents (teriparatide), and so on are recommended.

## Regulation of the catabolic cascade in osteoarthritis by the zinc·ZIP8·MTF1 axis



**Jang-Soo Chun**

Cell Dynamics Research Center and School of Life Sciences,  
Gwangju Institute of Science and Technology, Gwangju, Korea.

Osteoarthritis (OA), primarily characterized by cartilage degeneration, is caused by an imbalance between anabolic and catabolic factors. Here, we investigated the role of zinc ( $\text{Zn}^{2+}$ ) homeostasis,  $\text{Zn}^{2+}$  transporters, and  $\text{Zn}^{2+}$ -dependent transcription factors in OA pathogenesis. Among  $\text{Zn}^{2+}$  transporters, the  $\text{Zn}^{2+}$  importer ZIP8 was specifically upregulated in OA cartilage of humans and mice, resulting in increased levels of intracellular  $\text{Zn}^{2+}$  in chondrocytes. ZIP8-mediated  $\text{Zn}^{2+}$  influx upregulated the expression of matrix-degrading enzymes (MMP3, MMP9, MMP12, MMP13, and ADAMTS5) in chondrocytes. Ectopic expression of ZIP8 in mouse cartilage tissue caused OA cartilage destruction, whereas Zip8 knockout suppressed surgically induced OA pathogenesis, with concomitant modulation of  $\text{Zn}^{2+}$  influx and matrix-degrading enzymes. Furthermore, MTF1 was identified as an essential transcription factor in mediating  $\text{Zn}^{2+}$ /ZIP8-induced catabolic factor expression, and genetic modulation of Mtf1 in mice altered OA pathogenesis. We propose that the zinc·ZIP8·MTF1 axis is an essential catabolic regulator of OA pathogenesis.

## **Novel modes of action of anti-bone resorptive drugs revealed by intravital two-photon bone imaging technology**



**Masaru Ishii**

Department of Immunology and Cell Biology, Graduate School of Medicine and Frontier Biosciences, Osaka University, and JST, CREST  
Osaka, Japan

Intravital two-photon microscopy adopted for visualizing live bone tissues has undoubtedly revolutionized the research field of bone biology. Now that we can grasp the real mode of migration, interaction and function of different bone cell types *in vivo*, we could also dissect actual pharmacological actions of several drugs treating bone diseases. For example, we have recently identified that active vitamin D and its therapeutic analogues, whose therapeutic mechanisms had still been elusive, exerted their anti-bone resorptive activity by altering migratory behaviors of circulating monocytoïd cells, limiting the number of osteoclast precursors on the bone surfaces. Bisphosphonates and RANKL blocker were shown to have distinct properties for inhibiting osteoclastic bone destructions. These findings which could only be derived from intravital bone imaging technology enable us to deepen our understanding on current therapeutic regimens as well as to develop conceptually novel lines of treatment against bone diseases in future.

## Histological aspects on the biological function of osteocytes



**Norio Amizuka, Tomoka Hasegawa, Hiromi Hongo, Tomomaya Yamamoto**

Department of Developmental Biology of Hard Tissue, Graduate School of Dental Medicine,  
Hokkaido University  
Sapporo, Japan

Osteocytes build up functional syncytia, i.e., the osteocytic lacunar-canalicular system (OLCS). The osteocytes are connected each other by means of their cytoplasmic processes interconnected through gap junctions, which pass through narrow passageways referred to as osteocytic canaliculi. There are two possible pathways for molecular transport, one formed by the cytoplasmic processes connected by gap junctions, and the other being the pericellular space in the osteocytic canaliculi. The transport of minerals and small molecules carried through the OLCS serves as a fundament for osteocytes intimately involved in maintaining bone minerals, mechanosensing and regulating bone remodeling. In order to achieve these putative functions, a geometrically well-organized OLCS in mature bone seems to be efficiently functional. Recently, osteocyte-derived molecules, sclerostin, dentin matrix protein-1 (DMP-1), fibroblast growth factor 23 (FGF23), have been highlighted because these molecules may reflect osteocytic function responding to mechanosensing, regulation of bone remodeling and so forth. In our observations, FGF23 and sclerostin synthesis seemed to be associated with the spatial regularity of the OLCS, while DMP-1 was not related to the geometrical arrangement of OLCS.

More recently, the idea of “osteocytic osteolysis” has revisited, which is respondent to elevated concentration of parathyroid hormone (PTH) or low calcium diet, was proposed by Bélanger in 1960's. In order to clarify the occurrence of osteocytic osteolysis, we have examined osteocytes and their lacunae after the PTH administration in the tibial metaphysis and cortical bone of mice. At six hours after the PTH administration, enlarged osteocytic lacunae were observed mainly in the cortical bone, but not in the metaphysis. Transmission electron microscopy and von Kossa staining demonstrated broadly demineralized bone matrix surrounding osteocytes in the cortical bone. Intense immunoreactivity of vacuolar type H-ATPase was found in many osteocytes in the PTH-treated cortical bone, indicating that proton secreted by osteocytes might erode the surrounding bone minerals. Unlikely, the control bone without PTH administration did not reveal such histological alteration of osteocytic lacunae. In order to exclude the possible involvement of osteoclastic bone resorption after the PTH administration, we have examined OLCS in Rankl<sup>-/-</sup> mice which lack osteoclasts. As a consequent, the osteocytic lacunae were enlarged as was seen in the PTH-administered wild-type mice. Thus, it seems likely that osteocytes in cortical bone, rather in metaphysis, would participate, at least, in part, in controlling serum concentration of calcium and phosphate by responding to PTH, i.e., osteocytic osteolysis in bone.

This review will introduce our recent studies on the biological function of osteocytes.

# Investigating the dynamic biology of osteocytes and bone extracellular matrix assembly by live cell imaging approaches



**Sarah L. Dallas**

University of Missouri, Kansas City, MO, USA

Much of our understanding of skeletal biology comes from static imaging approaches, such as light and electron microscopy, combined with biochemical analysis and/or molecular genetic approaches. However, the biological processes occurring in the skeleton, such as bone development, remodeling and repair are highly dynamic events that include the dimension of time. To gain new insight into bone cell function, we have used live cell imaging techniques that enable visualization of temporal changes in living specimens, such as cells, tissues and intact animals and allow the quantitation of cellular, subcellular and tissue behavior as a function of time.

To gain insight into the process of osteocyte differentiation and embedding, we have generated transgenic mice expressing a membrane targeted GFP under control of the dentin matrix protein-1 promoter (Dmp1-memGFP mice). Live imaging in neonatal calvarial organ cultures and primary mineralizing osteoblast cultures from these mice as well as in live mice has revealed that osteocytes are highly dynamic cells. The Dmp1-memGFP transgene is switched on in a surface motile cell type prior to embedding that appears to be a non-dividing cell already committed to becoming an osteocyte. As this cell embeds and transitions to an osteocyte, it extends and retracts “exploratory dendrites”, which explore the entire area around the cell and appear to play a role in positioning/spacing of the osteocyte. Our studies have shown that the embedding and recently embedded osteocyte is highly dynamic and that its dendrites extend and contract, making transient dendritic connections between adjacent osteocytes. Osteocytes also showed deformations/undulating motions of their cell bodies within their lacunae and extensive membrane ruffling. A surprising finding was that osteocytes shed extracellular vesicles from their cell body and dendrites during embedding. These microvesicles contain a cargo of protein, mRNA and miRNA and may provide a mechanism for intercellular communication through delivery of this cargo to target cells to alter their function.

To investigate the dynamic processes of bone extracellular matrix assembly we have generated transgenic mice expressing a GFP-collagen fusion protein in which GFP replaces the N-terminal propeptide of  $\alpha 2(I)$ -collagen. Live imaging in primary osteoblasts from these mice showed that collagen assembly is a highly dynamic process involving extensive cell motions which stretched and contracted the fiber network during assembly. Upon addition of ascorbate, GFP-collagen translocated to vesicle-like structures which showed extensive intracellular movement to localized regions within the cell and appeared to be involved in the assembly process. During assembly, cells were able to physically reshape the collagen fiber network by pushing collagen outwards to generate holes resembling lacunae. Live imaging of cells from double transgenic mice expressing GFP-collagen together with a membrane TdTomato reporter enabled visualization of collagen assembly and cell membrane dynamics. Imaging of these cells seeded at low densities on wild type osteoblasts showed GFP-collagen deposition only in areas in which the cell body or cell processes had been, suggesting active placement of collagen by cells rather than diffusion of collagen away from the producer cell. Live imaging of collagen assembly in a wound healing assay showed that osteoblasts can assemble collagen “on the move”, that multiple cells contributed to the assembly of the collagen fiber network and that cells actively engaged in collagen assembly were able to divide and then resume assembly of collagen.

Together these studies are revealing the highly dynamic nature of bone cells and discovering novel aspects of osteocyte biology that were not previously appreciated. They have also shown that the bone matrix assembly process is highly dynamic, that multiple cells contribute to assembly of collagen fibers and that cells exert considerable forces on ECM fibrils during their assembly.



# **Work Shop**

---





# Proper bone histomorphometry in rats

**T.J. Wronski and J.I. Aguirre**

Department of Physiological Sciences,  
University of Florida, Gainesville, FL, USA

Bone histomorphometry is an important technique for evaluation of changes in bone structure and levels of bone formation and resorption in response to a variety of influences such as bone-active drugs, hormones, growth factors, and mechanical forces. Recommendations for proper bone histomorphometry in rats will be presented, including: 1) embedding undecalcified bone, 2) identification of osteoblasts and osteoclasts in stained histologic sections, 3) optimal regimens for fluorochrome labeling of cancellous bone in young and aged rats, 4) standardization of the region of interest for histomorphometric data collection in cancellous and cortical bone, and 5) the most important measurements of bone structure, formation, and resorption. These recommendations are intended to improve the quality of bone histomorphometry in preclinical studies of rat models.

## **Bone histomorphometry in mice: getting it right!**

**Natalie A Sims**

St. Vincent's Institute of Medical Research, University of Melbourne,  
Melbourne, Australia

Genetically altered mice are common tools used for discovery of novel pathways that regulate bone structure and bone cell function. In addition, the use of mice as models of bone and joint disease for testing pharmacological interventions is increasing because of their low cost compared to larger animals. Although information on structure can now be derived by micro-computed tomography, histomorphometry remains the best method for determining the changes in bone formation and resorption that lead to the changes in bone structure. However, differences in measurement methods, reporting of histomorphometric markers and selection of controls sometimes lead to confusion in the literature within the bone field when studies have been repeated in multiple laboratories.

This talk will focus on practical and theoretical issues of how to carry out histomorphometry on mouse models. It will consider issues such as selection of measurement sites, including methods for measuring cortical bone, the use of appropriate controls, including controls for Cre-directed genetic manipulation, and the ways that diet, genetic background, age, and sex modify bone remodelling parameters. Practical issues such as fluorochrome labelling protocols, paraffin vs plastic embedding techniques will be explored. Guidance will be given on how to report your histomorphometric data in a way that is accurate and meaningful and point out some limitations of how to measure and interpret standard histomorphometric parameters. It will also explore ways in which histomorphometric methods have been applied to more unusual features of bone structure, including analysis of growth plate dynamics, breast cancer metastasis, focal bone erosions, and the use of histomorphometric techniques for measuring immunohistochemical markers. Limitations of the mouse model compared to larger mammals will also be explored.

## **Luncheon & Evening Seminars**

---



# **Dynamic live imaging of bones : opening a new era with ‘bone histodynametry’**

**Masaru Ishii**

Osaka University Graduate School of Medicine and Frontier Biosciences, Japan,  
JST, CREST, Osaka, Japan

During the last decade, multi-photon fluorescent microscopy has launched a new trend in the field of biology. By using this advanced imaging technique we have established a new system for visualizing in situ behavior of a diversity of living cells within intact tissues and organs. Among them, we succeeded in visualizing the various dynamic phenomena within bones, a mysterious organ where various kinds of hematopoietic and immune cells are produced and functioning although poorly analyzed by conventional methodology such as histological analyses with decalcified bones. Especially we have focused on the behavior of osteoclast, a kind of specialized macrophage contributing to physiological bone remodeling as well as to bone destruction in arthritis and osteoporosis, and have been revealing novel mechanisms controlling migration and function of osteoclasts in situ. This novel ‘bone histodynametrical’ methodology is sure to, collaborating with conventional histomorphometrical analyses, contribute to opening a new era in the field of bone and mineral researches in future.

## **Locomotive syndrome –measures for increasing healthy life expectancy**

### **Kozo Nakamura**

President

National Rehabilitation Center for Persons with Disabilities

Saitama, Japan

Japan is now facing the advent of a super-aged society very rapidly. The difference between average life expectancy and healthy life expectancy is about nine years for men and twelve years for women, which is not short. The number of elderly who need nursing care service is increasing, and the increase has become an issue of great concern in our society.

The reasons for which the elderly aged 65 or older needed nursing care services include cerebrovascular disorders (21.5%), dementia (15.3%), and importantly, problems related to the locomotive organs, such as falls/fractures (10.2%) and joint disorders (10.9%). Most people recognize cerebrovascular disorders and dementia as a reason for nursing care services, but unfortunately not locomotive organ disorders.

Locomotive organ disorders hamper individuals in standing and walking. Since most elderly have plural disorders of locomotive organs, including bones, joints, cartilage, intervertebral discs, and muscles, we have to pay attention to their general walking function as well as their local symptoms.

This is a new affair in a super-aged society. We therefore need a new concept. The Japanese Orthopaedic Association (JOA) proposed locomotive syndrome in 2007. Locomotive syndrome refers to a decrease in walking function due to problems of the locomotive organs. The syndrome increases risk of requiring nursing care service.

Because gait speed and chair stand time are correlated with such risks, patients with locomotive syndrome are assessed using brief methods such as the two-step test, which involves dividing the maximum stride length by the height of the patient, and the stand-up test, which involves standing on one or both legs at different heights. The syndrome is also evaluated by “locomo-25”, the self reporting questionnaire, which consists of 25 items.

The goal of countermeasure against locomotive syndrome is to enable people to stand-up and walk independently even in old age. JOA recommends two exercises as a basic training. They are possible to do at home without any special equipment, and we have to avoid excess burden on already degenerated lumbar spine and knee joint. JOA calls this training as locomotion training, “loco-tra” for short. They are “one leg standing” and “squatting”.

This concept has been accepted and has spread quite rapidly in Japan. The syndrome has been included in National Health Promotion Movement (2013-2022).

# Morphological examination on anabolic effects of intermittent administration of PTH in bone

**Norio Amizuka**

Department of Developmental Biology of Hard Tissue, Graduate School of Dental Medicine,  
Hokkaido University  
Sapporo, Japan

In order to clarify the behavior of osteoblastic cells after intermittent PTH(1-34) treatment and to elucidate the role of osteoclasts on the mediation of PTH-driven bone anabolism, we have administered PTH intermittently to wild-type and c-fos<sup>-/-</sup> mice. Structural and kinetic parameters related to bone formation were increased in PTH-treated wild-type mice, whereas in the osteoclast-deficient c-fos<sup>-/-</sup> mice, there were no significant differences between groups. In wild-type and knockout mice, PTH administration led to significant increases in the number of preosteoblasts. Ultrastructural examinations showed two major preosteoblastic subtypes: one rich in endoplasmic reticulum (ER), the hypER cell, and other with fewer and dispersed ER, the misER cell. The latter constituted the most abundant preosteoblastic phenotype after PTH administration in the wild-type mice. In c-fos<sup>-/-</sup> mice, misER cells were present on the bone surfaces but did not seem to be actively producing bone matrix. We concluded that the absence of osteoclasts in c-fos<sup>-/-</sup> mice might hinder PTH-driven bone anabolism and that osteoclastic presence may be necessary for full osteoblastic differentiation and enhanced bone formation seen after intermittent PTH administration.

In Japan, daily and once-weekly administration of PTH(1-34), teriparatide, is approved treatments for osteoporosis. Both regimens enhance bone mineral density and bone mass in osteoporotic patients. To provide evidence of how the different intervals of PTH administration increase bone in vivo, we have examined the histology of mice femora subjected to different PTH administration intervals. Mice were randomly allocated to control or to three treatment groups (80µg/kg of PTH per dose, 80µg/kg of PTH daily, or 20µg/kg of PTH daily). For each group, PTH was injected once every other day, once daily, twice daily and four times/day during two weeks. In the 80µg/kg daily and in the 20µg/kg daily groups, more frequent PTH administration increased metaphyseal trabecular number. However, trabecular histology was different across the groups: thin metaphyseal trabeculae were common in the four times/day regimen, while the once daily PTH regimen formed thicker trabeculae. Cortical bone tended to change its compact profile into cancellous with the four times/day regimen. Higher PTH administration frequency (four times/day) showed a thick preosteoblastic cell layer and many osteoclasts, and the resultant bone matrix included scalloped cement lines that indicate osteoclastic bone resorption prior to new bone deposition. These findings suggest accelerated bone remodeling. In contrast, lower PTH administration frequency (once daily) did not induce the formation of a thick preosteoblastic cell layer, without any clear separation between the bone marrow and mature osteoblasts. These mature osteoblasts were occasionally localized atop mildly convex bone surfaces that featured smooth cement lines, identical to arrest lines. These findings suggest mini-modeling-based bone formation. Thus, it appears that higher PTH administration frequency rapidly increases bone mass by forming thin trabeculae through accelerated bone remodeling. On the other hand, lower PTH administration frequency forms thicker trabeculae not only through bone remodeling but also through mini-modeling.



## **Bone histomorphometry in orthopedic clinical practice**

**Noriaki Yamamoto, Hideaki Takahashi**

Niigata Bone Science Institute, Niigata, Japan

Department of Orthopedic Surgery, Niigata Rehabilitation Hospital, Niigata, Japan

Bone histomorphometry is a method for direct examination of bone metabolism, which obtains several information of bone remodeling.

Niigata bone science institute started since 1999 in Niigata rehabilitation hospital, and mainly conducted clinical histomorphometric work with orthopedic doctors in Japan. We have developed the new device for iliac bone biopsy more safety and easy way. Also we have published new text book of bone Histomorphometry to inform the bone histomorphometry method and standard knowledge to young doctors. In Japan we have a special group of bone histomorphimetry, and annual workshop was held to have technical consensus.

In clinical work, we orthopedic doctors experience atypical cases of fracture patients. Bone histomorphometry can provide the important information about bone metabolism and bone tissue, such as SSBT, osteomalacia, acute destructive joints and others. In this talk, I demonstrate some special clinical cases with iliac bone biopsy to show histomorphometric analysis.

Another topic of this talk is the concept of minimodeling which means new bone formation without previous bone resorption in trabecular surface. We had reported minimodeling was observed in hip osteoarthritis patients. Recently minimodeling measurement studies were indicated in some reports, but the definition of minimodeling is not established yet. We have been observed many minimodeling like structure in human trabecular bone, and wish to propose the final definition of minimodeling.

A last topic is Osteocyte evaluation in histomorphometry. Recently it was suggested that osteocytes play a key role in the regulation of bone remodeling. Bone histomorphometry demonstrate osteocyte density and empty lacuna density. We had some studies osteocyte measurement in human cortical and cancellus bone.

I strongly endorse the bone histomorphometry in clinical work to orthopedic doctors who handle the bone tissue directly.

# Imaging analysis of the effects of denosumab on bone structural properties

## Masako Ito

Center for Gender Equality  
Nagasaki University  
Nagasaki, Japan

Denosumab is a human monoclonal antibody that blocks the binding of RANK ligand (RANKL) to its receptor and selectively inhibits the activity of RANKL, thereby suppressing increased bone resorption in patients with osteoporosis. The effects of denosumab to reduce the risk of fracture have been demonstrated in clinical studies. There has been a progress in the elucidation of structural properties, mainly in non-clinical studies including the analysis of bone specimens collected primarily from experiments with ovariectomized (OVX) cynomolgus monkeys, as well as in clinical studies of human iliac bone biopsy specimens using micro-CT, and of in vivo radius and tibia morphometric analysis using high-resolution peripheral quantitative CT (HR-pQCT).

The effects of denosumab on cancellous bone microstructure have been reported. The results of studies on bone tissue from cynomolgus monkeys and iliac biopsy specimens from humans showed that BV/TV is maintained or increased with decreasing osteoblast surface/bone surface (%), osteoclast surface/bone surface (%), and eroded surface/bone surface (%). Moreover, with regard to the effects of denosumab on the cortical bone, a reduction in cortical porosity has been observed in human iliac biopsy specimens, and in cortical components of the radius and tibia using HR-pQCT. A number of studies have reported an increase of the cortical thickness due to suppression of endosteal resorption, and these effects have been shown to be greater than those of bisphosphonates, according to comparative studies with alendronate. Denosumab has been shown to have a great effect on improving cancellous and cortical bone microstructure, relative to the treatment with teriparatide, which is a bone formative agent. Furthermore, a recent study observed fluorochrome labeling, which showed that after treatment with denosumab, the endosteum of the cortical bone in the upper part of the femoral neck and the lower periosteum were markedly labeled over 6 - 16 months, whereas the cancellous bone was only slightly labeled. It indicates that modeling-based osteogenesis have been reported, which may explain the increase BMD during more than 7 years treatment with denosumab.

Clinically, the effects of denosumab have also been demonstrated by hip structure analysis (HSA) based on dual-energy X-ray absorptiometry (DXA) and imaging evaluation with radial-femoral quantitative CT.

In this lecture, I will discuss the effects of denosumab on bone structural characteristics and the mechanism of associated improvements in bone fragility based on imaging analysis data.

## **Denosumab for the treatment of osteoporosis**

**Sakae Tanaka**

Department of Orthopaedic Surgery,  
Faculty of Medicine, The University of Tokyo  
Tokyo, Japan

Osteoclasts are multinucleated giant cells primarily responsible for bone resorption. Osteoclasts are differentiated from monocyte/macrophage-lineage precursor cells in the presence of receptor activator of NF- $\kappa$ B (RANKL) and macrophage colony-stimulating factor. A number of studies have shown that RANKL-RANK pathways play essential roles in the pathologic bone resorption such as osteoporosis, rheumatoid arthritis, cancer bone metastasis and periodontal diseases. Denosumab, a fully human IgG2 monoclonal antibody that binds human RANKL with a high affinity, potently suppresses osteoclast development and reduces bone resorption. In a study of postmenopausal osteoporosis patients (FREEDOM), denosumab significantly reduced the risk of new vertebral fractures at 3 years by 68%, non-vertebral fractures by 20% and hip fractures by 40% relative to placebo. To examine the anti-fracture efficacy and safety of denosumab (60 mg subcutaneous injection every 6 months [Q6M]) in Japanese patients with primary osteoporosis, a randomized, double-blind, placebo-controlled trial with an open-label referential arm was conducted (DIRECT trial). Denosumab reduced the risk of new or worsening vertebral fracture, with incidences of 3.6% in the denosumab group and 10.3% in the placebo group in 24 months without increasing the risk of adverse events of interest. These results suggest that anti-RANKL therapy is effective in reducing osteoporosis fractures.

## Bone microarchitecture after alendronate treatment of osteoporotic women

**Robert R. Recker, M.D., M.A.C.P., F.A.C.E.**

Head of Creighton University's Osteoporosis Research Center  
Omaha, NE, USA

Alendronate was the first bisphosphonate to be approved for treatment of postmenopausal osteoporosis in the U.S. Preliminary studies demonstrated that it attached to bone surfaces, and markedly inhibited bone resorption by osteoclasts. Originally it was thought (hoped?) that during treatment with Alendronate, bone formation would continue, positive bone balance would ensue, bone mass/density (BMD by DXA) would increase and fractures would be prevented. The early studies did demonstrate increased BMD on treatment, but the increase reached a modest plateau at about 1½ years of continuous treatment. Clinical trials showed remarkable reduction in fractures of ~50% on treatment. At about the same time it became obvious from serum biomarker data that bone formation decreased to about the same extent as bone resorption. The bone resorption markers declined very precipitously after starting treatment, while the formation markers decreased gradually, reaching a plateau at about 6 months after starting treatment. Further, dynamic bone histomorphometry data from the human transiliac bone biopsies showed reduction in formation surfaces that mirrored the reduction in circulating bone formation markers. Thus, there was a relatively brief “uncoupling” of bone resorption from bone formation. However, the histomorphometry data showed that it was the bone resorption phase of bone remodeling that was affected by Alendronate, and that the activation frequency of new remodeling sites was decreased. Since the resorption phase at remodeling sites (Basic Multicellular Units, BMUs) is much shorter than the formation phase, it took much longer for the “remodeling space” to be filled, and this explained the delay in the plateau of positive bone balance. It was the reduction in activation frequency (Ac.f) of remodeling sites that was responsible for the gain in BMD. However, it was doubtful that this gain in BMD, ~6-8%, was enough to account for the reduction in fractures, since the reduction in BMD prior to treatment was much greater, ~15-20% or more. More refined anatomic measurements of trabecular microarchitecture (histomorphometry, Micro-CT) then suggested that the loss of trabecular volume, numbers, thickness, connectivity exaggerated the weakening due to bone loss beyond the reduction of overall BMD. This stimulated several reports of the effect of Alendronate treatment on microarchitecture, using histomorphometry and Micro-CT of trabecular bone in transiliac biopsies, as well as in vivo high resolution imaging. The findings generally showed increases in trabecular bone volume (BV/TV), thickness (Tb.Th), connectivity (Tb.C), number (Tb.N) and connectivity indices, along with reductions in trabecular spacing (Tb.Sp). The changes were +20%, +11%, +11% for BV/TV, Tb.N, and Tb.Th, respectively, and -15% for Tb.SP. These were regarded as respectable benefits to microarchitecture, but were they enough to account for the ~50% reduction in fractures, along with the rather modest gains in BMD? There are other potential explanations for more of the anti-fracture effect of Alendronate. For example, the high bone remodeling rates in the usual osteoporotic patient would reduce the overall age of the bone tissue, perhaps making it less mechanically competent. The reduction in Ac.f by Alendronate treatment would reverse this effect, and might contribute to the anti-fracture effect. Another benefit might accrue due to continued periosteal formation (which is not preceded by activation of resorption) coupled with inhibition of endocortical resorption. This might increase the moment of inertia of most bones in the skeleton, yielding an increase in mechanical strength out of proportion to the gain in BMD. As of yet, we do not have a complete explanation of the mechanism of the anti-fracture benefit of Alendronate, beyond its ability to reduce the remodeling space and thus result in some gain in bone mass.

## Geometry of lower extremities and atypical femoral fractures

**Muneaki Ishijima, M.D., Ph.D.**

Department of Medicine for Orthopaedics and Motor Organ  
Juntendo University Graduate School of Medicine, Tokyo, Japan

Osteoporotic fractures, most notably hip fractures, are associated with significant morbidity and mortality. Although osteoporosis had been thought to be a natural part of aging among women, it is no longer considered age- or sex-dependent. It becomes preventable due to the remarkable progress in the scientific understanding of its causes, diagnosis, and treatment. As bone strength primarily reflects the integration of bone mass and bone quality, treatment of osteoporosis is to increase the bone mass and, hopefully, to improve the bone quality. As bone is a remodeling organ and the recent development of bone biology, we are recently able to increase bone mass by modulating a bone remodeling processes. However, the goal of therapy is fracture prevention.

The bisphosphonates (BPs) are the current cornerstone of osteoporosis treatment and prevention. Treatment with BPs reduces the rate of bone resorption and increases bone mass, improving bone strength and reducing fracture risk. Denosumab, a fully human monoclonal antibody against the receptor activator of nuclear factor- $\kappa$ B ligand (RANKL), prevents the interaction of RANKL with RANK, its receptor, on osteoclasts and their precursors, thereby blocking the formation, function, and survival of osteoclasts. These anti-bone resorbing agents are only drugs currently available, those can reduce hip fractures in patients with osteoporosis. However, the treatments by these agents must be continued for 3 to 4 years for reducing the risk of these fractures in osteoporotic women.

In spite of its clinical benefits, the long-term treatment of BPs has been implicated in the rare but serious adverse events, such as atypical femoral fractures (AFFs). Although the recent studies with radiographic adjudication have indicated the significant associations between them, the pathogenesis of AFFs is not completely understood.

AFFs are characterized by unique radiographic features and also unique clinical features, such as prodromal pain and bilaterality, those resemble stress fractures or reactions. The ASBMR task force reported the original case definition to highlight the unusual radiographic features that distinguish AFFs from ordinary osteoporotic typical femoral fractures (TFFs). Although AFFs appear to be more common in patients who have been exposed to long-term BPs, usually for more than 3 years, every series includes patients who have not been treated with BPs, suggesting that the “background factors” of AFF in osteoporosis patients is not zero. The majority of studies have found a significant association with glucocorticoid use or duration. Although the relative risks of AFFs are very high in patients on BPs, their absolute risk is extremely low. Thus, these fractures are rare, particularly when considered against the incidence of common osteoporotic fractures of all types and ordinary TFFs, all of which have been proven to decrease with BP therapy. In addition, it has also been increasingly reported the cases suggesting the association between denosumab and AFFs. Therefore, it becomes more important to know the “background factors” of AFF to treat patients with osteoporosis who are susceptible for osteoporotic fractures.

We recently reported that the incidence of AFFs in the Japanese population was similar to that of those in Caucasians, and taking BPs and glucocorticoids and suffering from collagen diseases were the risk factors for developing AFFs (J Bone Miner Metab, 2014). We also reported that the fracture sites of AFFs are associated with the standing lower limb alignment and that the lower limb alignment is suggested to be one of the risk factors for AFFs (Bone, 2014). In this lecture, I'd like to focus on the “background factors” of AFF in addition to summarizing the epidemiology, risk factors and pathology of AFFs.

# Anabolic therapy for the skeleton with PTH

## – now and the future

### T.J. Martin

St Vincent's Institute of Medical Research;  
University of Melbourne Department of Medicine  
Melbourne, Australia

Anti-resorptive agents do not reconstruct the skeleton, but a new approach to achieving that has come with the development of PTH as an anabolic therapy, approved in several countries as PTH(1-34) and PTH(1-84). The anabolic effectiveness of PTH requires that it be administered intermittently, and this has been achieved with the use of daily injections which rapidly achieve a peak level in blood which is not maintained.

The pharmacokinetics required for this effect are that a peak of circulating PTH is required, returning to control levels within 3 hours. Prolongation of elevated levels brings into play the stimulation by PTH of osteoclast formation and bone resorption. This resorption effect is enhanced greatly with infusion of PTH over some hours, or with the consistently elevated PTH of primary hyperparathyroidism.

Studies of PTH pre- and post-treatment bone biopsies in women indicated that the predominant PTH effect is to increase remodelling, with some lesser effect on modelling. Current views of the anabolic action of PTH are that it increases the activation of BMU's in remodelling, that it acts on committed osteoblast precursors to promote their differentiation, inhibits osteoblast and osteocyte apoptosis and inhibits the production of the bone formation inhibitor, sclerostin. There is also much interest in the possibility that PTH treatment results in transient activation of osteoclasts, that in turn produce activities that enhances the osteoblast differentiation effect. The latter may be independent of resorption, and may result from the release of growth factors (TGF $\beta$ , IGF-1) in the resorption that enhance the availability of mesenchymal stem cells (TGF $\beta$ ), or their differentiation in the osteoblast lineage (IGF-1). When PTH treatment is stopped, the accrued bone is likely to be lost through resorption over a period of time, so courses of PTH treatment are likely to require treatment with anti-resorptive drugs to retain the newly formed bone. This is being actively investigated, as also is the question whether PTH could usefully be administered together with anti-resorptive? Some studies, but by no means all, indicate that co-treatment with bisphosphonate impairs the PTH effect. Much of this work is confounded by the use of BMD measurement as end-point. New methods of assessing bone quality will be needed to answer this question. There seems a sound logic in such combination, and this will be discussed.

We might now regard PTH in its application as a skeletal anabolic therapy as an attempt to reproduce the local action of PTHrP. This sharing of function between a hormone and its related cytokine is reminiscent of the relationship between growth hormone and IGF-1. If this is so, the pharmacological challenge comes from the fact that physiologically, PTHrP is generated and acts within those BMU's that require it. Pharmacological administration of PTH on the other hand, is presented globally to the skeleton, and able to activate BMU's generally. This might explain the increased bone resorption that inevitably begins after several weeks' treatment with daily PTH.

What does the future offer in relation to PTH in therapy? Attempts continue to find low molecular weight peptide or even non-peptide mimics that can activate through the specific G protein – coupled receptor PTHR1. Maybe alternative methods of delivery can be developed - e.g. intranasal or intrapulmonary, and perhaps PTH secretagogues, that provide a sharp burst of PTH release from the parathyroid gland, sufficient to promote the anabolic response, but not so prolonged that the resorption effect predominates. Efforts are being made to find such drugs by seeking antagonists of the calcium -sensing receptor. Such an approach, developing PTH secretagogues as anabolic agents, will have to satisfy the pharmacokinetic requirement of transiently increasing PTH in patients to the desired level. Reproducing the physiological function of PTHrP presents very much greater difficulty.



## **Oral Presentations**

---





# Histomorphometric analyses of cortical effects of teriparatide in postmenopausal women with or without long-term alendronate therapy

**Yanfei L. Ma, Qing Q. Zeng , Alan Y. Chiang<sup>1)</sup>, David Burr<sup>2)</sup>, Jiliang Li<sup>3)</sup>, Harald Dobnig , Astrid Fahrleitner-Pammer<sup>4)</sup>, Dana Michalská<sup>5)</sup>, Fernando Marin , Imre Pavo<sup>6)</sup>, Jan J. Stepan<sup>7)</sup>**

1) Lilly Research Lab, Indianapolis, IN, USA

2) Dept of Anatomy and Cell Biology, Indiana University, Indianapolis, IN, USA

3) Dept of Biology, Indiana University Purdue University, Indianapolis, IN, USA

4) Dept of Internal Medicine, , Medical University of Graz, Graz, Austria

5) 3rd Dept. of Internal Medicine, Charles University Faculty of Medicine 1, Prague, Czech Republic

6) Lilly Research Center, Windlesham, United Kingdom

7) Institute of Rheumatology, and Charles University Faculty of Medicine 1, Prague, Czech Republic

## Purposes:

Osteoporotic and age-related bone loss is characterized by a progressive thinning of cortical bone and increasing in intracortical porosity, consequently leading to increased risk of fracture. We assessed the cortical effects of teriparatide (TPTD) 20 µg/day sc treatments in postmenopausal women with osteoporosis previously receiving alendronate (ALN) treatment for a mean duration of 63.6 months or being treatment naïve (TN).

## Materials and methods:

Twenty-nine ALN and 16 TN paired tetracycline-labeled transiliac crest bone biopsies obtained from patients at baseline and after 24 months TPTD treatment were evaluated for bone formation activity at the periosteal, endosteal and intracortical osteonal bone surfaces using dynamic histomorphometry.

## Results:

At baseline, bone turnover was lower in patients previously treated with ALN compared to the TN patients. Double label prevalence in endocortical and periosteal surfaces were 28% and 3% in the ALN group compared to 50% and 38% in the TN group. The numbers of specimens without any tetracycline label on endocortical or periosteal surfaces were 38% and 59% in the ALN group compared to 6% and 13%, respectively, in the TN group. The percentage of quiescent osteons was also higher in the ALN (75%) specimens than TN (83%). Endocortical and periosteal mineralizing surface (MS/BS%), periosteal bone formation rate (BFR/BS), mineral apposition rate (MAR) and the number of intracortical forming osteons were significantly lower in specimens from the ALN-group than from the TN group. Following teriparatide treatment, the frequency of endocortical and periosteal unlabeled biopsies decreased in both ALN and TN groups; the percentage of quiescent osteons were reduced while forming osteons were increased in the ALN group. Teriparatide treatment resulted in significant increases of endocortical MAR in ALN- group, and periosteal MS/BS% in the periosteal compartment in both ALN and TN groups. Most indices of bone formation remained lower in the ALN-pretreated group compared with the TN group at study end. In the pooled analysis, percent changes in periosteal and endocortical MS/BS and BFR/BS; total cortical area, cortical thickness, and porosity area increased significantly after 24 months TPTD treatment compared to baseline. These results suggest that 24-month teriparatide treatment increases cortical bone formation activities in patients who were either treatment-naïve or had lower bone turnover initially due to previous alendronate therapy. The increased bone-building activities were associated with thicker cortex, increased cortical turnover in both patient groups.

# **In vivo bone microstructural analysis of osteoporosis using HR-pQCT**

**Ko Chiba, Masako Ito, Makoto Osaki<sup>1)</sup>,  
Andrew J. Burghardt, and Sharmila Majumdar<sup>2)</sup>**

1) Nagasaki University School of Medicine, Japan

2) University of California, San Francisco, USA

## **Introduction:**

It had been difficult to evaluate the bone microstructure of living human bones accurately using clinical imaging modalities. Due to the development of imaging technology in recent years, in vivo analysis of patients' bone microstructure has been attempted using various clinical modalities such as CT and MRI.

HR-pQCT is a clinical high resolution CT dedicated to patients' extremities. Using this CT, cancellous bone structure such as trabecular number (Tb.N) and trabecular separation (Tb.Sp), and cortical bone microstructure such as cortical thickness (Ct.Th) and cortical porosity (Ct.Po) can be measured. This CT is now widely used for the research of pathophysiology and drug development for osteoporosis.

## **Methods:**

A male osteoporosis study using HR-pQCT has been conducted at the University of California, San Francisco.

The subjects consisted of 80 male volunteers. The distal radius and tibia were scanned at the voxel size of 82  $\mu$ m, and Tb.N, Tb.Sp, Ct.Th, and Ct.Po, etc. were measured. Possible correlations between these parameters were analyzed, along with: age, height, weight, body mass index, smoking/drinking habits, serum calcium, vitamin D and testosterone value, bone mineral density value of the lumbar vertebra, proximal femur, distal radius measured by dual-energy x-ray absorptiometry (DXA).

## **Results:**

We obtained mainly two results: 1) It was impossible to estimate the existence of cortical porosity by DXA, although some micro-structural parameters of cancellous bone had correlations with DXA value. 2) The most significant factor that was associated with the formation of the cortical porosity was aging.

## **Discussion:**

HR-pQCT was developed in 2004 and now used in over 50 institutions all over the world, but not in Japan. In 2014, a new model of HR-pQCT was released, and it has been decided to install the CT in Japan this year. Research projects in 5 fields are under contemplation: 1) osteoporosis, 2) rheumatoid arthritis, 3) fracture healing, 4) osteoarthritis, and 5) anatomy. It is expected that new findings will emerge from these projects.

# Measurement of bone strength and medication evaluation can be achieved using medical CT images

**Nobuhito Nango<sup>1)</sup>, Shogo Kubota<sup>1)</sup>, Yusuke Horiguchi<sup>1)</sup>, Kazutaka Nomura<sup>1)</sup>  
and Masafumi Machida<sup>2)</sup>**

1) Ratoc System Engineering Co., Ltd.

2) National Hospital Organization Murayama Medical Center

## Introduction:

Prevention of fractures is a global issue in aging societies. Bone strength is determined by bone density and quality (NIH Consensus Statement 2000), and bone microstructure is a component comprising bone quality. Prediction of bone strength by measuring bone density and microstructure is an important step forward in preventing vertebral fractures. We can contribute to enhancing incentives for treatment by quantifying the effect of osteoporosis medications.

## Purposes:

We investigated whether human bone morphometry can be achieved using clinical CT (MDCT) images. Although human trabecular bone has a width of 0.1–0.3 mm, the MDCT scan has a slice thickness of 0.5 mm. Therefore, we examined the validity of numerical values obtained by measurement using MDCT images.

## Materials and methods:

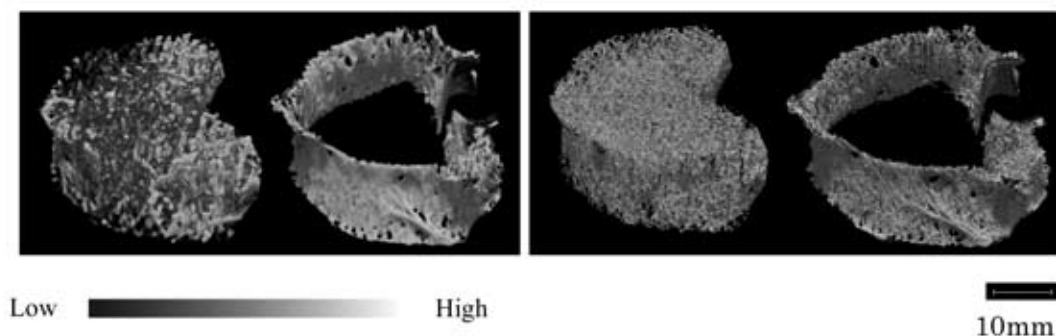
Specimens were T12, L1, L2, and L3 extracted vertebrae. We scanned them with MDCT using FOV of 100–150 mm and thickness of 0.5 mm. Specimens were scanned using  $\mu$ CT with a resolution higher than the trabecular bone width. Both CT images were converted to TMD images using an HA phantom. Volume position adjustment was performed for MDCT and  $\mu$ CT images, and trabecular bone and cortical shell were extracted from both the images to measure trabecular and cortical bones. We then ran the bone strength simulation of compression load and bone morphometric measurement.

## Results:

(1) The BMD value correlation between MDCT and  $\mu$ CT showed an  $R^2$  of  $>0.7$ . (2) The morphometry result showed an  $R^2$  of  $>0.6$  for correlation among indexes such as BV/TV, Tb.Th, V\*m.space, and V\*tr. (3) The shear stress was correlated with an  $R^2$  of  $>0.5$  ( $p < 0.00$ ).

## Discussion:

In MDCT, we could not separate trabecular bones individually, but its macroscopic bone shape was consistent with that on the  $\mu$ CT images. Based on the abovementioned results, trabecular bone morphometric values obtained using MDCT images may represent the state of bone accumulation. Thus, we suggest that MDCT images can be used for human bone morphometry measurement.



MDCT CT images (left), and  $\mu$ CT Images (right)

Trabecular bone and cortical shell were extracted.

MDCT macroscopic bone shape was consistent with that on the  $\mu$ CT images.

Comparison of TMD images obtained using MDCT and  $\mu$ CT.

## Comparative analysis of the development of periodontal disease in rice rats and lewis rats

**J. Ignacio. Aguirre<sup>1</sup>, Stephanie La<sup>2</sup>, Jonathan G. Messer<sup>2</sup>, Joshua F. Yarrow<sup>3</sup>,  
Mohammed P. Akhter<sup>4</sup>, Lakshmyya Kesavalu<sup>5</sup>, Deborah E. Kipp<sup>2</sup>, Donald B. Kimmel<sup>4</sup>,  
Thomas J. Wronski<sup>1</sup>**

1) Department of Physiological Sciences, University of Florida (UF), Gainesville, FL

2) Department of Nutrition, UNC Greensboro, Greensboro, NC

3) Research Service, Department of Veterans Affairs Medical Center, North Florida/South Georgia Veterans Health System, Gainesville, FL and Department of Applied Physiology and Kinesiology, UF

4) Osteoporosis Research Center, Creighton University, Omaha NE

5) Department of Periodontology and Oral Biology, College of Dentistry, UF

### Purposes:

Periodontal disease (PD) is a chronic dental disease resulting from a persistent immune-response to chronic infection in the mouth of humans/domestic animals. Identification of PD as a predisposing factor in the development of anti-resorptive-related osteonecrosis of the jaw (ARONJ) has generated interest in animal models of this disease. We have studied two rodent models of PD: 1) the rice rat (*Oryzomys palustris*), a species susceptible to spontaneous PD, which can be accelerated by feeding the rats with a diet high in sucrose/casein (H-SC), and 2) the Lewis rat, a strain used to study Th1-mediated-autoimmune diseases. We aim to compare the development of PD and coincident alveolar bone loss (ABL) in these two species.

### Materials and methods:

Three groups of rats (N=8-20) of each species were used. A group of rats of each species was euthanized at weaning age (baseline). The other two groups of each species were fed standard (STD) or H-SC diets for a period of 23/24 wks after weaning. Mandibles and maxillae were processed to assess vertical(v) and horizontal(h) ABL, and degree of inflammation (PD score), by MicroCT, histometry and qualitative histology, respectively.

### Results:

We found that compared to baseline, rice rats had greater vABL, hABL and PD scores (moderate/severe) in mandibles and maxillae of groups fed either the H-SC or the STD diet for 23/24 wks. In Lewis rats, there were no significant differences between baseline and STD groups for any parameter. However, slightly worse PD score (slight/mild) and significantly worse mandibular and maxillary vABL were observed in Lewis rats fed the H-SC diet for 23/24 wks.

### Conclusion:

These findings suggest that after 23/24 wks of dietary treatments: 1) STD rice rats develop PD comparable to H-SC rice rats with a moderate/severe degree; 2) no significant age-related PD develops in Lewis rats (STD); 3) the H-SC diet causes slight to mild PD and alveolar bone loss in Lewis rats; and 4) the H-SC diet-related PD develops more slowly in Lewis rats than in rice rats. These findings support use of rice rats with PD for preclinical studies of ARONJ, but the greater availability of Lewis rats merit further evaluation as a rodent model for PD.

## **G9a deficiency leads to impaired osteoblastic differentiation in mice**

**Akira Nifuji<sup>1)</sup>, Hisashi Ideno<sup>1)</sup>, Akemi Shimada<sup>1)</sup>, Koichiro Komatsu<sup>1)</sup>,  
Taichi Kamiunten<sup>1)</sup>, Yoshiki Nakamura<sup>1)</sup>, Kazuhisa Nakashima<sup>1)</sup>, Hiroshi Kimura<sup>2)</sup>,  
and Makoto Tachibana<sup>3)</sup>**

1) Tsurumi University School of Dental Medicine, Japan

2) Tokyo Institute of Technology, Japan

3) The University of Tokushima, Japan

### **Purposes:**

During development, histone H3K9 methyltransferases are expressed in many tissues and regulate cell differentiation. In this study, we investigated expression and function of an H3K9MTase, G9a, during osteoblastic differentiation,

### **Materials and methods :**

We investigated G9a expression during the differentiation of MC3T3E1 cells and primary calvarial cells. To examine G9a expression during embryonic bone formation, in situ hybridization (ISH) was carried out on sections prepared from mouse embryos at day 16.5 (E16.5). To investigate functions of G9a, we performed G9a knockdown by using siRNA against G9a. We also isolated primary osteoblasts from G9a(f/f) mice and deleted G9a by infection of cre-expressing adenovirus. To examine functions of G9a in skeletogenesis in vivo, mice carrying a floxed allele of G9a were crossed with mice expressing Cre recombinase under the control of the Sox9 promoter

### **Results and conclusion:**

G9a was expressed during osteoblastic differentiation in MC3T3E1 cells and primary calvarial cells. ISH revealed that G9a expression was observed in cells residing on bone surfaces. Knockdown or deletion of G9a in osteoblastic cells resulted in decreased cell proliferation rate and suppression of osteoblastic marker expression such as alkaline phosphatase. Conditional knockout mice showed impaired bone formation in cranial bones. Taken together, the H3K9MTase, G9a, is expressed during osteoblastic differentiation and its expression is required for proper development of bone.

## Osteocytic ephrinB2 restrains mineralisation of murine bone

**Christina Vrahnas<sup>1,2</sup>, Ingrid Poulton<sup>1</sup>, Huynh Nguyen<sup>3</sup>, Mark Forwood<sup>3</sup>, Keith Bambery<sup>4</sup>, Mark Tobin<sup>4</sup>, T John Martin<sup>1,2</sup>, Natalie Sims<sup>1,2</sup>**

1) St. Vincent's Institute of Medical Research, Melbourne, Australia

2) University of Melbourne, Australia

3) Griffith University, Gold Coast, Australia

4) Australian Synchrotron, Melbourne, Australia

Parathyroid hormone (PTH) rapidly upregulates expression of EphrinB2 in the osteoblast lineage. EphrinB2 deletion in osteoblasts and osteocytes (OsxCre.EphrinB2 f/f) caused a phenotype of compliant bones due to delayed mineralization and osteoblast apoptosis. In contrast, ephrinB2 deletion in osteocytes (Dmp1Cre.EphrinB2 f/f) results in increased bone brittleness, suggesting a different function for EphrinB2 in osteocytes. However, no defect in histomorphometric parameters of bone formation was observed. We have used synchrotron-based Fourier-Transform Infrared Microscopy (sFTIRM) to determine aspects of mineralisation that contribute most strongly to bone strength in the Dmp1Cre.EphrinB2 f/f mouse.

3µm tibial sections from 12 week old female Dmp1Cre.EphrinB2 f/f mice and littermate Dmp1Cre controls (w/w) (n = 13 per group) were analysed in 3 x 15 µm square regions commencing 1.5mm below the growth plate at the periosteal edge of the anterofibular cortex and concluding in the older mature bone. Regression analysis with 3-point bending data of femoral bones from the same mice was also conducted.

Our sFTIRM analysis revealed that the brittle bones from Dmp1Cre.EphrinB2 f/f mice had higher mineral/matrix (by 12%,  $p < 0.05$ ) and carbonate/mineral (by 37%,  $p < 0.05$ ) ratios than controls, even in the newly formed bone at the periosteal edge. This indicates that the greater brittleness of this bone occurred due to greater primary mineralization, rather than prolonged secondary mineralization. There was no significant change in collagen content (amide I band). The bone in this same region had altered collagen orientation (lower amide I/amide II ratio) (by 13%,  $p < 0.001$ ) which may underly the greater deposition of mineral in Dmp1Cre.EphrinB2 f/f mice. Regression analysis showed that while the energy absorbed to failure in 3-point bending tests correlated with the amount of collagen in control mice ( $r^2 = 0.40$ ,  $p < 0.05$ ), this relationship failed in Dmp1Cre.EphrinB2 f/f mice. Instead, ultimate strength of Dmp1Cre.EphrinB2 f/f bones was determined by the carbonate/mineral ratio ( $r^2 = 0.50$ ,  $p < 0.05$ ). sFTIRM analysis of the compliant OsxCre.EphrinB2 f/f bones showed no significant changes.

Deletion of ephrinB2 in osteocytes therefore accelerates the initial step of mineralisation on the periosteal surface, suggesting that osteocytic ephrinB2 restrains initial mineral deposition and may regulate collagen orientation.

# Quantitative local in vivo environment (live) Imaging of osteocytes during dynamic bone remodeling

**Andreas J. Trüssel<sup>1)</sup>, Felicitas R. Flohr<sup>1)</sup>, Gisela A. Kuhn<sup>1)</sup> and Ralph Müller<sup>1)</sup>**

1) Institute for Biomechanics, ETH Zurich, Zurich, Switzerland

## Purposes:

The maintenance and adaptation of the morphology of bone results from orchestrated remodeling processes. These processes are locally coordinated by osteocytes with biochemical signals that result in increased or decreased bone formation or resorption activities. To better understand the morphology, we therefore have to understand how osteocytes determine dynamic morphometric parameters within their local microenvironment.

We developed a local in vivo environment (LivE) imaging technique using in vivo micro-computed tomography (microCT) in combination with histology and image processing. LivE imaging allows us to quantify the mechanical and remodeling in vivo microenvironment of hundreds of individual osteocytes for several weeks prior to histological processing. Here, we used LivE imaging in trabecular mouse bone to show that dynamic morphometry is locally linked to quantitative single-cell gene expression.

## Materials and Methods:

The 6th caudal vertebrae of adult female C57BL/6 mice (n=9) were imaged three times over a period of two weeks by in vivo microCT. 3D dynamic morphometric parameters were assessed using advanced registration techniques. The local strain energy density (SED) was calculated for each timepoint by micro-finite element analysis performed on a supercomputer (Cray XT5, CSCS, Lugano, Switzerland). Cryosections were cut and registered into 3D microCT data. Osteocytes were identified, mapped into the microCT coordinate system, tracked back in time through LivE imaging and grouped according to their SED values within volumes around mineralizing, quiescent or eroding surfaces. By laser capture microdissection, osteocytes (n=720) were then isolated in subpopulations containing ten osteocytes on average and their gene expression was analyzed.

## Results and Discussion:

LivE imaging showed that osteocytes around eroding surfaces blocked bone formation activities by *Sfrp1*, a WNT antagonist and increased local bone resorption by MMPs. Osteocytes in areas of high SED increased not only WNT signaling by expression of  $\beta$ -catenin and connexin43 to enhance bone formation but also increased the expression level of the extracellular matrix protein *Col1a2* indicating active remodeling of their perilacunar matrix.

## Conclusion:

LivE imaging allows bridging the gap between dynamic morphometry and biochemical signaling and thereby help us to understand how osteocytes contribute to the dynamic remodeling of bone morphology on the molecular level.



# **Influence of subchondral bone plate integrity on subchondral bone homeostasis in osteoarthritis**

**Guangyi Li<sup>1,2)</sup>, Tak Cheng<sup>2)</sup>, Nathan Pavlos<sup>2)</sup>, Changqing Zhang<sup>1)</sup> and Minghao Zheng<sup>2)</sup>**

1) Department of Orthopaedic Surgery, Shanghai Jiao Tong University Affiliated Sixth People's Hospital, Shanghai, China

2) Centre for Orthopaedic Research, School of Surgery, The University of Western Australia, Perth, Australia

## **Purposes:**

To investigate the influence of subchondral bone plate (SBP) integrity on the homeostasis of underlying subchondral trabecular bone (STB) in osteoarthritis (OA).

## **Materials and methods:**

Subchondral bone cylinders were extracted in the load-bearing region of femoral heads from 110 patients with late-stage OA after hip replacement surgery. SBP integrity, STB microarchitecture and subchondral bone cysts (SBCs) were examined by micro-CT. Bone remodeling in STB and pathological changes inside SBCs were assessed by histology.

## **Results:**

All specimens were observed with SBP breach. 73 specimens displayed full-thickness breach of SBP with exposure of the underlying STB, while the remaining 37 specimens showed partial-thickness breach of SBP without exposure of STB. STB with full-thickness breach of SBP exhibited more sclerotic microarchitecture with higher bone remodeling level and SBCs frequency, as compared to those with partial-thickness breach of SBP. In samples with partial-thickness breach of SBP, microarchitecture and bone remodeling in STB did not correlate with either the thickness or porosity of SBP. However, in samples with full-thickness breach of SBP, microarchitecture and bone remodeling in STB were significantly associated with SBP defect size. A mixed pathology was detected within SBCs, including fibrous tissue, abnormal blood vessels, fibrocartilaginous tissue, hyaline cartilaginous tissue, remnant bone fragments and adipose tissue. The trabecular region immediately adjacent to SBCs exhibited more sclerotic microarchitecture and higher bone remodeling level, compared with distal regions.

## **Conclusion:**

SBP plays a pivotal role in the homeostasis of underlying STB in the progression of OA. It may act as a biomechanical and biochemical shield between the synovial space and STB.

# Intravital bone imaging by two-photon excitation microscopy to identify osteocytic osteolysis in vivo

**Hiroshige Sano<sup>1,2)</sup>, Junichi Kikuta<sup>1)</sup>, Masayuki Furuya<sup>1)</sup>, Naoki Kondo<sup>2)</sup>, Naoto Endo<sup>2)</sup>, and Masaru Ishii<sup>1)</sup>**

1) Department of Immunology and Cell Biology, Graduate School of Medicine and Frontier Biosciences, Osaka University, Osaka Japan

2) Department of Orthopedic Surgery, Graduate School of Medical and Dental Sciences, Niigata University, Niigata, Japan

## Purpose:

Bone is a highly dynamic organ in which several cell types function cooperatively. Among these, osteocytes have recently emerged as an important regulator of bone homeostasis. Moreover, it is revealed that osteocytes have various functions such as endocrine organ, although most of their mechanisms are still unclear. Recent circumstantial evidences support the enigmatic concept, 'osteocytic osteolysis'. However, no direct evidences have yet been presented. The aim of this study is to identify this phenomenon in vivo.

## Materials and methods:

Ten-week-old female C57BL/6 mice were subjected to unilateral sciatic neurectomy, and another side sham surgery (day 0) under isoflurane-induced anesthesia. Intravital bone imaging by two-photon excitation microscopy allowed us to directly visualize lacuno-canalicular systems in cortical bone of tibiae. Osteocyte lacunae and the canalicular network were detected by calcein (s.c.) staining, and local acidification areas in these structures were monitored using a topically applied pH sensor. Finally, we could identify 'osteocytic osteolysis', or resorption of bone in the lacuno-canalicular system by osteocyte in vivo.

## Results and conclusion:

We demonstrated that sciatic neurectomy causes significant acidification around osteocytic lacunae and enlargement of the areas. These results provide strong evidences for 'osteocytic osteolysis', and demonstrate that two-photon excitation microscopy is useful for analyzing the function of osteocytes in vivo.

## **Nck adaptor proteins control osteoblastic migration, bone formation and bone mass**

**Smriti Aryal A.C<sup>1</sup>, Yoichi Ezura<sup>1</sup>, Kentaro Miyai<sup>1</sup>, Izu Yayoi<sup>1</sup>, Tony Pawson<sup>2</sup>, Masaki Noda<sup>1</sup>**

Department of Molecular Pharmacology, Tokyo Medical and Dental University, Tokyo, Japan  
Mount Sinai Hospital, Samuel Lunenfeld Research Institute, Toronto, Canada

Osteoblastic migration and spreading are key events in the maintenance of bone remodeling and bone mass and they are under the control of cytoskeletal activity in osteoblasts through molecular mechanisms, which are incompletely understood. Ncks (non- catalytic region of tyrosine kinase) are SH2 SH3 domain containing adaptor proteins that play a major role in regulating actin cytoskeleton and cell migration. However the role of Nck in osteoblast cytoskeleton organization and migration is unknown.

Here, we present genetic evidence that osteoblast specific Nck conditional double knock-out mice (ob-Nck-dko) generated under the control of 2.3kb type I collagen promoter showed significant reduction in trabecular bone volume (BV/TV) and trabecular number (Tb.N/BS) resulting in osteoporosis, defect in primary osteoblast migration, suppression of repair and spreading after bone injury in vivo compared to control (Ct). Bone histomorphometry revealed that the mineral apposition rate (MAR), bone formation rate (BFR) and mineralized surface per bone surface (MS/BS) were all reduced in the trabecular bone of Ob-Nck-dko mice compared to Ct suggesting that the individual osteoblast activity and function were affected in the trabecular bone in the absence of Nck. Nck deficiency-induced reduction of bone formation was independent from the alteration in osteoclastic activity. Mechanistically, Nck regulates cytoskeletal reorganization and migration of osteoblasts. Nck also controls expression of genes encoding proteins related to osteoblastic phenotypes. These data indicate that Nck adaptors are playing a role in controlling cytoskeletal organization and bone formation to determine the levels of bone mass.

# Bone-implant interface: morphology and ultrastructure

**Anders Palmquist<sup>1,2</sup>, Furqan A. Shah<sup>1,2</sup>, Kathryn Grandfield<sup>3</sup>, Peter Thomsen<sup>1,2</sup>**

1) Department of Biomaterials, Sahlgrenska Academy at University of Gothenburg, Sweden

2) BIOMATCELL VINN Excellence Center of Biomaterials and Cell Therapy, Sweden

3) Department of Materials Science and Engineering, McMaster University, Canada

## Introduction:

The osseointegration of titanium has revolutionized the treatment of edentulousness. The underlying mechanisms for a direct bone-implant interface include both material and host related factors. However, until recently the vast majority of ex-vivo analyses of bone tissue have been restricted to the micrometer level and the light optical microscope. Bone is a highly hierarchical tissue with well-defined structures ranging from the nanoscale to the macroscale. Further, intentional implant surface modification at the nanoscale is emerging in the field of implantology, however, the specific role of this length-scale is unknown. The aim of the current paper is to provide a correlative methodology for multidimensional and multiscale evaluation of the bone-implant interface.

## Materials and methods:

The test material had a combination of micro- and nano-scale modifications created by laser ablation, confined to the thread valleys of a screw-shaped titanium implant. Bone-implant samples were retrieved from experimental animal studies in rabbits (8 weeks and 6 months healing), as well as retrieved clinical dental implants (2.5 months and 3.9 years healing). Samples were formalin fixed and resin embedded prior to analysis. Multiscale analyses included biomechanical testing, microCT, histology, backscattered electron SEM, FIB, TEM, and electron tomography.

## Results:

Significantly higher removal torque was needed to unscrew the modified implants as compared to unmodified controls, together with a different failure mechanism. Load-deformation plots indicated a fracture in the bone rather than at the interface, which was histologically confirmed. Comparable high amounts of bone had formed around both implant types, with increasing amounts after longer healing times. Clinically retrieved samples showed a high degree of osseointegration with > 80% bone-implant contact after 3.9 years in function. Well-defined osteonal bone occupied the thread area with osteocytes aligned with the implant surface and the bone lamellae. At the nano-scale, a chemical intermix of calcium and phosphorous was found with the nano-rough surface oxide, creating a graded interface. Osteocyte processes were frequently observed close to the implant surface.

## Conclusion:

The results clearly demonstrate the importance of using complementary analytical techniques ranging across the length-scales in order to increase the knowledge of the structural aspects of osseointegration and bone bonding.

## **Comparative histological study in maxillary sinus augmentation using coarse or fine particle of xenograft materials (preliminary report)**

**Paksinee Kamolratanakul DDS, Ph.D**

Associate Prof. Pornchai Jansisyanont, DDS, MS  
Chulalongkorn University, Thailand

### **Purposes:**

To compare the histology of the bone healing in maxillary sinus augmentation using coarse grained particle or fine grained particle of xenograft materials.

### **Materials and methods:**

Double blinded, clinical trial study was performed in 10 patients with posterior maxillary edentulous ridge associated with sinus pneumatization. Patients were subjected to lateral window technique of sinus lift procedure using xenograft material commercially prepared as coarse particle grafting (1-2mm) in first group and fine particle (0.25-1mm) in second group. Bone specimens were harvested after 6 months of augmentation and subjected to histomorphological analysis for newly-formed bone, residual particle and fibrous tissue formation.

### **Results:**

The preliminary data initially showed more newly-formed bone significantly ( $p$  value=0.002) in the group of sinus lift using coarse particle of xenograft (mean of percentage area=22.47%,) compared to the group using fine particle of xenograft(mean of percentage area=11.26%). Residual particle in the group of coarse particle xenograft (mean of percentage area=6.19%) was more than in the group of fine particle xenograft (mean of percentage area=1.88%) without the statistic significance. The group of fine particle xenograft revealed abandon of fibrous tissue surrounding the space of particle (mean of percentage area=86.85%) significantly compared to the group of coarse particle xenograft ( mean of percentage area=71.38%) with  $p$  value=0,021.

### **Results and conclusion:**

Coarse particle of xenograft material trends to promote more newly-formed bone in maxillary sinus augmentation which is possibly due to the more space between particle that provides enough space for ingrowth bone cell, cell adhesion and migration of neovascularization. We further study the immunohistochemistry to evaluate the bone healing and microstructure of newly-formed bone will be analyzed using micro-computerized tomography.

# Is it time to say goodbye to SMI?

**Phil Salmon<sup>(1)</sup>, Michael Doube<sup>(2)</sup>, Asa Tivesten<sup>(3)</sup>**

1) Bruker-microCT, Kontich, Belgium

2) Royal Veterinary College, University of London, UK

3) Sahlgrenska Institute, Goteborg, Sweden

## Purposes:

Osteoporotic deterioration of trabecular bone involves a transition from plate-like to rod-like architecture. The structure model index (SMI) [1] measures convex curvature and has long been used to quantify this transition. But it has a significant short-coming: it is confounded by porosity. Both high porosity and high percent volume result in extensive concave curvature, whose existence is ignored in the standard narrative of the shape-dependence of SMI. Traditionally SMI ranges from 0 (plate) to 3 (rod); however in real bone samples negative SMI routinely arises from high porosity. Different combinations of trabecular plate-rod architecture and porosity can give the same SMI. To improve upon SMI two alternatives are presented.

## Materials and methods:

The first is the Ellipsoid Factor (EF), a development of the 3D local thickness algorithm [2], but with fitted ellipsoids in place of spheres [3]. The ellipsoid has freedom to assume a spectrum of shapes from oblate (flat discus shaped,  $EF \rightarrow -1$ ) to prolate (long javelin shaped,  $EF \rightarrow 1$ ). Thus EF ranges from -1 (ideal plate) to +1 (ideal rod). The EF algorithm calculates both a mean value of EF and a 3D spatial map of local EF values. However EF is not a discretization method artificially dividing the trabecular continuum into connecting pieces in contrast to other proposed methods.

The second alternative to SMI is a much simpler parameter; the "unplate index" ( $uPi$ ) is introduced which is the ratio of the trabecular "direct" thickness measured in 3D by sphere-fitting,  $Th(d)$ , to that calculated from the histomorphometric plate model ( $2BV/BS$ ). Thus  $uPi = Th(d).BS/2BV$ . For an ideal plate  $uPi = 1$  and with departure from plate shape the value increases above 1.

## Results and conclusion:

MicroCT datasets of rat femoral trabecular bone from an OVX study into the efficacy of sex steroid drugs [4] is used to compare the values of SMI, EF and  $uPi$ . This study is a case where high  $BV/TV$  from anabolic drug treatment resulted in negative SMI. Both EF and  $uPi$  are shown to be free of this problem of out-of-range values arising from porosity which compromises SMI, and thus represent a potential step toward less ambiguous measurement of trabecular architecture.

1. Hildebrand T, Rueggsegger P (1997) *Comp. Meth. Biomech. Biomed. Eng.* 1: 15-23.
2. Remy E, Thiel E (2002). *Pattern Recognition Letters* 23: 649–661.
3. Doube M (2015) *Frontiers in Endocrinology / Bone Research*, Vol. 6 article 15. doi: 10.3389/fendo.2015.00015
4. Tivesten A et al.(2004) *J. Bone Miner. Res.* 2004; 19 (11):1833-1839.

# Labeling and seeding of MSCs on hydroxyapatite bone substitute: cell behavior and in vivo tracking

**Omar Omar<sup>1,2</sup>, Ibrahim Elgali<sup>1,2</sup>, Anders Palmquist<sup>1,2</sup>, Anna Johansson<sup>1,2</sup>, Birgitta Norlindh<sup>1,2</sup> and Peter Thomsen<sup>1,2</sup>**

1 Department of Biomaterials, Sahlgrenska Academy, University of Gothenburg, Sweden

2 BIOMATCELL, VINN Excellence center of Biomaterials and Cell Therapy, Gothenburg, Sweden

## Purposes:

The role of biomaterial properties for bone regeneration is not fully understood. This process includes material-induced effects on inflammatory cells and communication between monocytes/macrophages and mesenchymal stromal cells (MSCs). Further, priming of bone substitutes with MSCs has been suggested to trigger the recipient bone microenvironment and promote bone regeneration, but the mechanisms are largely unknown. This is partly due to the lack of few in vivo models that allow the tracking of the MSCs and their spatial distribution in the augmented defect. This study aimed to develop a model for seeding MSCs on hydroxyapatite (HA) granules, with possibilities to track the implanted cells in vivo, but yet without jeopardizing their osteogenic potential.

## Materials and methods:

Rat MSCs were labeled with iron oxide beads at different bead concentrations, and the effect of labeling was evaluated in vitro after 1, 6 and 28d. Thereafter, labeled MSCs were seeded on HA granules at different seeding densities. To determine the possibility to track the labeled MSCs in vivo, the combined MSCs-HA granules were implanted in rat femur defects and samples were retrieved, after 1h and 3d, for histology, BS-SEM and EDS analyses.

## Results:

After 1d, the viability was slightly lowered with the high bead concentration compared to medium and low. With FGF, the number of MSCs was doubled after 6d for all groups. Under osteogenic condition, higher Ca and P were recorded, after 28d, for the medium and high bead concentration groups. Viability of labeled MSCs was slightly lower in the high ( $5 \times 10^6$ ) seeding density group compared the medium ( $5 \times 10^5$ ) and low ( $2.5 \times 10^5$ ) seeding densities. In vivo, it was possible to detect the darkly stained cells, due iron content, using Prussian Blue staining. Detection of iron signal was also possible using BS-SEM and elemental mapping with EDS.

## Conclusion:

A model was developed consisting of a labeling procedure and in vivo implantation of combined MSCs-HA granules, which allowed for tracking of the implanted MSCs. In combination with morphological and molecular analytical tools, the model will enable detailed studies on the interactions between implanted MSCs, properties of the implanted material and the recipient local environment.

# Apatite orientation corresponds to the shape of the osteocyte lacuna in sheep trabecular bone

**Furqan A. Shah<sup>1,2</sup>, Ezio Zanghellini<sup>3</sup>, Aleksandar Matic<sup>3</sup>, Peter Thomsen<sup>1,2</sup>, Anders Palmquist<sup>1,2</sup>**

1 Department of Biomaterials, Sahlgrenska Academy at University of Gothenburg, Göteborg, Sweden

2 BIOMATCELL VINN Excellence Center of Biomaterials and Cell Therapy, Göteborg, Sweden

3 Department of Applied Physics, Chalmers University of Technology, Göteborg, Sweden

## Introduction:

Osteocyte lacunae (Ot.Lc) in lamellar bone are aligned parallel to the collagen fibre direction. While the organic matrix guides the mineral directionality, it is not entirely known what causes the organic phase to become organised and whether a parallel relationship exists between osteocytes and the mineral phase. Here, the ultrastructural relationship between the shape of the Ot.Lc and the orientation of nanoscale mineralised structures at the Ot.Lc floor was evaluated.

## Materials and methods:

2 mm thick longitudinal slices of trabecular bone obtained from the tibia and femur of sheep were deproteinised by soaking in NaOCl, followed by dehydration in a graded ethanol series. Scanning electron microscopy, energy dispersive x-ray spectroscopy (EDX), and Raman spectroscopy were utilised for structural characterisation and chemical analysis. The OrientationJ plugin for ImageJ, was used for image analysis.

## Results:

Following deproteinisation, the Ca/P ratio was  $1.69 \pm 0.1$  at the Ot.Lc floor and  $1.68 \pm 0.05$  externally. Raman spectra only showed peaks associated with carbonated apatite, while signals from collagen and other organic components were mostly absent. Compared to untreated bone, the apatite-to-collagen ratio of deproteinised bone was considerably higher; the mineral crystallinity and the carbonate-to-phosphate ratios however remained similar. Relative to the Ot.Lc long axis, the mean orientation (Fig. 1) of mineral structures at the Ot.Lc floor was  $19.01 \pm 14.35^\circ$  (tibia) and  $19.79 \pm 13.92^\circ$  (femur). The mean coherency was  $37 \pm 7\%$  (tibia) and  $38 \pm 9\%$  (femur). Linear regression analysis showed poor correlation between the coherency and orientation. Of all the Ot.Lc evaluated, 69.37% (tibia) and 74.77% (femur) exhibited a mean orientation of mineralised structures between  $0-25^\circ$ . The highest fraction of lacunae showed mineral orientation in the narrow  $15-20^\circ$  range; 17.12% (tibia) and 19.8% (femur).

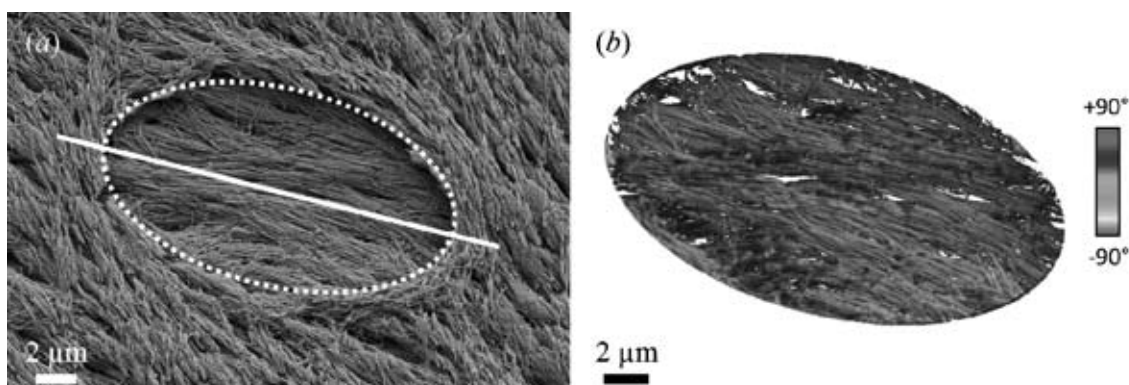


Fig. 1: (a) The shape of the osteocyte lacuna observed by scanning electron microscopy, and (b) the corresponding orientation/directionality analysis.

## Conclusion:

The directionality of the mineralised structures at the Ot.Lc floor closely follows the shape of the Ot.Lc suggesting that collagen production is a spatially and temporally synchronised process.



## **Housing mice at room temperature results in premature bone loss: Implications for the mouse as a model of osteoporosis**

**Urszula T. Iwaniec<sup>1</sup>, Kenneth A. Philbrick<sup>1</sup>, Carmen P. Wong<sup>1</sup>, Dawn A. Olson<sup>1</sup>, Adam J. Branscum<sup>2</sup>, and Russell T. Turner<sup>1</sup>**

1 Skeletal Biology Laboratory, School of Biological and Population Health Sciences, Oregon State University, Corvallis, OR, 97331, USA

2 Biostatistics Program, School of Biological and Population Health Sciences, Oregon State University, Corvallis, OR, 97331, USA

### **Purpose:**

Mice, because of their small size, short lifespan and ease of genetic manipulation, are a mainstay for cutting edge research in fundamental skeletal biology. However, in marked contrast to age-related cancellous bone loss in humans, cancellous bone loss in weight bearing long bones in mice begins during growth, even as cortical bone continues to be accrued. As a consequence, mice exhibit low cancellous bone volume fraction prior to skeletal maturity (4 months of age). Unlike humans who are homeotherms, mice are facultative daily heterotherms, experiencing cyclic changes in core temperature and bouts of torpor when subjected to cold stress (temperatures below thermoneutral; ~30°C for mice) and/or caloric restriction. Activation of sympathetic signaling is important for mice to successfully adapt to low temperature and suppression of sympathetic tone has been reported to increase cancellous bone in mice. We therefore hypothesized that premature age-related cancellous bone loss commonly seen in mice may be due to temperature stress induced by housing the animals at room temperature (20-24°C).

**Materials and methods:** 2-month-old female C57BL6/J mice were randomized to 1 of 2 temperatures (22°C or 32°C; n=10/group) and maintained for 2 months. Femora were evaluated by microcomputed tomography and histomorphometry.

### **Results:**

Mice housed at 32°C consumed less food than mice housed at 22°C. However, significant differences in body weight were not detected with temperature. Furthermore, there were minimal temperature-dependent effects on cortical bone. In contrast, mice housed at the warmer temperature maintained higher cancellous bone volume fraction in the distal femur metaphysis. The sparing effect of thermoneutral housing on cancellous bone was associated with increased bone marrow adiposity, higher bone formation and no change in bone resorption.

**Conclusions:** Our findings support the conclusion that mild cold stress has a major negative impact on cancellous bone mass in mice and that early onset cancellous bone loss in this species is due, in part, to cold adaptation. The findings also suggest that studies using mice as a preclinical model to investigate interactions between energy homeostasis and bone or the etiology of age-related bone loss need to account for confounding species differences in thermoregulation and energy metabolism.

# Texture analysis improvement in cortical evaluation: influence of osteophyte in femoral neck in osteoarthritis.

**Jean-Paul Roux, Gustavo Davi Rabelo, Nathalie Portero-Muzy, Stéphanie Boutroy, Roland Chapurlat, Pascale Chavassieux.**

INSERM UMR 1033 and Université de Lyon, Lyon, France

## Purposes:

Osteoarthritis (OA) is a multi-factorial disease characterized by cartilage and bone lesions. In hip OA, the subchondral plate is thickened and subchondral bone becomes sclerotic with the presence of osteophytes. It is usually acknowledged that OA might have a protective effect on fragility fracture and osteophytes have been suggested to play a role in the bone strength.

Many studies have shown the importance of the evaluation of cortical bone by itself, bone resistance to rupture depends on 40 to 90% of cortical bone at femoral neck. Cortical porosity is one major determinant of bone strength. However, the limit of resolution of clinical or laboratory computerized tomography underestimates of the cortical porosity and overestimates the pore diameter, principally due to partial volume effect. To overcome this resolution limitation, we propose the use of texture analysis.

## Materials and methods:

Femoral neck samples were obtained during arthroplasty for hip osteoarthritis in postmenopausal women (n=18; aged 66± 8 years). Microarchitecture was measured using a high-resolution peripheral quantitative computed tomography system (XtremeCT, Scanco Medical, Switzerland), with a nominal isotropic voxel size of 82 µm. The following cortical parameters were measured: thickness (Ct.Th), thickness heterogeneity (Ct.ThSD), porosity (Ct.Po), Fractal Dimension indicating how much an object fills up the space using threshold or unthreshold-based methods (respectively Ct.FD<sub>bin</sub>, Ct.FD<sub>gray</sub>) and Lacunarity (Ct.Lac), a scale dependent measure of heterogeneity of texture.

These approaches of evaluation were performed due to the possibility of the use of texture analysis by threshold or unthreshold-based methods, which allowed the identification of some extra characteristics of bone channels, related to their distribution and their spatial organization.

## Results:

Cortical analysis : osteophyte vs the opposite quadrant			
Parameter	Osteophyte quadrant	Opposite quadrant	p*
Ct.FD <sub>bin</sub>	2.62 (0.10) <sup>§</sup>	2.41 (0.34)	0.0048
Ct.FD <sub>gray</sub>	0.98 (0.18)	0.80 (0.20)	0.0020
Ct.Lac	1.11 (0.85)	1.40 (1.01)	0.4925
Ct.Th	1955 (427)	1053 (379)	<0.0001
Ct.Th <sub>SD</sub>	516 (139)	389 (152)	0.0138
Ct.Po	18.05 (11.23)	14.14 (6.71)	0.3073
<sup>§</sup> mean (SD), *Wilcoxon test			

## Results and conclusion:

The osteophyte area was characterized by a higher Ct.FD than the opposite quadrant of the femoral neck. Similar results were observed with the two methods (Ct.FD<sub>bin</sub> and Ct.FD<sub>gray</sub>). Ct.Th and Ct.ThSD were significantly higher in the osteophyte quadrant, than in the opposite part. Lacunarity and porosity were not significantly different between osteophyte and opposite quadrant. Osteophyte was characterized by a higher complexity than the other part of femoral neck. This may influence the mechanical properties of the femoral head.

## Accuracy of clinical computed tomography for measurement of bone quality: a study in cadavers

**Miyuki Takasu<sup>1)</sup>, Chikako Fujioka<sup>2)</sup>, Masao Kiguchi<sup>2)</sup>, Eiji Nishimaru<sup>2)</sup>, Koumei Takauchi<sup>2)</sup>, Masafumi Machida<sup>3)</sup>, Nobuhito Nango<sup>4)</sup>, Kazuo Awai<sup>1)</sup>**

1) Department of Diagnostic Radiology, Hiroshima University, Japan

2) Department of Radiology, Hiroshima University, Japan

3) National Institute of Musculo-Skeletal Disorders, Murayama Medical Center, Tokyo, Japan

4) Ratoc System Engineering Co., Ltd, Tokyo, Japan

### Purpose:

The application of clinical multidetector CT (MDCT) in evaluating bone quality has become a clinical research tool for in vivo studies. The purpose of this study was to determine the accuracy of MDCT for architectural measurements through a comparison with micro computed tomography (micro-CT) as the gold standard.

### Materials and Methods:

L1 and L2 vertebrae of 10 fresh human cadavers were scanned by 64-section MDCT (LightSpeed VCT; reconstruction kernel, BONEPLUS; collimation,  $64 \times 0.625$  mm), 16-section MDCT (LightSpeed Ultra16; BONEPLUS,  $16 \times 0.625$  mm), 320-section MDCT (Aquilion One; FC30,  $80 \times 0.5$  mm), 80-section MDCT (Aquilion One Vision Edition; FC30,  $80 \times 0.5$  mm), 16-section MDCT (Aquilion LB; FC30,  $16 \times 0.5$  mm), 32-section MDCT (Biograph mCT-S(64); B75f,  $64 \times 0.6$  mm), and by micro-CT (TOSCANER 30000). The reconstructed voxel sizes were  $0.2 \times 0.2 \times 0.16$  mm for MDCT and  $50 \times 50 \times 80$   $\mu$ m for micro-CT. Trabecular structural parameters and BMC/TV of the central 10-mm thickness portion of the vertebrae were calculated. Relationships between MDCT-derived and micro-CT-derived trabecular indices were compared using Spearman's correlation coefficient. The Scheffe's post hoc test was used to test for significant differences among the different MDCT systems and the micro-CT measurements.

### Results:

BMC/TV measured by MDCTs significantly correlated with micro-CT measures ( $\rho=0.84-0.88$ ). Seven of nine of morphological parameters measured by MDCTs significantly correlated with micro-CT measures. The correlation coefficient was the highest for bone volume/tissue volume (BV/TV,  $\rho=0.89-0.91$ ). Conversely, degree of anisotropy ( $\rho=0.14-0.6$ ) showed the lowest correlation with micro-CT. Trabecular thickness and trabecular width did not show significant correlation with micro-CT measures. The mean values of trabecular spacing, fractal dimension, and BV/TV did not differ from those of micro-CT. BMC/TV was significantly higher in five of six MDCTs than in micro-CT. For three out of nine morphological parameters, 80-section MDCT had the highest correlation with micro-CT measurements.

### Conclusion:

The validation here of MDCT against gold-standards micro-CT suggests that indices of bone quality including BV/TV may be appropriate for clinical monitoring of bone quality by MDCT. The degree of over- or underestimation of trabecular parameters is important when absolute values are needed.

# Melatonin suppresses the microgravity-induced activation of osteoclasts in cultured goldfish scale

**Mika Ikegame<sup>1)</sup>, Atsuhiko Hattori<sup>2)</sup>, Tatsuki Yamamoto<sup>3)</sup>, Kei-ichiro Kitamura<sup>4)</sup>, Yoshiaki Tabuchi<sup>5)</sup>, Masaki Nakano<sup>2)</sup>, Sachiko Yano<sup>6)</sup>, Toshio Yamamoto<sup>1)</sup>, and Nobuo Suzuki<sup>3)</sup>**

1) Okayama University Graduate School of Medicine, Dentistry and Pharmaceutical Sciences, Japan

2) College of Liberal Arts and Sciences, Tokyo Medical and Dental University, Japan

3) Institute of Nature and Environmental Technology, Kanazawa University, Japan

4) Institute of Medical, Pharmaceutical and Health Sciences, Kanazawa University, Japan

5) Life Science Research Center, University of Toyama, Japan, 6) Japan Aerospace Exploration Agency, Japan

## Purposes:

Melatonin is a hormone secreted from the pineal gland that controls circadian rhythms and that has recently been shown to affect various biological activities in peripheral tissues, including bone. In particular, melatonin has been reported to suppress osteoclast differentiation. Although previous studies indicate that microgravity influences osteoclast activity, the effect of melatonin on osteoclasts under microgravity conditions is unknown. Teleost scale is a calcified tissue similar to mammalian bone. Building upon our previous study showing that melatonin suppresses osteoclastic activity in goldfish scales, the present study investigated the effects of melatonin on scale osteoclasts under modeled microgravity.

## Materials and methods:

Microgravity was modeled by a three-dimensional clinostat, in which two axes rotate simultaneously to randomize the gravity vector. Regenerating goldfish scales in 96-well plates were set on the clinostat and rotated for 4 days with or without melatonin in the culture medium. Plates with control scales were incubated in the same environment but were not set on the clinostat. At the end of the culture period, scales were fixed with paraformaldehyde. We detected tartrate-resistant acid phosphatase activity as a marker of osteoclasts and assessed the presence of actin rings that form at the matrix adherent site of resorbing osteoclasts. We also examined the presence of melatonin receptors in the regenerating scales by immunohistochemistry.

## Results and conclusion:

Modeled microgravity significantly increased the number of nuclei and the formation of actin rings in scale osteoclasts. Melatonin significantly suppressed the microgravity-induced multinucleation and actin ring formation but not to the same extent as that in the control condition. Melatonin receptors were detected in osteoblastic cells on the periphery of the osseous layer and the surface of the fibrillary plate. Therefore, melatonin appears to exert a suppressive effect on the differentiation and activation of osteoclasts under modeled microgravity by interacting with osteoblastic cells in the scales.

# Histomorphometric analysis of bone to assess safety and mechanical performance of low dose fluoride

**Michael Dray<sup>1)</sup>, Andrew Grey<sup>2)</sup>, Karen Callon<sup>2)</sup>, Maureen Watson<sup>2)</sup>,  
Dharshini Sreenivasan<sup>3)</sup>, Justine Fernandez<sup>3)</sup> and Jillian Cornish<sup>2)</sup>**

1) Histology Department, Waikato Hospital, New Zealand

2) Department of Medicine, University of Auckland, New Zealand

3) School of Engineering Sciences, University of Auckland, New Zealand

## Purposes:

To investigate the skeletal effects of low dose fluoride

## Materials and methods:

A cohort of 24 post-menopausal women from a larger group of 180 participants with osteopenia in a double-blind, placebo-controlled randomized trial volunteered for transiliac bone biopsy after tetracycline double labeling. Prior to preparation of undecalcified sections for histomorphometric analysis the alcohol fixed cores of bone underwent micro-CT scanning. Histomorphometric and micro-CT derived parameters relating to mineralization and trabecular bone structure were submitted for further computational modeling.

## Results:

23 of 24 biopsies were evaluable. Placebo, 2.5, 5, and 10mg fluoride per day groups showed differences in mineralization. Osteoid surface tended to be higher in the fluoride treated group,  $P=0.08$ , with values in 4 participants exceeding the published normal range. Osteoid volume was not different,  $P=0.17$ , although the same 4 participants exceeded the normal range. Osteoid thickness, mineralization lag time, and mineral apposition rate did not differ. Pooled data from the fluoride treated group showed an increase in osteoid surface  $P=0.02$ , and osteoid volume  $P=0.03$ , but no difference in other parameters. By comparison participants in an earlier trial who received 20mg/day for 4 years showed hyperosteoridosis and prolongation of mineralization lag time.

Computational modeling of the micro-CT structural data enabled estimation of bone strength, assessment of bone surface density, trabecular separation and intersection surface, in addition to percentage bone volume, trabecular thickness and trabecular number. This 3D data was compared to the measured 2D histomorphometric data.

Percentage bone volume was observed to be a strong surrogate for mechanical strength  $R^2=0.83$ , while bone surface density  $R^2=0.6$ , trabecular thickness  $R^2=0.5$ , and intersection surface  $R^2=0.6$ , showed moderate correlation. Trabecular separation  $R^2=0.31$ , and trabecular number  $R^2=0.35$ , were only mildly correlated. Substituting the 3D indices with 2D measurements decreased the correlation by up to 58%.

## Results and conclusion:

Even small doses of fluoride show mild impairment of mineralization and a tendency towards hyperosteoridosis without showing an anabolic effect on structural parameters. Micro-CT examination can give good structural data upon which to base computational modeling and assess bone strength. Dynamic mineralization and osteoid parameters to assess drug safety remain an important role of 2D histomorphometric analysis.

# **Craniofacial anomalies in cartilage calcification insufficient (CCI) rat**

**Hitoshi Amano<sup>1)</sup>, Kakei Ryu<sup>2)</sup>, Minoru Watanabe<sup>3)</sup>, Motohiko Nagayama<sup>4)</sup>,  
Shunichi Shibata<sup>5)</sup>, Junichi Tanuma<sup>4)</sup>, Masami Tanaka<sup>6)</sup>, Kiyoshi Ohura<sup>1)</sup>**

1) Osaka Dental University, Japan

2) Showa University School of Medicine, Japan

3) Inst. Animal Exp.St. Marianna University, Japan

4) Asahi University School of Dentistry, Japan

5) The University of Aizu, Japan

6) Tokyo Medical and Dental University, Japan

## **Purposes:**

The cartilage calcification-insufficient (CCI) rats were established as a naturally occurring dwarf mutant caused by an autosomal recessive mutation. Sprague-Dawley rat-derived CCI rats show impaired development accompanied by short limbs, tail and overall size reduction as systemic changes. In this study, we further characterize the craniofacial skeletal phenotype of the CCI rat strain.

## **Materials and methods:**

Carcasses of 4, 8 and 13-week-old rats were fixed in 4% neutral buffered glutaraldehyde solution after the skin and visceral organs had been removed [1]. The head and the bilateral femurs and tibias were excised. Radiograms were acquired using soft X-ray apparatus. Specimens were embedded in Epon 812 without decalcification. Two µm-thick sections were stained with toluidine blue and von Kossa stain. Other specimen were decalcified and embedded in paraffin using standard procedures. Serial 5 µm-thick sections were used for immunohistochemistry.

## **Results:**

CCI rats are characterized by systemic ossification deficiency of cartilage observed in soft X-ray and histological analyses. An immunohistochemical examination detected an aggrecan synthesis disorder, which might have led to delayed calcification and increased growth plate thickening in the dwarf rats. CCI rat exhibit that the mandibular bone moved forward as compared with maxillary bone, and an edge-to-edge bite phenotype associated with craniofacial dysmorphism.

## **Results and conclusion:**

We hypothesized that the principal characteristics of the CCI rats were systemically induced by insufficient cartilage calcification in their skeletal growth.

## **Temporal association of tensin 1 and p130Cas at focal adhesions links actin inward flux to cell migration**

**Zhihai Zhao<sup>1)</sup>, Song Hui Tan<sup>1)</sup>, Hiroaki Hirata<sup>1)</sup> and Yasuhiro Sawada<sup>1), 2)</sup>**

1) National University of Singapore, Singapore

2) National Rehabilitation Center for Persons with Disabilities, Japan

### **Purposes:**

p130Cas (Crk-associated substrate; hereafter Cas) has been reported to be involved in various cellular processes, including the mechano-sensing by which physical information is converted to a biochemical event (Sawada et al., Cell 2006). However, the molecular mechanism of how Cas relates to force-bearing or –generating cell machinery, i.e., actomyosin system, is poorly understood. We have recently reported that actomyosin contraction displaces Cas molecules from focal adhesions depending upon their phosphorylation, thereby promoting cell migration (Machiyama et al., J. Cell Sci. 2014). The purpose of this study is to further delineate the mechanism underlying the Cas dissociation from the adhesion complexes.

### **Materials and methods:**

An actin-binding protein tensin1 is tested as a candidate that links actin cytoskeletons to phosphorylated Cas at focal adhesions. We analyzed the co-localization of Cas and tensin1 with particular reference to the phosphorylation of Cas and the domain specificity of tensin1. We biochemically examined the phosphorylation-dependent, domain-specific interaction between Cas and tensin1 by GST-pull down or co-immunoprecipitation experiments. Conducting FRAP (fluorescence recovery after photobleaching) analysis using a TIRF (total internal reflection fluorescence) microscope, we examined whether tensin1 regulated the turnover of Cas molecules at focal adhesions.

### **Results:**

Analysis of the subcellular distribution reveals that tensin1 co-localizes with Cas, but not its phosphorylation-defective mutant at the cell lamellipodia. While a truncation mutant of tensin1 that lacks the phosphotyrosine-binding region, SH2PTB domain, does not co-localize with Cas, bacterially expressed recombinant tensin1-SH2PTB protein binds to Cas in vitro in a Cas phosphorylation-dependent manner. Furthermore, the exogenous expression of tensin1-SH2PTB, which is devoid of the actin-interacting motifs, interferes with the Cas-driven cell migration, slows down the inward flux of Cas molecules, and impedes the displacement of Cas molecules from focal adhesions.

### **Results and conclusion:**

Tensin1 transmits actomyosin contractility to adhesion sites by temporally binding to phosphorylated Cas, providing a clutch that supports cell migration.

## Poster Sessions

---





# Alveolar bone healing after the removal of temporary anchorage devices

**Eunji Kim, Yoon Jeong Choi, Kyung-Ho Kim, and Chooryung J. Chung**

Department of Orthodontics, Gangnam Severance Dental Hospital, College of Dentistry, Yonsei University, Korea

## Purposes:

Temporary anchorage devices (TADs) such as miniscrews are frequently used for contemporary orthodontic treatment. However, visible scarring is noted at the removal sites and the bone healing process after the removal of TADs is still unknown. Therefore, the purpose of the study is to evaluate the course of alveolar bone healing after the removal of orthodontic miniscrews.

## Materials and methods:

Total of 32 orthodontic miniscrews (1.6mm in diameter) were inserted in the interdental bone (both maxilla and the mandible) of two beagle dogs. Miniscrews were removed serially and calcein/ tetracycline was systemically injected for florescent labeling. Micro CTs were taken just after, 4,7, and 10 weeks after the removal the miniscrews (n=4). Bone volume (BV)/ tissue volume (TV) of the miniscrew removal sites were measured and compared to the neighboring interdental bone (control) followed by histologic evaluation of mineral apposition rate and bone formation rates of the interdental bone after the removal of miniscrews.

## Results:

Just after the removal, BV/TV of the removal sites was significantly reduced compared to the control interdental bone ( $p<0.05$ ). BV/TV was gradually increased and reached the levels of the control bone after 7 weeks in both the maxilla and the mandible. However, in some mandibular removal sites, rough irregular cortical surfaces were noted even after 10 weeks.

## Results and conclusion:

Because of the small diameter and atraumatic insertion and removal procedures of TADs, many clinicians expect complete healing after its removal. However, the removal of TADs leaves a transit full thickness defect penetrating the oral cavity, soft tissue and the underlying alveolar bone. Fortunately, BV/TV reached similar levels to the control after the period of 7 weeks in both the maxilla and the mandible indicating natural healing of the alveolar bone. However, some cortical surface roughness remained in the mandible even after 10 weeks. Thus, long term bone remodeling of the TAD removal sites should be monitored carefully in the clinical setting.

## **Inhibition of histone deacetylases enhances the osteogenic differentiation of human periodontal ligament cells**

**Nam Cong-Nhat Huynh<sup>1) 4)</sup>, Vincent Everts<sup>2)</sup>, Prasit Pavasan<sup>t 1) 3)</sup>,  
Ruchanee Salingcarnboriboon Ampornaramveth<sup>4)</sup>**

1) Mineralized Tissue Research Unit, Faculty of Dentistry Chulalongkorn University, Bangkok, Thailand.

2) Department of Oral Cell Biology, Academic Centre for Dentistry Amsterdam (ACTA), University of Amsterdam and VU University Amsterdam, Research Institute MOVE, Gustav Mahlerlaan 3004, 1081 LA Amsterdam, The Netherlands.

3) Department of anatomy, Faculty of Dentistry Chulalongkorn University, Bangkok, Thailand.

4) DRU in Oral Microbiology, Microbiology department, Faculty of Dentistry Chulalongkorn University, Bangkok, Thailand

The purpose of this study was to investigate the possible role of histone deacetylases (HDACs) in osteogenic differentiation of human periodontal ligament (hPDL) cells.

### **Methods:**

The activity of HDACs was blocked by using the inhibitor trichostatin A (TSA). The effect of TSA on proliferation and cytotoxicity of primary hPDL cells was tested by MTT assay. Osteogenic and adipogenic differentiation were induced in the presence of various concentrations of TSA. Gene expression was assessed by semi-quantitative and real time RT-PCR. ALP activity and mineral deposition assays were used to assess osteoblast phenotype. Western blotting was used to investigate the effect of TSA on histone acetylation and the expression of different HDACs.

### **Results:**

During the course of osteogenic differentiation in the presence of the HDAC inhibitor, osteoblast-related gene expression was increased by hPDL cells. ALP activity as well as bone nodule formation were also enhanced under these conditions. Inhibition of HDACs did not induce differentiation into the adipocyte lineage. hPDL highly expressed HDACs of both class I (HDAC 1, 2, 3) and class II (HDAC 4, 6). During osteogenic differentiation HDAC 3 expression gradually decreased. This was apparent in the absence and presence of the inhibitor. The level of acetylated Histone H3 was increased during osteogenic differentiation. Inhibition of HDAC activity induced hyperacetylation of Histone H3 therefore demonstrating Histone 3 as a candidate target molecule for HDAC inhibition in our model. In conclusion, hPDL cell express a distinguished series of HDACs and these enzymes appear to be involved in the osteogenic differentiation; their inhibition promotes the latter process.

# Principles of selection methods of radiation diagnosis of postmenopausal osteoporosis

**Zakharov IS, Kolpinskiy GI, Ushakova GA, Shkaraburov AS, Popova OP**

Russia, Kemerovo State Medical Academy

The main characteristic of osteoporosis is a decrease in bone mineral density (BMD). BMD determined radiation methods – dual energy X-ray absorptiometry (DXA) and quantitative computed tomography (QCT). Studies, including a comparative assessment of the diagnostic value of the QCT and the DXA in identifying postmenopausal osteoporosis, few (Bansal SC, 2011; Pickhardt PJ, 2011), and the question about the benefits of a particular method remains open. Given that most actively decreased bone mineral density in women occurred at the age of 50 years, comparing the results of different modalities of diagnostic imaging in the evaluation of BMD in postmenopausal women is relevant.

The aim of the study was a comprehensive assessment of indicators of bone mineral density in women aged 50 years and older by dual-energy X-ray absorptiometry and quantitative computed tomography.

## Material and methods:

The study included 210 postmenopausal women who are in the range of 1–2 weeks densitometry was performed by dual-energy X-ray absorptiometry and quantitative computed tomography. Depending on patient age were divided into four groups: I group (50–59 years, n=73), II group (60–69 years, n=58), III group (70–79 years, n=53), IV group (80 years and older, n=26).

## Results:

Assessment of BMD in women in the age group 50-59 years did not reveal significant differences in the results of densitometry. In carrying out the DXA osteoporosis was diagnosed in 15.1%, with QCT – 20.5% of the patients. From the age of 60 years and older incidence of osteoporosis by QCT was higher than in the DXA (44.8% and 24.1%, respectively,  $p=0.001$ ). In assessing the correlation was determined positive correlation of moderate intensity between the results of the DXA and the QCT, which decreased with increasing age, with a significant difference was observed with 70 years ( $p=0.02$ ). Probably, these results are due to age-related degenerative involutional processes in the vertebrae, causing occurs overstatement of the BMD during the DXA.

## Conclusions:

Thus, with increasing age of the women surveyed noted the discrepancy densitometry results depending on the method used. Women after 60 years of age is recommended densitometry by QCT to improve the quality of diagnosis of osteoporosis.

## **TGF-beta impairs cilia morphology via suppression of Ift88 expression in chondrocytic ATDC5 cells**

**Makiri Kawasaki, Tadayoshi Hayata, Tetsuya Nakamoto, Takuya Notomi, Shuichi Moriya, Takayuki Yamada, Yayoi Izu, Yoichi Ezura, Masaki Noda**

Tokyo Medical and Dental University, Japan

### **Purposes:**

Osteoarthritis is a serious disease affecting over 25 million patients, while molecular and cellular bases are still incompletely understood. Cilium is a critical structure for chondrocytes and cartilage. However, how this structure is controlled by cytokines that play critical roles in osteoarthritis is not well understood. Therefore, we examined the effects of TGF beta on the morphology of cilia in a chondrocytic cell line, ATDC5.

### **Materials and methods:**

We cultured ATDC5 cells under the presence of various concentrations of recombinant human TGF beta. For immunocytochemistry, primary cilia were stained with anti-acetylated alpha-tubulin. Real-time PCR was performed using SYBR Green after RNA extraction and subsequent reverse transcription.

### **Results:**

TGF beta treatment reduced the number of cilia positive cells. TGF beta treatment not only reduced the cilia positive cell population size but also suppressed the average length of cilia. Analysis of cilia length variation indicated that TGF beta treatment reduced mode, median and minimum lengths of cilia. Interestingly, maximum length of cilia was not affected indicating the heterogeneity in the sensitivity of length parameters to TGF beta treatment. As a mechanism for this action, TGF beta suppressed Ift88 mRNA expression in ATDC5 cells. TGF beta suppressed the levels of Ift88 mRNA in a dose-dependent manner starting from as low as 0.5 ng/ml and reaching maximal at around 2 ng/ml. TGF beta suppressed the protein levels of Ift88. TGF beta suppression was not affected by the presence of a protein synthesis inhibitor and a transcriptional inhibitor. In contrast, TGF beta treatment suppressed the levels of Ift88 mRNA stability. Knockdown of Ift88 by siRNA enhanced TGF beta-induced increase in type II collagen mRNA expression revealing the suppressive role of Ift88 on TGF beta-induced regulation of extracellular matrix protein expression.

### **Results and conclusion:**

TGF beta impairs cilia morphology via suppressing Ift88 posttranscriptionally and this suppression leads to further enhancement of TGF beta-induced increase in the expression of extracellular matrix protein.

# Membrane depolarization regulates intracellular RANKL transport in non-excitabile osteoblasts

**Takuya Notomi<sup>1)</sup>, Miyuki Kuno<sup>2)</sup>, Yoichi Ezura<sup>3)</sup>, Kiyoshi Ohura<sup>1)</sup>, and Masaki Noda<sup>3)</sup>**

1) Osaka Dental University, Japan

2) Osaka City University, Japan

3) Tokyo Medical and Dental University, Japan

Parathyroid hormone (PTH) are important factors in  $\text{Ca}^{2+}$  homeostasis, and promote osteoclastogenesis by modulating receptor activator of nuclear factor kappa-B ligand (RANKL) mRNA expression. However, their contribution to RANKL intracellular transport, including the trigger for RANKL lysosomal vesicle fusion to the cell membrane, is unclear. In neurons, depolarization of membrane potential increases intracellular  $\text{Ca}^{2+}$  level ( $[\text{Ca}^{2+}]_i$ ) and promotes neurotransmitter release via fusion of synaptic vesicles to the cell membrane. To determine whether membrane depolarization also regulates cellular processes such as RANKL intracellular transport in MC3T3-E1 osteoblasts (OBs), we generated a light-sensitive OB cell line and developed a system for altering their membrane potential via delivery of a blue light stimulus. In the membrane fraction of RANKL-overexpressing OBs, PTH increased membrane-bound RANKL 10 min after application without affecting the mRNA expression level, and depolarized the cell membrane while transiently increasing  $[\text{Ca}^{2+}]_i$ . In our novel OB line stably expressing channelrhodopsin, wide receiver blue light-induced depolarization increased membrane-bound RANKL, which was reversed by blockers for voltage-gated  $\text{Ca}^{2+}$  channels and  $\text{Ca}^{2+}$  release from endoplasmic reticulum. In co-cultures of osteoclast precursor-like RAW264.7 cells and light-sensitive OBs overexpressing RANKL, light stimulation induced an increase in tartrate-resistant acid phosphatase activity and promoted osteoclast differentiation. These results indicate that depolarization of the cell membrane is a trigger for RANKL lysosomal vesicle fusion to the membrane, and that membrane potential contributes to the function of non-excitabile OBs. Elucidating the mechanism of RANKL intracellular transport regulation by PTH will be useful for the development of drugs to prevent bone loss in osteoporosis and other bone diseases.

## **Poldip2 is expressed in osteoblasts and its expression is enhanced by osteogenic differentiation medium containing beta glycerophosphate and ascorbic acid or BMP.**

**Sakie Katsumura, Yoichi Ezura, Yayoi Izu, Takayuki Yamada, Kiyoshi Harada, Kathy Griendling, Masaki Noda**

Tokyo Medical and Dental University, Japan

Emory University School of Medicine, Atlanta, USA

### **Purposes:**

Osteoporosis is a bone disease that is characterized by a decrease in bone mass and density. This decrease is due to the imbalance of bone formation by osteoblasts and bone resorption by osteoclasts. Osteoblastic cells are under the control of oxidative stress, cell adhesion, aging and cell cycle progression. One of the molecules related to these modulating components is Poldip2. Poldip2 binds to p22phox and activates NADPH oxidase 4 (Nox4). This Nox4 is required for BMP2-induced alkaline phosphatase as well as BMP2 gene expression in osteoblasts. However, it is not known whether Poldip2 is expressed in osteoblasts and if so, whether expression of this gene is regulated in osteoblasts. Therefore, we examined these points by using osteoblast-like cell line, MC3T3E1 cells.

### **Materials and methods:**

Osteoblast like MC3T3E-1 were cultured in  $\alpha$ -medium in the presence or the absence of BMP2. Some cultures were conducted in the presence or the absence of ascorbic acid and  $\beta$ -glycerophosphate. The expression levels of Poldip2 and osteoblast-related mRNAs were examined based on real-time PCR.

### **Results and Conclusion:**

We first examined the expression of Poldip2 mRNA in the cell cultures of MC3T3E1 cells and found that these cells express Poldip2 mRNA constitutively. When the cells were cultured in the presence of beta glycerophosphate and ascorbic acid (osteogenic medium) to induce differentiation, Poldip2 mRNA levels were increased along with time course in conjunction with the increase of alkaline phosphatase mRNA. These observations indicate that Poldip2 is not only expressed in osteoblasts but its expression is regulated developmentally in these cells. As it was reported that one of the factors that could play a role in such osteogenic medium would be BMP, we further examined whether BMP alone regulates Poldip2 mRNA expression in these osteoblasts. BMP treatment enhanced the expression of Poldip2 mRNA in these osteoblasts. This BMP effect was time dependent with a peak at 24 hours of the treatment. We further examined if BMP effects on Poldip2 is dependent on dosage of BMP. Treatment with 50ng/ml BMP did not significantly enhance Poldip2 mRNA expression while 100ng/ml BMP significantly enhance the expression of Poldip2 mRNA in these osteoblastic cells. These data indicated that Poldip2 is one of the BMP target genes in osteoblasts.

# **Bone regeneration is increased with local application of Lactoferrin in critical-sized rat calvarial defects**

**Maureen Watson<sup>1</sup>, Ryan Gao<sup>1</sup>, Karen Callon<sup>1</sup>, Donna Tuari<sup>1</sup>, Jacob Munro<sup>2</sup>, David Musson<sup>1</sup>, Jillian Cornish<sup>1</sup>**

1) University of Auckland, Auckland, New Zealand

2) Department of Orthopaedic Surgery, Auckland District Health Board, New Zealand

## **Purposes:**

Lactoferrin is an iron-binding glycoprotein which is present in milk and exocrine secretions in mammals. In vitro, lactoferrin functions as a potent bone anabolic factor by increasing the proliferation, differentiation and survival of osteoblasts and by inhibiting osteoclastogenesis. In vivo, local injection of lactoferrin above the hemicalvaria of adult mice results in substantial increases in the dynamic histomorphometric indices of bone formation and bone area. The objective of this study was to assess the ability of bovine lactoferrin to increase bone regeneration in a rat critical-sized calvarial defect model.

## **Materials and methods:**

Critical-sized defects (5mm diameter) were created in the right parietal bone of 60 male Sprague-Dawley rats with the left parietal bone used as a contralateral control. The rats were randomised into three groups: Group 1- empty defect; Group 2-collagen gel and Group 3- collagen gel containing 10µg bovine lactoferrin. The rats were sacrificed at 4 or 12 weeks post-operatively and the calvaria were imaged by micro-CT (Skyscan 1172) with a 12µm voxel size. Cylindrical volumes of interest were created and the percentage of bone formed in the defect was calculated and referenced to the contralateral control.

## **Results:**

The relative percentage of new bone formation in the defects, at both 4 and 12 weeks was significantly greater in the group treated with lactoferrin compared with other groups. The relative percentage of new bone formation in groups 1, 2 and 3 was 42.7±4.2%, 35.9±5.9% and 62.6±2.5%, respectively, at 4 weeks (P=0.0019); and 41.3±5.2%, 45.8±4.8% and 74.6±4.3%, respectively, at 12 weeks (P<0.0001).

## **Results and conclusion:**

This study demonstrated that local application of lactoferrin significantly increased bone regeneration in a rat critical-sized calvarial defect model. These findings suggest that lactoferrin has therapeutic potential for the treatment of bony defects and fracture non-union.



## **Collagens VI and XII form complexes mediating osteoblast interaction during osteogenesis.**

**Yayoi Izu <sup>1)</sup>, Yoichi Ezura <sup>1)</sup>, Manuel Koch <sup>2)</sup>, David E. Birk <sup>3)</sup>, Masaki Noda <sup>1)</sup>**

1) Tokyo Medical and Dental University, Japan

2) University of Cologne, Germany

3) University of South Florida, USA

### **Purposes:**

Ullrich congenital muscular dystrophy (UCMD) and Bethlem myopathy (BM) are diseases representing overlapping phenotypes of connective tissue and muscle. Both diseases are caused by genetic mutations in the genes encoding collagen VI. Recently COL12A1 gene mutations were identified in UCMD and BM-like patients harboring no COL6 mutations, indicating shared functions of these collagens for connective tissue homeostasis. We have previously demonstrated that the genetic deletion of Col6a1 or Col12a1 in mice cause bone mass reduction and fragility. The purpose of this study is to determine whether collagens VI and XII have coordinate regulatory role (s) during bone formation.

### **Materials and methods:**

Primary osteoblasts were obtained from neonatal mouse calvariae and were cultured in a medium supplemented with 10% FBS or osteogenic medium. The cells were harvested on day 2, 4, and 11 and then analyzed based on immunofluorescence microscopy using antibodies against collagen I, VI, and XII.

### **Results:**

The double staining analysis revealed that co-localization of collagen VI and XII was detected in the matrix bridges between adjacent cells on day 2 and 4 when osteoblasts were still considered in migration and proliferation phase. On the other hand, collagen I was localized in a region close to the cell surface where it colocalized with collagen XII. The percentage of the cells harboring collagens bridges was analyzed based on the immunostaining, demonstrating that matrix bridges were made via collagen VI and XII but not via collagen I.

### **Conclusion:**

Our data indicate that collagen VI and XII have a novel coordinate function in the formation of cell communicating networks at bone forming sites during bone formation.

# A rankl-binding peptide accelerates BMP-induced bone regeneration in murine maxilla by subperiosteal injections.

**Tomoki Uehara<sup>1)</sup>, Setsuko Mise<sup>2)</sup>, Yuki Arai<sup>3)</sup>, Yasutaka Sugamori<sup>2)</sup>, Genki Kato<sup>2)</sup>, Yukihiro Tamura<sup>2)</sup>, Yasuhiko Tabata<sup>4)</sup>, Ramachandran Murali<sup>5)</sup>, Noriyuki Wakabayashi<sup>3)</sup>, Michiyo Miyashin<sup>1)</sup>, Kazuhiro Aoki<sup>2)</sup>**

- 1) Department of Pediatric Dentistry, Division of Oral Health Sciences, Graduate School, Tokyo Medical and Dental University (TMDU), Japan
- 2) Section of Pharmacology, Department of Bio-matrix, Graduate School, TMDU, Japan
- 3) Section of Removable Partial Prosthodontics, Department of Masticatory Function Rehabilitation, Graduate School, TMDU, Japan
- 4) Department of Biomaterials, Field of Tissue Engineering, Institute for Frontier Medical Sciences, Kyoto University, Japan
- 5) Department of Biomedical Sciences, Cedars-Sinai Medical Center, Los Angeles, CA, USA

## Purposes:

Although the beneficial effects of recombinant human BMP-2 on bone regeneration have been shown in many clinical cases, recent evidences clearly revealed that BMP-2 increased cancer risk. To decrease the cancer risk, the BMP-2 amount needs to be reduced. Several cytokines has already known to be effective to reduce a BMP amount to accelerate BMP-2-induced bone tissue, but the protein drug is tend to cause sometimes life-compromising side effects. We have recently developed peptide X, which binds to receptor activator of NF- $\kappa$ B ligand (RANKL), thereby having the bone resorption inhibitory activities. Since the other RANKL-binding peptide WP9QY can accelerate bone formation, we hypothesized that this peptide X could have the same effect. The aim of this study is to investigate whether peptide X can promote BMP-2- induced bone formation in murine maxilla. In this study, we have developed a unique drug delivery system to induce bone formation at the site of injection toward a clinical application using this peptide X.

## Materials and methods:

Twenty-four eight-week-old male C57BL/6J mice were used. Gelatin hydrogel was used as a carrier of the peptide X and BMP-2. Mice were divided into 4 groups (n=6) depending on materials incorporated in the carrier; 1) BMP-2(1  $\mu$ g), 2) BMP-2(1  $\mu$ g) + peptide X (0.56 mg), 3) BMP-2(1  $\mu$ g) + control peptide (0.56 mg) or 4) vehicle. Those carriers were subperiosteally injected into the maxillary diastema between the right incisor and the first molar. Calcein and demeclocycline were subcutaneously injected on day 12 and 26, respectively. The mice were sacrificed 4 weeks after the subperiosteal injections, and the local bone formation was analyzed radiologically and histologically.

## Results and conclusion:

Micro-CT analyses showed the highest radio-opacity at the site of injection in the group 2) compared with the other experimental groups. Bone mineral density and bone mineral content measured by pQCT confirmed these observations. Histomorphometric analyses revealed that demeclocycline-labeled area was significantly increased in the group 2) compared with the other 3 groups. Interestingly, calcein-labeled area was observed outside of the demeclocycline-labeled area. These results suggest that peptide X could accelerate the bone regenerating efficiency induced by BMP-2.

## **BMP-2 induction of LGR4 expression in osteoblastic MC3T3-E1 cells.**

**Chantida Pawaputanon na mahasarakham<sup>1,2)</sup>, Makiri Kawasaki<sup>1)</sup>, Shuichi Moriya<sup>1)</sup>, Takayuki Yamada<sup>1)</sup>, Yayoi Izu<sup>1)</sup>, Yoichi Ezura<sup>1)</sup>, Katsuhiko Nishimori<sup>3)</sup> Yuichi Izumi<sup>2)</sup>, Masaki Noda<sup>1)</sup>**

1) Department of Molecular Pharmacology, Medical Research Institute, Tokyo Medical and Dental University, Japan

2) Department of Periodontology, Tokyo Medical and Dental University, Japan

3) Graduate School of Agricultural Science, Tohoku University, Japan

### **Purposes:**

The leucine-rich repeat containing G protein-coupled receptor4 (LGR4) is a subfamily of GPCRs that plays an important role in stem cell/progenitor proliferation. A nonsense mutation of LGR4 was found to be associated with several human diseases. Strikingly, this mutation is strongly associated with low BMD and osteoporotic fractures. Consistently, the deletion of LGR4 in mice have delayed embryonic and postnatal bone formation and down-regulated Runx2, Atf4, Ocn and Bsp. LGR4 is also thought to play a potential role in osteoblast differentiation and bone formation. However, the regulation of LGR4 expression in osteoblasts is not known. The present study therefore examines the effects of BMP2 on LGR4 expression in osteoblast-like MC3T3-E1.

### **Materials and methods:**

Osteoblast like MC3T3-E1 cells were cultured in medium supplemented with or without BMP2. The expression levels of LGR4 and osteogenic-related mRNAs were examined based on real-time RT-PCR. Furthermore, the function of LGR4 on BMP signaling-induced transcription was analysed by examining the influence of the down regulation of LGR4 on BMP response element (BRE)-luciferase activity.

### **Results and conclusion:**

We examined the response of LGR4 in Osteoblast like MC3T3-E1 cells. These cells expressed LGR4 mRNA and its baseline levels slightly declined along with time course. BMP2 treatment enhanced the expression of LGR4 mRNA level. This enhancement started at 10hours after BMP2 treatment in MC3T3-E1 osteoblastic cells and peaked at 24 hours and then, maintained for 3 days. BMP2 enhanced LGR4 mRNA levels in these cells in a dose-dependent manner starting at 10ng/ml and saturated at 50-100ng/ml. BMP2 enhancement of LGR4 expression was no longer observed in the presence of a transcriptional inhibitor, DRB, and a protein synthesis inhibitor, CHX. Therefore, LGR4 is regulated in a manner at least in part through transcriptional events and requires new protein synthesis. The knockdown of LGR4 down-regulated the mRNA expression of OSX, ALP and BSP. Finally, LGR4 mRNA knockdown also enhanced the BRE-reporter expression.

### **Conclusion:**

Our data reveal for the first time that LGR4 is a novel target for BMP in these cells.

# Paradoxical effects of partial leptin deficiency on bone in growing female mice

**Kenneth A. Philbrick<sup>1</sup>, Russell T. Turner<sup>1</sup>, Adam J. Branscum<sup>2</sup>, Carmen P. Wong<sup>1</sup>, and Urszula T. Iwaniec<sup>1</sup>**

1) Skeletal Biology Laboratory, School of Biological and Population Health Sciences, Oregon State University, Corvallis, OR, 97331, USA

2) Biostatistics Program, School of Biological and Population Health Sciences, Oregon State University, Corvallis, OR, 97331, USA

## Purpose:

Morbidly obese, leptin-deficient ob/ob mice display low bone mass, mild osteoclast-rich osteopetrosis, and increased bone marrow adiposity. Partial leptin deficiency results in increased weight. However, the skeletal manifestations of partial leptin deficiency are not well defined. We therefore analyzed femora and lumbar vertebrae in growing (7-week-old) female C57BL/6 wildtype (WT) mice, partial leptin-deficient ob/+ mice, and leptin-deficient ob/ob mice.

## Materials and methods:

Bones were evaluated by dual energy absorptiometry, microcomputed tomography, and histomorphometry.

## Results:

As expected, ob/+ mice were heavier, had more white adipose tissue, and lower serum leptin than WT mice, but were lighter and had less white adipose tissue than ob/ob mice. Bone mass, density and indices of bone architecture in ob/+ mice were not intermediate between WT mice and ob/ob mice. In general, cancellous bone architecture, cell (osteoblast, osteoclast, and adipocyte), and dynamic measurements were similar between WT and ob/+ mice. In contrast, ob/ob mice differed from WT and ob/+ mice in that ob/ob mice had lower cancellous bone volume fraction and higher bone marrow adiposity in the femur metaphysis, and higher cancellous bone volume fraction in lumbar vertebra. Paradoxically, ob/+ mice had greater femoral cross-sectional bone volume, cortical volume, marrow volume, and polar moment of inertia than WT mice and longer femora and higher bone mineral content and bone volume compared to either WT or ob/ob mice. There was a positive correlation between body weight and femur volume in all three genotypes. However, the positive effect of body weight on bone volume occurred at much lower body weight in mice that produced leptin.

## Conclusions:

The paradoxical differences in bone size among WT, ob/+, and ob/ob mice may be explained if leptin, in addition to stimulating bone growth and cancellous bone turnover, acts directly or indirectly to lower the set-point at which increased body weight leads to a commensurate increase in bone size.

## **Osteocytes in primary cultures express higher levels of $\beta_2$ -adrenergic receptor mRNA while MLOY4 cells exhibit culture period dependent regulation of the expression levels.**

**Koji Mineta , Yoichi Ezura ,Yayoi Izu , Masaki Noda**

Department of Molecular Pharmacology, Medical Research Institute, Tokyo Medical & Dental University, Japan

### **Introduction**

Osteocytes are becoming more considered to play key roles in regulation of bone metabolism in addition to the actions of osteoblasts and osteoclasts. Osteocytes have been reported to express RANKL, FGF23, Phex, Sost and DMP-1. Although osteocytes are consisting about 90% of the cells in bone, full repertoire of its actions is still incompletely understood. One of the functions of osteocytes is considered to be the mediation of mechanical stimuli to bone. Based on the unloading-induced bone loss model using tail suspension, sympathetic tone has been suggested to be related to such unloading-induced bone loss. However, the profile of sympathetic signaling-related molecules in osteocytes is not well understood. Sympathetic tone suppresses bone formation and enhances bone resorption in way similar to unloading-induced modulation of each arms of bone metabolism. In particular,  $\beta_2$  adrenergic receptor (Adrb<sub>2</sub>) is a major entry point of sympathetic tone. Isoproterenol binds to  $\beta_2$  adrenergic receptor and enhances osteopontin expression while loss of osteopontin attenuates  $\beta_2$  adrenergic receptor related events. Since osteopontin is also required for the unloading-induced bone loss on both side of suppression of bone formation and enhancement of bone resorption and it is expressed in osteocytes, we focused on the expression of  $\beta_2$  adrenergic receptor in osteocytes.

### **Methods**

Primary osteocytes were obtained from 7-week-old mouse long bones. The cells were separated into early fractions (2-4) and late fraction (5-9). The cells were cultured for 10 days. These cells were subjected to the analyses of mRNA expression of osteocyte markers (Sost, Dmp1, Phex, Fgf23), osteoblast markers (Alp, Col1a1) and Adrb<sub>2</sub> by real-time PCR. MLO-Y4 cells were also used.

### **Results and Conclusion**

We found that mRNA of Adrb<sub>2</sub> was expressed in primary osteocytes obtained from 7-week-old mice. When comparing diverse fractions, we observed that cells in late fractions (5-9) demonstrated high levels of mRNA of Adrb<sub>2</sub> in association with high levels of osteocyte markers including Dmp1 and Fgf23. In contrast, cells in early fractions (2- including 4) expressed lower levels of mRNA of Adrb<sub>2</sub> in association with high levels of osteoblast markers alkaline phosphatase. We also found that an osteocytic cell line MLO-Y4 expressed mRNA of Adrb<sub>2</sub>. The levels of Adrb<sub>2</sub> mRNA expression in MLO-Y4 altered in a culture period dependent manner. When MLO-Y4 cells were cultured for longer period of time, the levels of expressed mRNA of Adrb<sub>2</sub> were declined. These result suggest that primary cultures of osteocytes and osteocytic cell line MLO-Y4 express  $\beta_2$  adrenergic receptor.

## Potential role of osteocyte in the fracture healing: comparison of fishes with and without osteocytes

**Mari Sato<sup>1</sup>, Tatsuya Shimizu<sup>1</sup>, Takashi Okubo<sup>2</sup>, Takuya Hosoki<sup>3</sup>, Masato Tamura<sup>1</sup>, Itsuro Koizumi<sup>2</sup>**

1) Biochemistry and Molecular Biology, Graduate School of Dental Medicine., Hokkaido Univ., Japan,

2) Animal Ecology, Graduate School of Environmental Earth Science, Hokkaido Univ., Japan,

3) School of Fisheries Science, Hokkaido Univ., Japan

### Purposes:

The human have acquired bones with osteocytes through evolution. However, it is a mystery why our bones need osteocytes. Interestingly, many fishes have bone that lack osteocytes, whereas all other vertebrates have osteocytes. However, it remains unclear when and why some fishes have acquired or lost osteocytes. Bone fracture caused by predatory attacks and aggressive competitions may be one of the lethal factors for fishes, living in hard environment exposed various mechanical stress such as big waves or rapid flows. In human and some other mammals osteocytes contribute to bone homeostasis by converting mechanical stress to biological signals. Therefore, osteocytes may be involved in the acceleration of fracture healing by mechanical stimuli including ultrasound stimulation. In this study, we examined the effect of low-intensity pulsed ultrasound (LIPUS) for the fracture healing in two types of fish which have bones with or without osteocytes. Our goal is to understand the adaptive significance of osteocytes, especially solving the enigma of fish bones without osteocytes.

### Methods:

Zebrafish and medaka were our study species that have bones with and without osteocytes, respectively. We fractured the bones in caudal fin rays using sharp-edged tungsten needles. 1 day after fracture, fishes were stimulated by LIPUS (Teijin) every day. The process of fracture healing was determined by Alizarin red and Alcian blue staining.

### Results and conclusion:

We decided the point at which the fracture healing finished was when we could observe Alizarine red-positive calcified smooth new bone. Medaka required around 24 days to complete fracture healing, whereas zebrafish required only around 18 days. LIPUS stimulation accelerated the healing periods significantly only in zebrafish. These results suggest that bone with osteocytes may have an advantage in the bone fracture healing and acceleration of it by LIPUS in fishes, although we cannot rule out other possibilities (e.g. higher metabolic rate). In future studies, we will increase sample sizes and also use other fish species with or without osteocytes. We will also investigate the correlations between fishes with/without osteocytes and their habitats, ecology, and evolutionary histories.

## **Dullard/Ctdnep1 regulates endochondral ossification via suppression of TGF- $\beta$ signaling**

**Tadayoshi Hayata<sup>1,2)</sup>, Yoichi Ezura<sup>3)</sup>, Makoto Asashima<sup>4)</sup>, Ryuichi Nishinakamura<sup>5)</sup>, Masaki Noda<sup>3)</sup>**

1) Department of Biological Signaling and Regulation, Faculty of Medicine, University of Tsukuba, Japan

2) Ph.D. Program in Life Science Innovation, University of Tsukuba

3) Department of Molecular Pharmacology, Medical Research Institute, Tokyo Medical and Dental University, Japan

4) Research Center for Stem Cell Engineering, National Institute of Advanced Industrial Science and Technology (AIST), Japan

5) Department of Kidney Development, Institute of Molecular Embryology and Genetics, Kumamoto University, Japan

Transforming growth factor (TGF)- $\beta$  signaling plays critical roles during skeletal development and its excessive signaling causes genetic diseases of connective tissues including Marfan syndrome and acromelic dysplasia. However, the mechanisms underlying prevention of excessive TGF- $\beta$  signaling in skeletogenesis remain unclear. We previously reported that Dullard/Ctdnep1 encoding a small phosphatase is required for nephron maintenance after birth through suppression of bone morphogenetic protein (BMP) signaling. Unexpectedly, we found that Dullard is involved in suppression of TGF- $\beta$  signaling during endochondral ossification. Conditional Dullard-deficient mice in the limb and sternum mesenchyme by Prx1-Cre displayed the impaired growth and ossification of skeletal elements leading to postnatal lethality. Dullard was expressed in early cartilage condensations and later in growth plate chondrocytes. The tibia growth plate of newborn Dullard mutant mice showed reduction of the proliferative and hypertrophic chondrocyte layers. The sternum showed deformity of cartilage primordia and delayed hypertrophy. Micromass culture experiments revealed that Dullard deficiency enhanced early cartilage condensation and differentiation, but suppressed mineralized hypertrophic chondrocyte differentiation, which was reversed by treatment with TGF- $\beta$  type I receptor kinase blocker LY-364947. Dullard deficiency induced upregulation of protein levels of both phospho-Smad2/3 and total Smad2/3 in micromass cultures without increase of Smad2/3 mRNA levels, suggesting that Dullard may affect Smad2/3 protein stability. The phospho-Smad2/3 level was also upregulated in perichondrium and hypertrophic chondrocytes in Dullard-deficient embryos. Response to TGF- $\beta$  signaling was enhanced in Dullard-deficient primary chondrocyte cultures at late, but not early, time point. Moreover, perinatal administration of LY-364947 ameliorated the sternum deformity in vivo. Thus, we identified Dullard as a new negative regulator of TGF- $\beta$  signaling in endochondral ossification.

# Masticatory activity affects bone remodeling in mice

**Huayue Chen<sup>1)</sup>, Takao Senda<sup>1)</sup>, and Kin-ya Kubo<sup>2)</sup>**

1) Gifu University Graduate School of Medicine, Japan

2) Seijoh University, Japan

## Purposes:

Mastication is very important not only for food intake, but also for preserving and promoting the general health.

We hypothesize that mastication affects bone health. To test this hypothesis, we examine the effects of masticatory activity on bone remodeling in mice.

## Materials and methods:

We used male senescence-accelerated mouse strain P8 (SAMP8). For masticatory dysfunction experiment, mice were divided into control and toothless groups. All upper molar teeth were removed at 1 month of age in toothless group. Bone response was evaluated at 2, 5 and 9 months. For active mastication experiment, mice were divided into control, stress, and stress/chewing groups. Mice in the stress and stress/ chewing groups were placed in a ventilated restraint tube for 60minutes, twice a day for 4weeks. The restrained mice were simultaneously subjected daily to one of the following stressors: water immersion, physical shaking and flashing lights. Mice in the stress/chewing group were allowed to chew a wooden stick during the experimental period. After experiments, bone response was evaluated using quantitative micro computed tomography, bone histomorphometry, and biochemical markers.

## Results and conclusion:

Tooth loss caused an increase in circulating corticosterone level with age. Bone formation was suppressed, bone resorption was activated, and trabecular bone volume fraction of vertebra and femur was decreased in the toothless mice with age. Chewing under chronic stress prevented the increase in circulating corticosterone level. Exposure of mice to chronic stress resulted in a reduction of bone formation and an activation of bone resorption. Chewing under chronic stress improved reduced bone formation, activated bone resorption and trabecular bone loss. The present findings indicated that tooth loss induced masticatory dysfunction, impaired dynamic homeostasis of bone formation and bone resorption, leading to reduced bone strength with age. Active mastication can ameliorate chronic stress-induced bone loss in mice.



## **β2-adrenergic receptor expression in osteoblastic MC3T3-E1 cells is regulated by PTH**

**Shuichi Moriya<sup>1,2)</sup>, Tadayoshi Hayata<sup>1)</sup>, Takayuki Yamada<sup>1)</sup>, Jumpei Shirakawa<sup>1)</sup>, Makiri Kawasaki<sup>1)</sup>, Kazuo Kaneko<sup>2)</sup>, Yoichi Ezura<sup>1)</sup>, Masaki Noda<sup>1)</sup>**

1) Tokyo Medical & Dental University, Medical Research Institute, Japan

2) A Department of Orthopaedic Surgery, Juntendo University School of Medicine, Japan,

### **Purposes:**

The molecular bases underlying the regulation of bone mass and remodeling are still incompletely understood. Beta2 adrenergic receptor and a receptor for parathyroid hormone (PTH) are co-expressed in osteoblasts. PTH acts as an anabolic agent for bone used for osteoporosis. However, whether beta2 adrenergic receptor is under the regulation by PTH or no is not still to be elucidated. We therefore examined the effects of PTH in beta2 adrenergic receptor gene expression in osteoblastic cells.

### **Materials and methods:**

Osteoblastic cell line, MC3T3E1 were used for all experiments. si-RNA for ADRB2 or control si-RNA, RNAs from cells were subjected to quantitative RT-PCR. cyclic AMP response element Luciferase assay and Western blot for cyclic AMP response element binding protein (CREB) antibody and phosphorylation CREB antibody of analyses were carried out.

### **Results:**

The expression levels of beta2 adrenergic receptor mRNA was immediately suppressed by PTH treatment. This PTH-induced ADRB2 mRNA suppression was observed in a dose-dependent manner. A transcriptional inhibitor, DRB, inhibited such PTH effects while by a protein synthesis inhibitor, cycloheximide did not, suggesting direct transcription control. In terms of function, we observed that knockdown of beta2 adrenergic receptor enhanced PTH-induced expression of c-fos, an immediate early response gene. With respect to molecular bases for this phenomenon, knockdown of beta2 adrenergic receptor enhanced PTH induced transcriptional activity of cyclic AMP response element-luciferase construct in osteoblasts. Knockdown of beta2 adrenergic receptors tended to enhance caPPR (constitutive active mutant of PTH receptor, H223R)-induced luciferase expressions. Finally, knockdown of beta2 adrenergic receptor enhanced base line level as well as PTH-induced phosphorylation of cyclic AMP response element binding protein (CREB).

### **Conclusion:**

Our data reveal that PTH regulates beta2 adrenergic receptor as a hormonal target suppresses beta2 adrenergic receptor in osteoblasts.

# Quantification analysis of cranial bones development among primates species using geometric morphometrics method

**Wataru Yano<sup>1)</sup>, Takeshi Nishimura<sup>2)</sup>, Ryuta Watanabe<sup>1)</sup>, Kazuhiko Satoh<sup>1)</sup>,  
Sadakazu Ejiri<sup>1)</sup>**

1) Asahi University, School of Dentistry, Japan

2) Primates Research Institute, Kyoto University, Japan

Cranial morphology plays a particularly important role in the primate evolution. Although the previous studies<sup>1,2</sup> elucidated cranial variation among extant primates, it is unknown the timing and location in which cranial bone components accelerate/retard. The knowledge is, however, essential in linking the morphological evolution of primates skull with potential physical and physiological factors inducing them. The growth pattern of each bones, yet, were not easily quantified with traditional linear measurements due to the complex configuration and articulation of cranial bones. New morphological techniques are anticipated to quantify cranial bone configuration in high dimensions.

## Purposes:

We aimed to identify the timing and location of bone growth crucial for the phylogenetic variation by quantification of cranial form of three primates species (Chimpanzee, Japanese macaque and Baboon) using the Geometric morphometrics method (GM).

## Materials and methods:

Dried crania of three primates species (Chimpanzee (n=8), Japanese macaque (n=18) and Baboon (n=16)) were used. The specimens are CT-scanned and external surface models are reconstructed. 31 anatomical landmarks and 46 semilandmarks were dotted on the sagittal plane to trace the outline of 12 bone parts. By defining the total variance of landmark coordinates as a quantity of form difference, the form information of each specimen was projected onto the high dimensional shape space. Subsequently, they were decomposed into scaling, rotation, transition, and non-affine deformation factors. The relative growth score is calculated by standardizing them with the score of maximum adult specimens. Then, the temporal change is induced by regressing these scores by the size of whole cranium as time proxy.

## Results and conclusion:

The original GM method successfully quantified the shape of cranial bones in high dimensions. Based on relative growth scores, we identified crucial change of developmental pattern which leads to the cranial shape evolution, specifically relative retardation of palatine bone growth and accelerated development of premaxilla in Chimpanzees. The method and data of this study will underlie the future study on human craniofacial evolution.

<sup>1</sup> Yano, Wataru, et al. *Primates* 51.3 (2010): 263-271.

<sup>2</sup> Nishimura, Takeshi D., Yano, Wataru, et al. *Anthropological Science* 122.2 (2014): 101-113.

## Deletion of Pfn1 have an effect on bone formation

**Wanting Lin<sup>1),2)</sup>, Yoichi Ezura<sup>1)</sup>, Yayoi Izu<sup>1)</sup>, Keiji Moriyama<sup>2)</sup>, Masaki Noda<sup>1)</sup>**

1) Department of Molecular Pharmacology, Medical Research Institute, Tokyo Medical and Dental University, Tokyo, Japan

2) Department of Maxillofacial Orthognathics, Tokyo Medical and Dental University, Tokyo, Japan

### Purposes

Bone development is a dynamic process that requires cell motility and morphological adaptation under the control of actin cytoskeleton. This actin cytoskeleton system is regulated by critical modulators including actin-binding proteins. Among them, profilin 1 (Pfn 1) is a key player to control actin fiber structure and it is involved in a number of cellular functions such as migration. BMPs are multifunctional cytokines involved in cell proliferation and differentiation. BMP2, an osteoinductive factor, is clinically approved for use in bone regeneration and repair. Although multiple transcription factors and secreted proteins are known to mediate BMP signal intensity or duration, less is known about mechanisms determining lineage specificity in response to BMP. In this study, we examined the role of Pfn1 in BMP-induced osteogenic activities

### Materials and Methods.

As for cells, we used MC3T3E1 cells and MLO-Y4 cells. These cells were cultured as reported previously. To estimate the levels of gene expression, RNAs were isolated and were subjected to real-time RT-PCR. For knock down of Pfn1, siRNAs were used. To examine transcriptional activity, luciferase reporter linked to BMP response element (BRE) was used.

### Results and Conclusion.

In MC3T3E1 cells, Pfn1 mRNA is expressed constitutively and BMP treatment of these cell suppressed the levels of Pfn1. This effect was time dependent and suppression was more when the BMP treatment was continued for a longer period of time. Along with this time course, alkaline phosphatase mRNA levels were enhance in a time dependent manner as described before. To address the functional role of Pfn1 during BMP-induced differentiation of MC3T3 cells, we knocked down Pfn1 via siRNA technique. The efficiency of Pfn1 knock down (KD) by si-RNA was confirmed by quantitative RT-PCR. The result shows that about 80% expression of Pfn-1 was observed. Interestingly, Pfn1 KD enhanced basal levels of alkaline phosphatase (Alp) activity in MC3T3-E1 cells. When Pfn1 KD was done in the cells treated with BMP, BMP-induced expression of Alp activity in MC3T3-E1 cells were further enhanced. Surprisingly, such Pfn1 KD enhancement of Alp was still observed even when the BMP concentration was increased to 200ng/ml. Pfn1 KD enhancement of Alp was time-dependent. As for underlying mechanism, Pfn1 KD enhanced BMP-induced Alp mRNA expression. For transcription, Pfn1 KD enhanced BMP-induced enhancement of BRE-luciferase activity. In osteocytic MLO-Y4, Pfn1 KD decreased the number of cellular processes and disorganized the cytoskeletal patterns. These results demonstrated that the Pfn1 is a novel target of BMP and acts as an endogenous suppressor of BMP actions via at least in part transcriptional events.

# A novel measurement method for the morphology of the mandibular ramus using homologous modeling

**Hiroyuki NAKANO<sup>1)</sup>, Kazuya Inoue<sup>2)</sup>, Tomoki SUMIDA<sup>1)</sup>, Naruto OTAWA<sup>2)</sup>, Naoyuki FUKUDA<sup>2)</sup>, Tomohiro YAMADA<sup>3)</sup>, Katsuhiko MINAMI<sup>4)</sup>, Katsuaki Mishima<sup>5)</sup>, Makiko Kouchi<sup>6)</sup>, Yoshihide MORI<sup>7)</sup>**

- 1) Senior Assistant Professor, Section of Oral and Maxillofacial Surgery, Division of Maxillofacial Diagnostic and Surgical Sciences, Faculty of Dental Science, Kyushu University, Higashi-ku, Fukuoka, Japan
- 2) Assistant Professor, Section of Oral and Maxillofacial Surgery, Division of Maxillofacial Diagnostic and Surgical Sciences, Faculty of Dental Science, Kyushu University, Higashi-ku, Fukuoka, Japan
- 3) Associate Professor, Section of Oral and Maxillofacial Surgery, Division of Maxillofacial Diagnostic and Surgical Sciences, Faculty of Dental Science, Kyushu University, Higashi-ku, Fukuoka, Japan
- 4) Senior Assistant Professor, Division of Research and Treatment for Oral and Maxillofacial Congenital Anomalies, Faculty of Dentistry, Aichi-Gakuin University, Chikusa, Nagoya, Aichi, Japan
- 5) Associate Professor, Department of Oral and Maxillofacial Surgery, Yamaguchi University Graduate School of Medicine, Minamikogushi, Ube, Yamaguchi, Japan
- 6) Digital Human Research Center, National Institute of Advanced Industrial Science and Technology, Koto-ku, Tokyo, Japan
- 7) Professor and chairman, Section of Oral and Maxillofacial Surgery, Division of Maxillofacial Diagnostic and Surgical Sciences, Faculty of Dental Science, Kyushu University, Higashi-ku, Fukuoka, Japan

## Abstract

Some three-dimensional (3D) studies on facial asymmetry have reported differences in linear and angle measurements between the deviated and contralateral sides in asymmetric mandibles. However, these studies cannot clarify the 3D morphology of ramus. In this study, we aimed to evaluate the mandibular ramus between the deviated and contralateral sides in asymmetric mandibles using traditional and homologous model methods.

Fifteen Japanese females with jaw deformities treated by orthodontic surgery were enrolled. 3D computed tomography (CT) images were reconstructed and 13 landmarks identified on the model surface. Homologous ramus models were constructed for each sample.

Principal component analysis revealed that >80% ramus morphology was suggested by principal components 1–8. The 3 principal components were significantly different between the deviated and contralateral sides. The t-values for the mandibular ramus height, posterior mandibular ramus height, condylar width, condylar head height, coronoid process height, horizontal and vertical dilated ramus angles, and ramus angle were 2.45, 2.30, 3.48, 2.36, –2.24, –2.08, –4.67, and 2.19, respectively. The F-values for the mandibular ramus height, condylar width, and horizontal and vertical dilated ramus angles were 18.34, 15.56, 11.94, and 16.88, respectively. The squared multiple correlation coefficient adjusted for the degrees of freedom was 0.815. Visual simulation revealed a larger condylar head on the contralateral side, a larger coronoid process on the deviated side, and a mandibular angle that was turned inwards to a greater extent on the deviated side. In conclusion, we successfully created a homologous model of the mandibular ramus and demonstrated the effectiveness of this model in the 3D comparison of ramus morphology between contralateral and deviated sides in asymmetric mandibles.

## **BMP-induced alkaline phosphatase expression in osteoblast-like MC3T3E1 cells is suppressed by $\beta_2$ adrenergic receptor activation.**

**Takayuki Yamada<sup>1), 2), 3)</sup>, Yoichi Ezura<sup>1)</sup>, Tadayoshi Hayata<sup>1)</sup>, Shuichi Moriya<sup>1)</sup>, Junpei Shirakawa<sup>1), 3)</sup>, Takuya Notomi<sup>1), 3)</sup>, Smriti Arayal<sup>1)</sup>, Makiri Kawasaki<sup>1)</sup>, Yayoi Izu<sup>1)</sup>, Kiyoshi Harada<sup>2)</sup>, Masaki Noda<sup>1), 3)</sup>**

1) Department of Molecular Pharmacology, Medical Research Institute, Tokyo Medical and Dental University, Tokyo, Japan

2) Department of Oral and Maxillofacial Surgery, Tokyo Medical and Dental University, Tokyo, Japan

3) Global COE program, Tokyo Medical and Dental University, Tokyo, Japan

### **Purposes:**

In vivo  $\beta$  adrenergic stimulation suppresses bone formation while its actions in osteoblastic differentiation are not fully understood. Therefore, we examined the effects of  $\beta_2$  adrenergic stimulation on osteoblast-like MC3T3-E1 cells focusing on BMP-induced alkaline phosphatase (ALP) expression in vitro.

### **Materials and methods:**

For cell culture, osteoblast-like cell line, MC3T3E-1 was used. ALP activity measurement and protein determination were performed according to PNPP method. For ALP staining, we used BM purple (Roche), and analyzed the ALP-positive area using Image-J software. For Real-time PCR, StepOne™ system (life technology) was used to gene expression analysis. For luciferase assay, reporter activity was measured by using a LIMAT LB9507 (Berthold). The data was standardized in Renilla luciferase reporter activity. Differences between groups were analyzed by Student's t-test. P values less than 0.05 or 0.01 were considered to be significant.

### **Results:**

In terms of morphology, isoproterenol (ISO) treatment reduces BMP-induced increase in the numbers of small ALP-positive foci in the cultures of MC3T3-E1 cells. With respect to biochemical effects, ISO treatment inhibits BMP-induced enzymatic activity of ALP in a dose-dependent manner. Isoproterenol treatment suppressed BMP-induced ALP activity even at higher dosage of BMP was used. Regarding cell density, ISO treatment tends to inhibit BMP-induced increase in ALP activity compared to those at lower cell density. In addition, we observed that ISO treatment did not affect cell proliferation in MTT assay. In terms of treatment protocol, continuous ISO treatment is compared to cyclic treatment. Continuous ISO treatment is more suppressive against BMP-induced increase in ALP activity than cyclic regimen. At molecular level, ISO treatment inhibits BMP-induced enhancement of ALP mRNA expression. With regard to the mode of ISO action, ISO inhibits BMP-induced BRE-luciferase activity. These data suggest that ISO regulates BMP-induced ALP expression in osteoblast-like MC3T3E1 cells.

### **Conclusion:**

ISO treatment suppresses BMP-induced ALP expression in osteoblast-like MC3T3-E1 cells. BMP-induced enhancement of osteoblastic differentiation may be one of the target points of sympathetic tone-dependent suppression of osteoblastic activity, such phenomena may be relevant to those in disuse osteoporosis.

# **Voluntary exercise prevents deterioration of trabecular bone architecture in diabetes mellitus model rats**

**Akira Minematsu, Tomoko Hanaoka, Yoshihiro Takada, Shunji Okuda, Hidetaka Imagita, and Susumu Sakata <sup>1)</sup>.**

1) Kio University, Japan

## **Purpose:**

Type 2 diabetes mellitus (DM) is well-known to cause bone fragility and increase in fracture risk, although bone mass remains unchanged. In patients with type 2 DM, regular physical exercise may improve not only DM symptom but also bone fragility that appears to be caused by poor bone quality. The purpose of this study is to examine the effects of voluntary wheel-running on trabecular bone architecture of lower limb in type 2 DM model Otsuka Long-Evans Tokushima Fatty (OLETF) rats.

## **Materials and methods:**

Five-week-old male OLETF rats were used as experimental animals and male Long-Evans Tokushima Otsuka (LETO) rats as control animals. Half of the OLETF rats performed daily voluntary wheel-running throughout the experimental period of 16 months (OLETF-EXE), and the remainder of the OLETF and LETO rats did not perform the wheel-running. After 16 months, left distal femur and proximal tibia were scanned with micro-CT, and were analyzed for trabecular bone architecture.

## **Results:**

Long-term voluntary wheel-running prevented the deterioration of trabecular bone architecture in the femur and tibia, where bone volume, bone volume fraction, trabecular number, and connectivity density were significantly lower in the OLETF than in the OLETF-EXE and LETO rats. In addition, the OLETF-EXE rats showed a significant decrease in tissue volume compared with the OLETF and LETO rats.

## **Conclusion:**

Although trabecular bone architecture of femur and tibia was deteriorated in type 2 DM model OLETF rats aged 17 months, this deterioration was prevented by daily voluntary wheel-running that started at the age of 1 month. Based on these results, we conclude that regular physical exercise would be a potent strategy for preventing the deterioration of trabecular bone architecture in patients with type 2 DM.

## **Morphological and dynamic analysis of migration linked to FUCCI-indicated cell cycle under the influence of PTH and mechanical flow signals**

**Shirakawa J<sup>(1,2,3)</sup>, Ezura Y<sup>(1)</sup>, Moriya S<sup>(1)</sup>, Kawasaki M<sup>(1)</sup>, Yamada T<sup>(1)</sup>, Notomi T<sup>(1)</sup>, Hayata T<sup>(1)</sup>, Miyawaki A<sup>(3)</sup>, Omura K<sup>(2)</sup>, Noda M<sup>(1)</sup>.**

1) Dept. Molecular Pharmacology, Medical Research Institute, Tokyo Medical and Dental University, Japan

2) Dept. Oral and Maxillofacial Surgery, Tokyo Medical and Dental University, Japan

3) Laboratory for Cell Dynamics, Brain Science Institute, RIKEN, Japan

Bone Cellular responses to hormones and mechanical stress may be linked to the cell morphology and migration. Osteoblasts are responding to Parathyroid hormone (PTH) and also mechanical stress. However, how these signals regulate cell migration and cell cycle when the two signals are together is still incompletely understood. To address this point, we subjected osteoblasts to PTH and mechanical signaling and monitored the behavior by using fluorescent ubiquitination-based cell cycle indicator (FUCCI) reporter system. This FUCCI system allows simultaneous monitoring of cell migration and cell cycle as G1 as well as S/G2 /M phase can be detected due to the marker expression specific to each cell cycle stage. We found that osteoblastic cells in S/G2 / M phase migrate faster than those in G1 phase. Parathyroid hormone as an anabolic agent also regulates migration velocity of the osteoblasts. Flow induced mechanical stress increased migration speed. The presence of both PTH and mechanical stress, the migration velocity got back to the base line levels. These observations suggest that cell migration is influenced by the PTH and mechanical flow and these two signals my influence each other. Our data show that morphological monitoring of osteoblasts could reveal complex interactions of PTH and mechanical stress in osteoblasts.

# **Influence of magnet implant on tibial trabecular bone microarchitecture in ovariectomized rats.**

**Yasue Nishii<sup>1)</sup>, Hidetaka Imagita and Akira Minematsu<sup>2)</sup>**

1) Graduate school of Health Science, Kio University, Japan

2) Department of Physical Therapy, Faculty of Health Science, Kio University, Japan

## **Purposes:**

Static magnetic field (SMF) was reported to inhibit reduction of bone mineral density (BMD) in ovariectomized (OVX) rats. Those were assessed by dual energy X-ray absorptiometry and there are few studies to investigate the effects of SMF on bone structure. The purpose of this study is to examine the influence of SMF on trabecular bone microarchitecture (TBMA) in OVX rats.

## **Materials and methods:**

Female SD rats (mean body weight  $376.8 \pm 10.5$  g) were used. They underwent either ovariectomy (OVX, n=14) or sham-operation (SHAM, n=6). Half of OVX rats (OVX+MG group) were surgically implanted disk-shaped neodymium magnet and stainless steel in lateral part of the right and left knee joints, respectively. The remainder of the OVX rats (OVX group) and SHAM rats (SHAM group) were surgically implanted stainless steel in lateral part of the both knee joints. The right knee joints were harvested after 20-week intervention. Then, the proximal tibias were scanned using x-ray micro-computed tomography and were analyzed for TBMA with 3D bone analysis software.

## **Results:**

Final body weights of the OVX+MG and OVX groups were significantly heavier than the SHAM group. TBMA was remarkably deteriorated by OVX. The ratio of decrease for bone volume fraction was 81% in the OVX group and 69% in the OVX+MG group compared with the SHAM group. Parameters of TBMA in the OVX+MG group tended to be maintained compared with the OVX group, for trabecular thickness and width were significantly higher in the OVX+MG group than in the SHAM group. In addition, trabecular star volume ( $V^*_{tr}$ ) as osteoporotic index was higher in OVX+MG group than in the OVX and SHAM groups.

## **Results and conclusion:**

OVX caused deterioration of TBMA. Compared with the OVX group, the degree of deterioration in TBMA was smaller and  $V^*_{tr}$  was significantly higher in the OVX+MG group. These results suggested that SMF was likely to inhibit deterioration of TBMA, especially trabecular thickness and width, in OVX rats. We need to consider the SMF conditions, the timing and term of interventions, and histomorphological study.



## **PTH-induced proliferation in osteoblasts requires ubiquitin specific peptidase 2 (Usp2)**

**Jumpei Shirakawa<sup>1)</sup>, Yoichi Ezura<sup>1)</sup>, Yayoi Izu<sup>1)</sup>, Masaki Noda<sup>1)</sup>**

1) Dept. Molecular Pharmacology, Medical Research Institute, Tokyo Medical and Dental University, Japan,

### **Purposes:**

Osteoporosis is a common disease that affects mainly the elderly individuals by increasing the fragility fracture risk. Teriparatide (PTH) is the only agent that induces anabolic action of bone forming osteoblastic lineage cells. Though the molecular bases the anabolic action of PTH has been investigated from various aspects, the mechanism of its action is still incompletely understood. We were interested in the genes directly induced by cAMP pathway as possible downstream targets leading to osteoblast proliferation. Ubiquitin specific peptidase 2 (Usp2, also named as Ubp41) was suggested be one of the direct target genes of PTH. However, the functional role of Usp2 gene in PTH effects on osteoblast proliferation is not known.

### **Materials and methods:**

Murine osteoblast-like MC3T3-E1 cells and primary calvarial osteoblasts isolated from newborn double Fucci-transgenic mice were used. To examine the role of Usp2 enhanced by PTH treatment we transfected si-Usp2. Protein levels were determined by western blot. We also used real time PCR and live imaging.

### **Results:**

PTH1-34 induced Usp2 expression in MC3T3E1 cells. Usp2 has three isoforms and all of them were expressed and induced by PTH in osteoblasts. Cycloheximide (CHX) treatment did not affect the Usp2 induction by PTH treatment. To examine if the Usp2 expression could be induced by cyclic AMP-PKA pathway, MC3T3E1 cells were treated with forskolin. Forskolin induced Usp2 expression through PKA pathway. These results suggested that PTH induced Usp2 expression through cyclic AMP pathway directly. Then we analyzed whether knocking down of Usp2 would influence the proliferation-inducing effect of PTH on osteoblasts, using live imaging of the calvarial osteoblasts obtained from Fucci-transgenic mice. PTH induced osteoblast proliferation by increasing the numbers of cells that enter the S/G2/M phase from G0/G1 phase. However, the cells transfected with si-Usp2 did not show significant increase of the proliferating cells that enter the S/G2/M phase after PTH treatment. These results indicated that Usp2 play a role in regulation of proliferation in osteoblasts after PTH treatment.

### **Conclusion:**

Usp2 gene is a target of PTH is involved in PTH-induced regulation of proliferation in osteoblasts.

## This image shows a full page of a handwriting practice worksheet. It consists of multiple rows of horizontal dashed lines spaced evenly down the page, providing a guide for letter height and placement. The background is plain white, and there are no other markings or text present.

[illegible]



日本発。  
強い骨には、理由がある。



骨粗鬆症治療剤(ミノドロン酸水和物錠)

薬価基準収載

**ボノデオ®錠1mg/50mg**

劇薬、処方箋医薬品  
(注意—医師等の処方箋により使用すること)

**Bonoteo®**

#### 【禁忌(次の患者には投与しないこと)】

- (1) 食道狭窄又はアカラシア(食道弛緩不能症)等の食道通過を遅延させる障害のある患者[本剤の食道通過が遅延することにより、食道局所における副作用発現の危険性が高くなる。]
- (2) 服用時に上体を30分以上起こしていることのできない患者
- (3) 本剤の成分あるいは他のビスホスホネート系薬剤に対し過敏症の既往歴のある患者
- (4) 低カルシウム血症の患者[血清カルシウム値が低下し低カルシウム血症の症状が悪化するおそれがある。]
- (5) 妊婦又は妊娠している可能性のある婦人(「妊婦、産婦、授乳婦等への投与」の項参照)

#### 【効能・効果】骨粗鬆症

【効能・効果に関連する使用上の注意】 本剤の適用にあたっては、日本骨代謝学会の診断基準等を参考に、骨粗鬆症との診断が確定している患者を対象とすること。

【用法・用量】(1mg) 通常、成人にはミノドロン酸水和物として1mgを1日1回、起床時に十分量(約180mL)の水(又はぬるま湯)とともに経口投与する。なお、服用後少なくとも30分は横にならず、飲食(水を除く)並びに他の薬剤の経口摂取も避けること。(50mg) 通常、成人にはミノドロン酸水和物として50mgを4週に1回、起床時に十分量(約180mL)の水(又はぬるま湯)とともに経口投与する。なお、服用後少なくとも30分は横にならず、飲食(水を除く)並びに他の薬剤の経口摂取も避けること。

#### 【用法・用量に関連する使用上の注意】

投与にあたっては次の点を患者に指導すること。(1) 本剤は水(又はぬるま湯)で服用すること。水以外の飲料(Ca、Mg等の含量の特に高いミネラルウォーターを含む)、食物及び他の薬剤と一緒に服用すると、吸収を妨げることがあるので、起床後、最初の飲食前に服用し、かつ服用後少なくとも30分は水以外の飲食を避ける。(2) 食道及び局所への副作用の可能性を低下させるため、速やかに胃内へと到達させることが重要である。服用に際しては、以下の事項に注意すること。1) 口腔咽頭刺激の可能性があるので、本剤を嚥んだり又は口中で溶かしたりしないこと。2) 十分量(約180mL)の水(又はぬるま湯)とともに服用し、服用後30分は横たわらないこと。3) 就寝時又は起床前に服用しないこと。(3) (50mgのみ) 本剤は4週に1回服用する薬剤であるため、飲み忘れないように注意すること。本剤の服用を忘れた場合は、翌日1錠服用すること。

#### 【使用上の注意】(抜粋)

1. 慎重投与(次の患者には慎重に投与すること) (1) 嚥下困難、食道炎、胃炎、十二指腸炎、又は潰瘍等の上部消化管障害がある患者[上部消化管粘膜に対し、刺激作用を示すことがあるので基礎疾患を悪化させるおそれがある。] (2) 重篤な腎障害のある患者[排泄が遅延するおそれがある。] 2. 重要な基本的注意 (1) 上部消化管に関する副作用が報告されているので、これらの症状があらわれた場合は、本剤の服用を中止して診察を受けるよう指導すること。(2) 骨粗鬆症の発症にエストロゲン欠乏、加齢以外の要因が関与していることもあるので、治療に際してはこのような要因を考慮する必要がある。(3) (1mg) 患者の食事によるカルシウム、ビタミンDの摂取が不十分な場合は、カルシウム又はビタミンDを補給すること。ただし、カルシウム補給剤及びカルシウム、アルミニウム、マグネシウム含有製剤は、本剤の吸収を妨げることがあるので、服用時刻を変えて服用させること。〔相互作用〕の項参照) (50mg) 本剤投与後は、血清カルシウム値が低下する可能性があるため、血清カルシウムの変動に注意し、必要に応じて、カルシウム及びビタミンDを補給すること。ただし、カルシウム補給剤及びカルシウム、アルミニウム、マグネシウム含有製剤は、本剤の吸収を妨げることがあるので、服用時刻を変えて服用させること。〔相互作用〕の項参照)

ム、アルミニウム、マグネシウム含有製剤は、本剤の吸収を妨げることがあるので、服用時刻を変えて服用させること。〔相互作用〕の項参照) (4) 本剤を含むビスホスホネート系薬剤による治療を受けている患者において、顎骨壊死・顎骨骨髓炎があらわれることがある。報告された症例の多くが、抜歯等の顎骨に対する侵襲的な歯科処置や局所感染に関連して発現している。リスク因子としては、悪性腫瘍、化学療法、コルチコステロイド治療、放射線療法、口腔の不衛生、歯科処置の既往等が知られている。本剤の投与開始前は口腔内の管理状態を確認し、必要に応じて、患者に対し適切な歯科処置を受け、侵襲的な歯科処置をできる限り済ませておくよう指導すること。本剤投与中に侵襲的な歯科処置が必要になった場合には本剤の休薬等を考慮すること。また、口腔内を清潔に保つこと、定期的な歯科検査を受けること、歯科受診時に本剤の使用を歯科医師に告知して侵襲的な歯科処置はできる限り避けることなどを患者に十分説明し、異常が認められた場合には、直ちに歯科・口腔外科を受診するように指導すること。(5) ビスホスホネート系薬剤を長期使用している患者において、非外傷性の大腿骨転子下及び近位大腿骨骨幹部の非定型骨折が報告されている。これらの報告では、完全骨折が起る数週間から数カ月前に大腿部や鼠径部等において前駆痛が認められている報告もあることから、このような症状が認められた場合には、X線検査等を行い、適切な処置を行うこと。また、両側性の骨折が生じる可能性があることから、片側で非定型骨折が起きた場合には、反対側の大腿骨の症状等を確認し、X線検査を行うなど、慎重に観察すること。X線検査時には骨皮質の肥厚等、特徴的な画像所見がみられており、そのような場合には適切な処置を行うこと。 3. 相互作用 併用注意(併用に注意すること) 水以外の飲料、食物(特に牛乳や乳製品のような高カルシウム含有飲食物)、多価陽イオン(カルシウム、鉄、マグネシウム、アルミニウム等)含有製剤(ミネラル入りビタミン剤、制酸剤等) 4. 副作用 (1mg) 承認時までの臨床試験における1,108例中206例(18.6%)に副作用(臨床検査値の異常を含む)が認められた。主なものは胃・腹部不快感35例(3.2%)、腹痛27例(2.4%)、血中カルシウム減少22例(2.0%)及び胃炎15例(1.4%)等であった。(承認時:2009年1月) (50mg) 承認時までの臨床試験における228例中30例(13.2%)に副作用(臨床検査値の異常を含む)が認められた。主なものは胃・腹部不快感5例(2.2%)、腹痛3例(1.3%)、胃炎3例(1.3%)及びアルカリホスファターゼ減少3例(1.3%)等であった。(承認時:2011年7月)

(1) 重大な副作用 1) (1mg) 上部消化管障害: 十二指腸潰瘍(0.3%)、胃潰瘍(0.1%)等の上部消化管障害があらわれることがあるので、観察を十分に行い、異常が認められた場合には投与を中止するなど、適切な処置を行うこと。(50mg) 上部消化管障害: 十二指腸潰瘍(0.4%)、胃潰瘍(頻度不明)等の上部消化管障害があらわれることがあるので、観察を十分に行い、異常が認められた場合には投与を中止するなど、適切な処置を行うこと。2) 顎骨壊死・顎骨骨髓炎・顎骨壊死・顎骨骨髓炎(頻度不明)があらわれることがあるので、観察を十分に行い、異常が認められた場合には投与を中止するなど、適切な処置を行うこと。3) 大腿骨転子下及び近位大腿骨骨幹部の非定型骨折(頻度不明)を生じることがあるので、観察を十分に行い、異常が認められた場合には投与を中止するなど、適切な処置を行うこと。4) 肝機能障害、黄疸: AST(GOT)、ALT(GPT)等の上昇を伴う肝機能障害、黄疸(いずれも頻度不明)があらわれることがあるので、観察を十分に行い、異常が認められた場合には投与を中止し、適切な処置を行うこと。(50mgのみ) 注) 1mg製剤の承認時までの臨床試験成績又は自発報告に基づく記載のため頻度不明とした。(2) 重大な副作用(類薬) 低カルシウム血症: 他のビスホスホネート系薬剤において、極端な、テタニー、しびれ、失見当識、QT延長等を伴う低カルシウム血症があらわれるとの報告があるので、観察を十分に行い、異常が認められた場合には投与を中止し、適切な処置を行うこと。

■その他の使用上の注意等につきましては、製品添付文書をご参照ください。

製造販売 **アステラス製薬株式会社**  
東京都中央区日本橋本町2-5-1

[資料請求・お問い合わせ先] DIセンター ☎0120-189-371

2014年11月作成 A4



## エーザイの骨粗鬆症関連製品

骨粗鬆症治療剤

日本薬局方 リセドロン酸ナトリウム錠

劇薬 処方箋医薬品：注意 一医師等の処方箋により使用すること

〔薬価基準収載〕

**アクトネル<sup>®</sup> 錠 75mg**

骨粗鬆症治療用ビタミン K<sub>2</sub> 剤

メナテトレノン製剤

〔薬価基準収載〕

**グラケ<sup>®</sup> カプセル 15mg**

体外診断用医薬品 (電気化学発光免疫測定法)

低カルボキシル化オステオカルシンキット [検体検査実施料収載]

血清中低カルボキシル化オステオカルシン (ucOC) 測定用医薬品

**ピコルミ<sup>®</sup> ucOC<sup>※</sup>**

※ 販売提携品

● 効能・効果、用法・用量、禁忌を含む使用上の注意等については添付文書をご参照ください。



エーザイ株式会社

東京都文京区小石川4-6-10

製品情報お問い合わせ先：エーザイ株式会社 hhcホットライン

フリーダイヤル 0120-419-497 9～18時(土、日、祝日 9～17時)

ACL1410M01

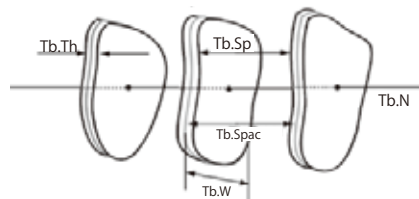
# TRI/3D-BON-FCS64

Measures bone morphometry, bone fine structure, and bone matrix mineralization.

Specializes in 3D bone morphometric measurements and dramatically improves bone observations.

## Bone morphometric measurement

CT-scanned bone can be measured using 3D bone morphometry. The software measures bone volume, BV (cm<sup>3</sup>), bone volume density, BV/TV (%), trabecular dimensions (thickness Tb.Th; width Tb.W; pore space Tb.SP; and trabecular number, Tb.N). The measurement provides a 3D perspective of trabecular bone fine structure. The structure model index (SMI), which is an index of the trabeculae in the form of a plate and rod, indicates the condition of the bone, such as an increase and decrease in bone volume, or change in the morphometric features of each region. Bone volume dimensions can be measured accurately using a direct measurement method. Commonly found measurement functions are available at very reasonable prices. This system includes various options, such as Node Strut measurement, a full trabecular bone measurement package, and cortical measurement functions.



1. Beehive-form concave structure



SMI  $\approx$  0

2. Plate-form



SMI  $\approx$  0

3. Rod-form



SMI  $\approx$  3.00



RAT OVX 14W Tibia



Mouse Femur  
RedTB WhiteCB

## Bone volume density measurement

A CT image is used to produce a BMD image in which the BMD is the same as the pixel value. This is performed using a phantom image scan, where the BMD value is already known and the scan conditions are the same as for bone. Bone density, bone mineral content (BMC; mg), and tissue bone density (BMD/TV) of each trabecular and cortical bone can be measured. Tissue bone density reflects decreased bone volume and is an indicator of osteoporosis. The BMD and BMC values can be measured in each region, regardless of scanning conditions. Bone can be extracted from the BMD value and compared to previously acquired data, regardless of scan conditions, and fine bone morphometric measurements become possible.



0 500mg/cm<sup>3</sup>

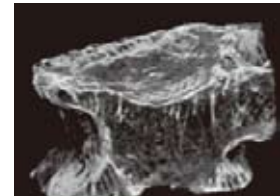
## Bone intensity measurement (option)

Measure stress toward the outer load, based on bone density by calculating Young's modulus, which reflects the bone matrix.

Items to be measured:

- Principal stress
- Principal strain
- Shear stress
- Shear strain

shear stress  
0 SMPa



Compressed load 500N

MDCT Human L3 Shear stress image

## Measurement parameters

### Trabecular bone morphometric measurement

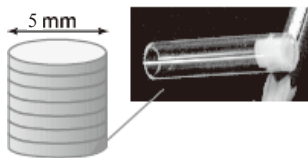
- Bone volume density; TV, BV, BV/TV
- Trabecular dimensions  
Thickness, Tb.Th, width, Tb.W;  
Trabecular space, Tb.SP;  
Trabecular central distance, Tb.Space;  
Trabecular number, Tb.N;
- Structural model index, SMI

### Bone density measurement

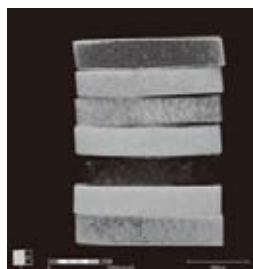
- Volume bone density (vBMD; mg/cm<sup>3</sup>)
- Bone volume (cm<sup>3</sup>)
- Bone mineral content (BMC; mg)
- Tissue bone density (BMC/TV; mg/cm<sup>3</sup>)

## BMD phantom for $\mu$ CT

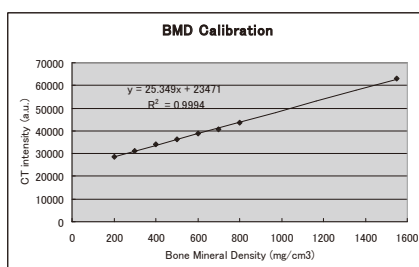
Hydroxyapatite mixed phantom in polyurethane resin structure



Structure:  
200-800 mg/cm<sup>3</sup>, one set including seven disks with 100 mg variances.  
The diameter of each disk is 5 mm, and the height is 1 mm.



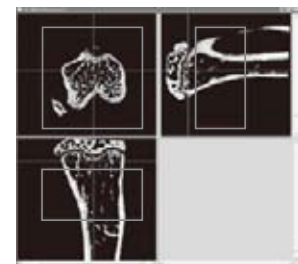
Phantom



BMD phantom analytical curve

## Cut measurement area

Morphometric measurements in each region



## Cut measurement area



Trabecular Bone (TB)



Cortical Bone (CB)

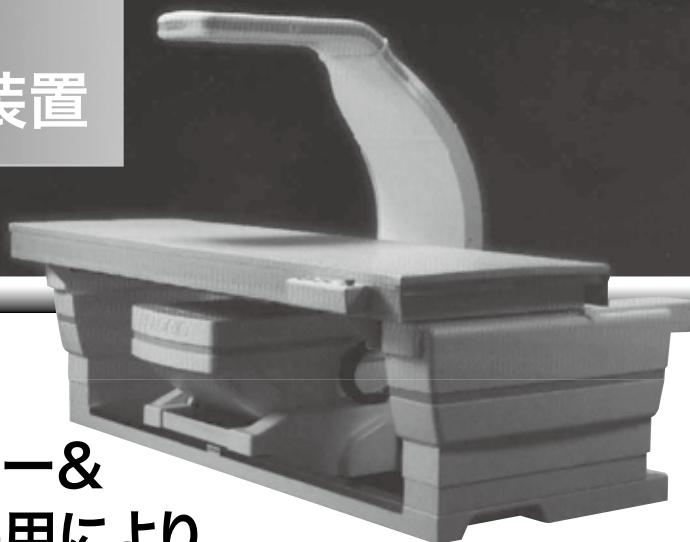


Ratoc System Engineering Co., Ltd.  
Toho Edogawabashi Bldg. 1-24-8 Sekiguchi, Bunkyo-ku, Tokyo 112-0014  
TEL: +81-3-3268-8411 FAX: +81-3-3268-8411  
E-mail: info@ratoc.co.jp URL: http://www.ratoc.co.jp



プレミアム高画質の贅沢をHorizonで  
**Horizon**  
**X線骨密度測定装置**

Horizon™  
QDR SERIES



**最新の  
セラミックディテクター&  
高周波X線管球の採用により  
体厚のある受診者の画像もより鮮明に描出します。**

**主な機能と特長**

DXA法による腰椎・大腿骨・全身・ラテラル・前腕骨の骨密度測定装置です。

- 最新のセラミックディテクター&高周波X線管球の採用(Discovery 比)
- X線管球の小型化により、前腕骨測定のポジショニングが容易に  
(Discovery 比)
- 従来のQDRシリーズとのデータ互換性を確保することで、  
蓄積してきた受診者データを有効活用
- 10秒(L2-L4)で測定可能なBMD測定性能
- ホロジック社のみが有するラテラル測定機能
- ヒストグラム解析により、椎間の判別しにくかった受診者の解析が容易に
- ホロジック社独自の「自動内部リファレンスシステム」
- ON/OFFボタンを押すことでベッドが前に、アームが横に移動。  
受診者の容易な乗降を実現
- 臨床・研究ともに豊富な測定アプリケーションソフト



**TOYO  
MEDIC**

■米国・HOLOGIC社 日本総代理店

**東洋メディック株式会社**

本 社／〒162-0813 東京都新宿区東五軒町2-13

TEL.(03)3268-0021(代表) FAX.(03)3268-0318

事業所／東京・大阪・名古屋・福岡・札幌・新潟・仙台・岡山

<http://www.toyo-medico.co.jp/>

// MICROSCOPY  
MADE BY ZEISS

# Revolutionize Your Confocal Imaging **ZEISS LSM 880 with Airyscan**



## Revolutionize Your Confocal Imaging

Discover ZEISS LSM 880 with Airyscan – the new confocal laser scanning microscope that offers high sensitivity, improved resolution in x, y and z, and high speed.

All in one system. Find out more and book a hands-on demonstration in one of our ZEISS Microscopy Labs now.



[www.zeiss.com/lsm880](http://www.zeiss.com/lsm880)



We make it visible.



# Wiley Blackwell Commercial Sales

Supporting the communication needs of your industry

## Maximizing the Impact of your Brand

Through our extensive range of clinical and professional publications we can develop a customized communications plan to support your promotional strategy. Whether in print or digital formats, our global sales team is ready to help shape your brand strategy.

- Reprints
- Advertising (Print and Online)
- Supplements
- Sponsored subscriptions and books
- Custom publications in English or local languages

Email or call us today:

**[corporatesalesjapan@wiley.com](mailto:corporatesalesjapan@wiley.com)**

**03 3830 1221**



**[wileyonlinelibrary.com](http://wileyonlinelibrary.com)**

**WILEY**

**Wiley  
Online  
Library**

# リガク社製 実験動物用3DマイクロX線CTシステム

小型実験動物用3DマイクロX線CT

## CosmoScan GX

高速（最速8秒）、高解像（最高解像度 $4.5\mu\text{m}$ ・最大画素 $8,000\times 8,000$ ）、広視野（最大 $72\text{mm}$ ）を高い次元で両立したかつてないプレミアムCT

- ハイスピード撮影モードでは、わずか8秒でCT画像を取得し、さらに約10秒程度で3D画像再構成まで完了します。
- 撮影部位を高速にCTスキャン後、画像劣化なくさらに任意のポイントを超解像ズームし、最高解像度 $4.5\mu\text{m}$ で表示可能。
- 最大 $72\text{mm}$ の広視野を1スキャンで撮影可能。長時間撮影が可能なことから、in vivo実験に加え、ex vivoニーズにもお応えします。



**業界初!!**

中型実験動物用3DマイクロX線CT

## CosmoScan AX

約15Kgまでの中型動物を最高 $60\mu\text{m}$ の画素サイズで撮影可能。X線自己遮蔽型で中型動物を用いた安全性試験や薬効薬理試験に最適なニューコンセプトCT

- 撮影室直径 $32.2\text{cm}$ 、最大視野領域 $22\text{cm}$ 、最高画素サイズ $60\mu\text{m}$ を有しており、中型動物の生体内構造を高解像度に撮影可能です。
- 人用CTと異なり自己遮蔽型のため、CT室の設置は不要で置き場所を選びません。また専任の技術者も不要です。
- 100V電源で稼働し、キャスター付きで移動も容易です。



総販売元

# Focus on the Science

理科研グループは、研究用試薬・理化学機器の販売を通じて、生命科学に貢献する会社です

## 理科研株式会社

- 本 社 〒463-8528 名古屋市守山区元郷二丁目107番地  
TEL: (052)798-6151(代) Email: honsya@rikaken.co.jp
- 三 重 支 店 〒514-0103 三重県津市栗真中山町43番地1  
TEL: (059)236-5511 Email: mie@rikaken.co.jp
- 岐 阜 営 業 所 〒500-8225 岐阜県岐阜市岩地二丁目25番2号  
TEL: (058)240-0721 Email: gifu@rikaken.co.jp
- 東 京 支 社 〒113-0033 東京都文京区本郷七丁目2番1号  
TEL: (03)3815-8951(代) Email: tokyo@rikaken.co.jp
- 多 摩 営 業 所 〒187-0022 東京都小平市上水本町2丁目18番20号  
TEL: (042)329-8651 Email: tama@rikaken.co.jp
- つ く ば 支 店 〒305-0074 茨城県つくば市高野台3丁目16-2  
TEL: (029)839-1251 Email: tsukuba@rikaken.co.jp
- 柏 営 業 所 〒277-0871 千葉県柏市若柴197番地17  
TEL: (04)7135-6651 Email: kashiwa@rikaken.co.jp
- 千 葉 営 業 所 〒260-0842 千葉市中央区南町3丁目2番1号 青木ビル1階  
TEL: (043)305-1751 Email: chiba@rikaken.co.jp
- 仙 台 営 業 所 〒984-0051 仙台市若林区新寺三丁目5番40号  
TEL: (022)352-4851 Email: sendai@rikaken.co.jp

グループ会社一覧

 並木薬品株式会社

- 〒930-0834 富山県富山市問屋町三丁目1番33号 TEL:(076)451-4545(代)

- 岡 崎 営 業 所 〒444-0864 愛知県岡崎市明大寺町字西長峰50番  
TEL: (0564)57-1751 Email: okazaki@rikaken.co.jp
- 静 岡 営 業 所 〒422-8005 静岡市駿河区池田379番地  
TEL: (054)208-5351 Email: shizuoka@rikaken.co.jp
- 福 井 営 業 所 〒910-0842 福井県福井市開発三丁目3010  
TEL: (0776)52-1651 Email: fukui@rikaken.co.jp
- 神 奈 川 支 店 〒227-0045 横浜市青葉区若草台1番地5  
TEL: (045)530-0151 Email: kanagawa@rikaken.co.jp
- 鶴 見 営 業 所 〒230-0033 横浜市鶴見区朝日町一丁目49番地  
TEL: (045)500-4551 Email: tsurumi@rikaken.co.jp
- 平 塚 営 業 所 〒254-0035 神奈川県平塚市宮の前1番2号 エバース第7平塚ビル3階  
TEL: (0463)79-8851 Email: hiratsuka@rikaken.co.jp
- 三 島 営 業 所 〒411-0943 静岡県駿東郡長泉町下土狩217番地1  
TEL: (055)980-1101 Email: mishima@rikaken.co.jp

 株式会社 片 岡

- 〒920-1158 石川県金沢市朝霧台二丁目27番地 TEL:(076)263-2011(代)

# 骨・歯等の生体サンプルの撮像には “EASY”・“SPEEDY”・“COMPACT” な inspeXio SMX-90CT Plus

Easy, Speedy, and Compact inspeXio SMX-90CT Plus System  
for CT Imaging of Bones, Teeth, and Other Biological Samples

## inspeXio SMX-90CT Plus

inspeXio SMX-90CT Plus は “EASY”、 “SPEEDY”、 “COMPACT” をコンセプトにした卓上型 X 線 CT システムです。キャリブレーションフリーを主とする操作性や卓上型のコンパクトさに加え、超高速演算処理システム HPCinspeXio や DICOM 変換機能などの機能を搭載し、誰でも簡単に生体、医薬品・骨等の CT 撮像・解析を実現します。

Built to be easy to use, speedy, and compact, the inspeXio SMX-90CT Plus benchtop X-ray CT system makes CT imaging simple for everyone.

In addition to user-friendly operability and its compact benchtop design, the inspeXio SMX-90CT Plus also includes an HPC inspeXio high-performance computing system, a DICOM conversion function, and other features that allow anyone to perform CT imaging and data analysis on biological, pharmaceutical, bone, or other samples.

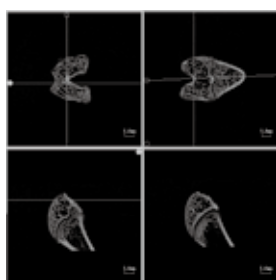


透視画像分解能	Fluoroscopic Image Resolution	10 $\mu$ m (チャート分解)	10 $\mu$ m (chart resolution)
X 線出力	X-Ray Generator	90 kV – 250 $\mu$ A, 10 W	90 kV – 250 $\mu$ A, 10 W
搭載可能なサンプルの大きさ	Sample Size Capacity	$\varnothing$ 160 $\times$ H100 mm	160 mm dia. $\times$ H100 mm
搭載可能なサンプル重さ	Sample Weight Capacity	4 kg	4 kg
CT スキャン領域 (FOV)	Max. CT Scan Area (FOV)	$\varnothing$ 50 mm	50 mm dia.

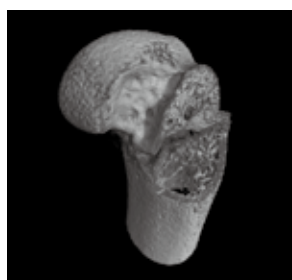
### ラット大腿骨の観察・BMD解析 Observation and BMD Analysis of Rat Femur

ラット大腿骨を inspeXio SMX-90CT Plus で撮像した後、ラトックシステムエンジニアリング社製ソフトウェア TRI/3D-BON と専用ファントムの CT データを用いて BMD 解析を行いました。各部位の骨密度 (BMD 値) 分布をカラーマップで表示可能です。

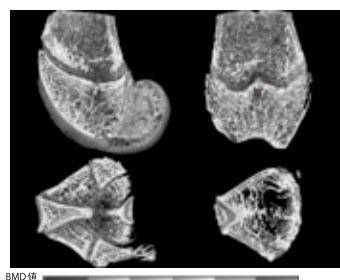
A rat femur image was obtained with an inspeXio SMX-90CT Plus system and then TRI/3D-BON software from Ratoc System Engineering was used to analyze the bone density (BMD) from CT data acquired using a specialized phantom. This made it possible to display a color-coded map of the bone density (BMD value) distribution in each area.



MPR (FOV = 14.7 mm)



VR



BMD 解析結果 BMD Analysis Results

**株式会社 島津製作所** 分析計測事業部

<http://www.an.shimadzu.co.jp/ndi/>

■ 東京 (03) 3219-5735	■ 北関東 (048) 646-0082	■ 神戸 (078) 331-9665
■ 関西 (06) 6373-6661	■ 横浜 (045) 311-4106	■ 岡山 (086) 221-2511
■ 札幌 (011) 700-6605	■ 静岡 (054) 285-0124	■ 四国 (087) 823-6623
■ 東北 (022) 221-6231	■ 名古屋 (052) 565-7532	■ 広島 (082) 248-4312
■ 郡山 (024) 939-3790	■ 京都 (075) 823-1602	■ 九州 (092) 283-3334
■ つくば (029) 851-8515		

SHIMADZU Corporation

HEAD OFFICE

1, Nishinokyo-Kuwabara-cho, Nakagyo-ku, Kyoto 604-8511, Japan  
Phone: 81(75)823-1111



**International Society of Bone Morphometry**